4-20-2016 12:00 AM

Minor Whey Protein Purification Using Ion-Exchange Column Chromatography

Naeimeh Faraji Dizaji
The University of Western Ontario

Supervisor
Dr Ajay Kumar Ray
The University of Western Ontario

Graduate Program in Chemical and Biochemical Engineering
A thesis submitted in partial fulfillment of the requirements for the degree in Doctor of Philosophy

Abstract

This thesis is concerned with application of mechanistic models for recovery and purification of two minor milk proteins to develop an efficient and robust process. A fundamental and quantitative understanding of the underlying mechanisms assists to evaluate chances and challenges in non-linear chromatography.

The first chapter considers adsorption isotherm data of two minor whey proteins on cation exchanger under various conditions and used as the basis to develop a predictive approach for correlating adsorption behavior using a mechanistic isotherm model. The SMA isotherm model explicitly considers the contributions of protein-adsorbent and protein-protein interactions in the simulation of salt gradients in ion exchange chromatography.Sensitivity and robustness analysis by factorial design of experiments within this framework showed to be highly consistent and even allowed for upscale predictions with an excellent quality.

In the next part of the thesis, the nonlinear gradient elution was to be optimized by three process factors the length of gradient, final salt concentration at the end of gradient and flow velocity. Predictions based on response surface modeling (RSM) approach were applied to reveal significant process factors. The optimal operating point was then determined by calibrated mechanistic model within and outside the design space. The operating conditions containing optimal information were experimentally verified which confirmed simulations accuracy.

The third chapter considers the effects of scale-up and operating conditions on dynamic adsorption of proteins. For two columns having similar bed height, flow distribution properties was observed under non-binding conditions. Elution profiles were employed to determine dominant mass transport mechanisms. Breakthrough profiles were compared at different flow rates and protein loading concentrations.The efficiency of the columns in terms of HETP and dynamic binding capacity were calculated and compared for two columns.

The outcomes resulting from the application of mechanistic models to the purification of lactoperoxidase and lactoferrin in this thesis exploit the platform for the next step towards the recovery of high-value proteins at industrial scales.

Keywords

Ion-exchange chromatography, Whey proteins, Mechanistic modeling, Steric mass action, Process development

Co-Authorship Statement

Chapter 3: Faraji, N.; Zhang, Y.; Ray, A.K. Determination of Adsorption Isotherm Parameters for Minor Whey Proteins by Gradient Elution Preparative Liquid Chromatography. *J. Chromatogr. A.* (2015) 1412 67-74

Chapter 4: Faraji, N.; Zhang, Y.; Ray, A.K. Model-based Optimization of Lactoperoxidase Separation on an Ion-Exchange Chromatography Step. (Prepared for submission)

Chapter 5: Faraji, N.; Zhang, Y.; Ray, A.K. Impact of operating conditions on chromatography column performance- Experimental study of high-value minor whey proteins adsorption. (Prepared for submission)

The manuscripts were prepared by the author and reviewed by Dr. Y. Zhang and Dr. A.K. Ray.

To my mom, Robab, for her unconditional love and support

&

to the blessed memory of my dad, Nosrat, for his love and inspiration

Acknowledgments

I would like to thank my enthusiastic supervisor, Professor Dr. Ajay Ray. My PhD has been an incredible experience and I thank him wholeheartedly, not only for his tremendous academic support, but also for giving me so many wonderful opportunities.

I am also hugely appreciative to Dr. Yan Zhang, especially for sharing her expertise in chromatography so willingly, and for being so dedicated to her role as my secondary supervisor. She has been actively interested in my work and has always been available to advise me.

Similar, profound gratitude goes to Dr. Ferdinando Crapulli, for his patience and immense knowledge in statistics that, taken together, make him a great mentor.

I am particularly indebted to Atieh Motaghi for her support when so generously helping me with mathematical modeling and for spreading happiness on those scientifically dark days. I have very fond memories of my time with her in the office.

I especially thank our lab coordinator, Mrs. Fate Hashemi. Fate has been helpful for organizing our research group with instrumentation and general lab inquiries. I like to think of her as the guardian angel of our group before she left to start her new position as research and training coordinator in the department.

Special mention goes to Dr. Ghodsieh Malekshoar, for going far beyond the call of friendship. I cannot express my gratitude and feelings for this gregarious woman. To Maliheh Mehdizadeh, for providing me with a fantastic lab training. And to Dr. Nillohit Mitra Ray and Shreyas Yadahalli, for nurturing my enthusiasm for biotechnology.

My deep appreciation goes out to all my friends in London who opened their homes to me during my time at Western and who were always so helpful in numerous ways. Special thanks to Zahra and Nina.

Lastly, but by no means least, thanks goes to my family; mum, Monir and Mostafa for their unbelievable support and encouraging me to follow my dreams. I love them all dearly.

Table of Contents

List of Tables

List of Figures

List of Appendices

Abbreviations

AC	Affinity chromatography
ANOVA	Analysis of variance
BSA	Bovine serum albumin
CV	Column volume
DBC	Dynamic binding capacity
DOE	Design of experiments
FDA	US Food and Drugs Administration
HIC	Hydrophobic interaction chromatography
FPLC	Fast protein liquid chromatography
LF	Lactoferrin
LP	Lactoperoxidase
MC	Membrane chromatography
MOL	Method of line
MW	Molecular weight
IEC	Ion-exchange chromatography
PAT	Process Analytical Technology
pI	Isoelectric point
RSM	Response surface model
RPC	Reverse phase chromatography
SEC	Size exclusion chromatography
SMA	Steric mass action isotherm
SP FF	Sulphopropyle fast flow
UV	Ultra violet
WPI	Whey protein isolate

Nomenclature

A	coefficient in van Deemter equation (5-7) (m)
B	coefficient in van Deemter equation (5-7) (m^2/s)
B_b	Bed permeability (m^2/s)
C	coefficient in van Deemter equation (5-7) (s)

$c_{p,i}$	concentration of protein *i* in the pores of the adsorbent (M)
$c_{p,salt}$	salt concentration in the pores of the adsorbent (M)
c_i	protein concentration i in the mobile phase (M)
c_{prot}	Concentration of protein *i* in stock solution (M)
c_{salt}	salt concentration in buffer (M)
c_0	initial concentrations of salt and protein at column inlet (M)
$c_{a,s}$	salt concentration at gradient begin (M)
$c_{e,s}$	salt concentration at gradient end (M)
d_p	Particle diameter (m)
D_{ax}	axial dispersion coefficient (m^2/s)
D_m	molecular diffusivity in mobile phase (m^2/s)
D_e	effective diffusivity (m^2/s)
h	reduced HETP ($=H/d_p$)
H	Height equivalent to plate number (HETP) (m)
$k_{eff,i}$	effective mass transfer coefficient of protein *i* (m/s)
$k_{ads,i}$	adsorption coefficient of protein *i* in the SMA isotherm ($s/M^{-\nu}$)
$k_{des,i}$	desorption coefficient of protein *i* in the SMA isotherm ($s/M^{-\nu}$)
$k_{eq,i}$	equilibrium coefficient of protein *i*
L	length of the column (m)
ΔP	column pressure drop (Pa)
q_i	protein concentration i on the adsorbent phase (M)
r_p	particle radius (m)
u_0	Superficial velocity of the fluid (m/s)
u_{int}	interstitial velocity of the fluid (m/s)
Y	recovery yield
V_c	column volume (m^3)

Greek symbols

ε_c	column void fraction
ε_p	Intra-particle void fraction
ε_t	total column void fraction

$1-\varepsilon_t/\varepsilon_t$	ratio of stationary and mobile phase volumes in column
Λ	total ionic capacity (M)
η	mobile phase viscosity (Pa.s)
μ_1	first moment of pulse response peak (s)
μ_2	second moment of pulse response peak
v_i	characteristic charge of protein *i* in SMA isotherm
σ_i	steric factor of protein *i* in the SMA isotherm

Dimensionless transport parameters

Pe	Péclet number ($=u_{int}\,L/D_{ax}$)
Re	Reynolds number ($=\rho u d_p/\eta$)
Sc	Schmidt number ($=\eta/\rho D_m$)
Sh	Sherwood number ($=k_{eff}\,d_p/D_m$)
Bi	Biot number ($=k_{eff}r_p/\varepsilon_p D_e$)

Chapter 1

Introduction

1.1 Whey protein purification

The commercial recovery of by-products from waste food streams has recently drawn a great attention. Future initiatives to improve the recovery of by-products require further research to look into potential uses for high value waste-stream components and to develop profitable techniques for their recovery [1]. An example of by-product recovery is the purification of proteins from milk whey using chromatographic techniques [2].

Whey is a by-product from the cheese and curd manufacturing present at low concentrations. Only 10-20% (w/w) of the raw milk is utilized to obtain cheese or curd as the final product; the residue of the raw milk yields whey. Thus, the problem of whey consumption is that an enormous amount of whey in the order of 150 million tonnes is produced worldwide annually. Whey is typically utilized in three major types: animal feedstocks, production of whey powders and production of lactose [3]. It has long been considered as a waste product of dairy processes rather than a by-product and this whey contains of very dilute concentrations of high biological value proteins and other components. Whey protein constitutes about 20% of the total milk proteins and its namely the major components are β-Lactoglobulin (β-Lg), α-Lactalbumin (α-La), bovine serum albumin (BSA) and immunoglobulins (Ig), representing 90% of the whey fraction [4]. In addition, whey contains numerous minor proteins, such as lactoperoxidase (LP), lactoferrin (LF), lysozyme (LYS), proteose peptone (PP), and osteopontin (OPN) [5]. Table 1-1 presents the main characteristics of the major and two minor proteins present in whey [5,6].

The dairy industry has convinced the food industry that whey is a marvelous product. Whey protein products are usually available in three major types: concentrates (WPC), isolates (WPI) and hydrolysates (WPH). These products, best known for their versatile functional properties, are widely utilized in the food processing industry as food additives in the production of a variety of baked goods, meats, dairy products, and beverages [7]. However, the approval of above mentioned products by the food industry has been restricted due to inconsistency in the gross composition and functionality [8]. Moreover, presence of lipid and protein impurities develops a stale off-flavor in commercial whey

protein concentrates [9]. Individual whey proteins are generally unrealized in whey products due to interactions between components and degradation during processing. Each whey protein has unique attributes for nutritional, therapeutic and food ingredient applications [10]. They exhibit better functionality in comparison to crude protein mixtures [11]; therefore there is a great commercial interest in recovering pure whey protein fractions without damaging structural and functional properties of protein [9].

Table 1-1 Characteristics of whey proteins

Protein	Concentration in whey (g/l)	Molecuolar weight (kDa)	Isoelectric point
β-Lactoglobulin	2-4	18	5.2
α-Lactalbumin	1.2-1.5	14	4.5-4.8
Immunoglobulins	0.6-0.9	150-1000	5.5-8.3
BSA	0.3-0.6	69	4.7-4.9
Lactoferrin	0.02-0.2	78-92	8-9.5
Lactoperoxidase	0.02-0.05	78-89	9.5

The present study will focus on downstream purification of the two minor whey proteins, lactoperoxidase (LP) and lactoferrin (LF), as they correspond to about less than 10% wt. of the total whey proteins. These components with high nutritional and biological properties have unique attributes in nutraceutical, pharmaceutical and therapeutic applications. LP and LF are known to be effective against microorganisms; many biological activities have been reported such as immune system modulation, anti-microbial, anti-parasitic and anti-inflammatory activities [12,13]. LF has been confirmed to function as an iron absorption regulator, an anti-infective agent and inhibits the outbreak of infections. LP is one the most dominant enzymes in bovine milk and catalyzes the inactivation of a wide range of microorganisms; hence it acts as a natural preservative in milk [14].

The dairy industry has been employed different technologies to purify single whey proteins; such as selective precipitation, membrane filtration and chromatography. Selective separation based on molecular weight requires a large difference in and for that

reason would be limited to separating only specific components of whey proteins [15]. Due to the fairly similar physicochemical properties of whey proteins, membrane separation has demonstrated to be challenging. Moreover, precipitation and membrane techniques may result in unacceptable consequences on changes in native structure shifting functional properties of the whey proteins. Liquid chromatographic processes are of particular interest in the biotechnology industry as they can provide high-purity products, are relatively simple to develop, and can be easily scaled from the laboratory scale to the preferred manufacturing scale with low cost [16].

1.2 Chromatography

Chromatography, to write with colors literally translated from its Greek roots (χρῶμα [chroma]: color and γράφειν [graphein]: to write), has now been applied for separation purposes for over 100 years. In 1903, the Russian botanist Mikhail Tswett coined and screened adsorption-based methods for the separation of plant pigments on a column of calcium carbonate. Later, in 1906, he introduced the term chromatography. It is an invaluable laboratory tool to separate and analyze a mixture as a result of differential distribution of its components between two phases. The stationary adsorbing medium remains settled in place as the mobile phase spreads out the components of the mixture around or over the stationary medium. The stationary phase acts as a restraint on various components in the mixture, slowing them down to move slower than the mobile phase. The movement of the components in the mobile phase is controlled by the importance of their interactions with stationary and/or the mobile phase. Because of the differences in the strength of components affinities for the stationary phase and factors such as the solubility of particular components in the mobile phase and, some components will travel more rapidly than others, thus assisting the separation of the components within that mixture.The different modes of chromatography are briefly described:

Size exclusion chromatography (SEC) separates components based on their molecular size; large molecules are excluded from the pores of the SEC medium, while smaller ones are retained in the bead and eluted later on. As the only chromatographic method with gentle non-adsorptive interaction with the sample, SEC enables the high retention of biomolecular activity.

Ion-exchange chromatography (IEC) separates proteins on the basis of their ionic charge, where molecules with an opposite charge bind to charged functional groups of IEC media. In anion-exchange chromatography negatively charged proteins are attracted to a positively charged group. Conversely in cation-exchange chromatography positively charged proteins bind to a negatively charged media. .

Hydrophobic interaction chromatography (HIC) is a method to separate proteins based upon their surface hydrophobicity. Proteins with hydrophobic patches on surface form hydrophobic cavities in the mobile phase. Adding of salt enhances the interaction between hydrophobic areas on a protein and hydrophobic surfaces of a chromatography medium, while by lowering the salt concentration hydrophobic interaction weakens and results in desorption from the solid support.

Affinity chromatography (AC) is a technique on the basis of molecular recognition. The specific ligands coupled to a chromatography matrix function via reversible biological interactions due to electrostatic or hydrophobic interactions, van der Waals' forces and/or hydrogen bonding. This makes the binding of the protein of interest highly selective. Hence AC can potentially provide one-step purification and concentrated form of the target protein. However, the utilization of the specialized mediums at lager scales is often very costly.

Reversed-phase chromatography (RPC), like HIC, separates proteins according to differences in their hydrophobicity however on a surface of a more hydrophobic RPC medium used in HIC. After purification by RPC, the protein in solution can simply be lyophilized. However, RPC may exploit more denaturing environment and is hence not appropriate for proteins that do not spontaneously refold.

1.3 Ion-exchange chromatography of whey proteins

Proteins are often characterized by their isoelectric points (pI), the pH value at which they carry no net charge [17]. It is assumed that the proteins will not bind to the chromatography media at their pI, but will be retained by cation resins at pH below their pI; or by anion resins above their pI [18]. At the pH of rennet whey (pH 6.2 to 6.4), whey

proteins give two specific groups: the major whey proteins, β-Lg, α-La and BSA that have a negative charge; and minor whey proteins, LP and LF that are positively charged. This distinctive property presents the potential for separation of the desired protein from other proteins employing IEC. One encouraging ion exchange technology that has been applied to fractionate whey proteins is membrane chromatography (MC) [19,20]. The key advantage of MC over column chromatography have been mainly attributed to shorter diffusion times, as the association between target proteins and functional groups occurs through pores rather than in a stagnant fluid inside the pores of the beads. Thus, the process can be efficiently operated at high flow rates with low pressure drop. Other advantages of MC are lower buffer usages due to low void volume and ease of scale-up for process development [21]. Some researchers [21,22] using an ion exchange membrane, were able to separate protein fractions from whey. In spite of the promise of ion exchange membrane chromatography, it is worth noting that currently available membranes display lower binding capacities compared to the ones achieved with packed bed columns with similar geometries, because of a larger surface area obtained when using IEC beads. Generally, ion-exchange packed column chromatography, the focus of this thesis, is an advantageous method for protein purification due to its high binding capacity, relatively low cost compared to other methods (e.g. protein A affinity chromatography), ability to resist under intense cleaning procedures, and the ease of control [23].

As a practical straightforward process for isolating and separating the two minor whey proteins, lactoperoxidase and lactoferrin from whey, ion-exchange adsorption approach is therefore adopted. According to the pH of natural milk (6.6-6.8), cation exchange column chromatography was selected for the purpose of this work. This implies that the two proteins must be in the form of cations. In other words, the working pH is below the lower pI of the two proteins. The selected adsorption media is the strong cation-exchanger SP Sepharose FF. It has been well-proven for great flow characteristics and reasonable mechanical stability due to high chemical cross-linking.

However, the variety of process factors complicates quantitative studies of IEC. Due to the nature of the separation mechanism, factors such as buffer type, pH, temperature and

salt concentration all play significant roles in controlling process performance. These effects are influenced by the complex adsorbent, protein properties and transport issues involved. A priori prediction of chromatographic processes is tremendously challenging. Moreover with over 50-80% constituting the downstream cost [24], downstream processing is reflected as an "unresolved bottleneck" [25]. Therefore, an absolute need for strategies that can offer solutions to these challenges by providing more insight into bio-separation process development [26,27].

1.4 Objective and outline of thesis

The objective of this work is to investigate a framework enabling knowledge-based fast development of two minor whey proteins separation process. The projected outcome of the research is of potential significance to preparative and nonlinear IEC, in such respects as process optimization and scale up consideration. The ultimate advantages include cost-effective and efficient usage of resources as well as well-timed process development (i.e. better understanding of the critical process and product quality attributes). The approaches taken to accomplish these goals are outlined and the structure of this thesis is as follows.

This introductory chapter (**Chapter 1**) provides the background and motivation for the research, the research objectives and an overview of the research approach. Prior to this research, there already existed a great body of information on whey purification using ion-exchange adsorption, but no study on model-based process development and optimization of lactoperoxidase and lactoferrin separation. Hence, brief reviews of protein purification using ion-exchange chromatography and major concepts of process development in this direction are highlighted in **Chapter 2**.

Chapter 3 focuses on the determination of sorption model parameters of proteins based on inverse method to nonlinear adsorption isotherm. A set of experimental data on a commercial cation-exchange column under various elution conditions is used to calibrate steric mass action model. To verify predictive capability of the calibrated mechanistic model, full-factorial design experiments are carried out on a larger bed height column. The results show a realistic agreement with the experiments providing reproducible

column elution profile and reduced experimental work. To evaluate model parameters quality in real conditions, whey protein isolate was introduced as a feed sample.

Chapter 4 expands the importance of process understanding, as well as sensitivity and robustness analyses emphasized in the Process Analytical Technology (PAT) guidelines of US Food and Drug Administration (FDA) [28]. Thus, the objective of the separation step is defined by yield and product purity constraint. The optimization starts with multivariate optimization approach based on design of experiments (DoE) and response surface modeling (RSM) for characterization of the design factor spaces, primary predictions with respect to optimal factor settings and providing adequate experiments for the calibration of the mechanistic model. In the next step, the calibrated mechanistic model is employed for accurate predictions on the process.

In **Chapter 5**, we study the adsorption of protein with experimental approach in an attempt to evaluate the behavior of employed columns in order to achieve an effective scale-up of a real separation problem. Despite of effective separation protocol at a typical scale from laboratory already presented, complex biochemical feedstocks often show only a few aspects of predictions in realistic applications. This chapter includes a necessary preliminary study to scale-up and insights into the column performance involved in scale-up.

Lastly, **Chapter 6** presents the conclusions from this work and some perspectives on future study.

References

[1] S. Beszedits, A. Netzer, Protein recovery from food-processing wastewaters, Food Technology 37(1983) 160.

[2] L.S. Conrado, V. Veredas, E.S. Nobrega, C.C. Santana, Concentration of α-lactalbumin from cow milk whey through expanded bed adsorption using a hydrophobic resin, Brazilian Journal of Chemical Engineering, 22 (2005) 501-509.

[3] T. Sienkiewicz, Nomenclature and some properties of whey proteins, Nahrung-food 25 (1981) 329-343.

[4] S. Jovanovic, M. Barac, O. Macej, T. Vucic, C. Lacnjevac, SDS–PAGE analysis of soluble proteins in reconstituted milk exposed to different heat treatments, Sensors 7 (2007) 371–383.

[5] R. Hahn, P.M. Schulz, C. Schaupp, A. Jungbauer, Bovine whey fractionation based on cation-exchange chromatography, J. Chromatogr. A 795 (1998) 277– 287.

[6] H. Korhonen, A. Pihlanto-Leppälä, P. Rantamäki, T. Tupasela, Impact of processing on bioactive proteins and peptides, Trends Food Sci. Technology 9 (1998) 307-319.

[7] P. Cayot, D. Lorient, Structure function relationships of whey proteins, in: Food proteins and their applications, S. Damodaran, A. Paraf, Marcel Dekker, New York (1997) 225-256.

[8] C.V. Morr, E.Y.W. Ha, Off-flavours of whey protein concentrates: A literature review, International Dairy Journal 1 (1991) 1-11.

[9] Andrew L. Zydney, Protein separations using membrane filtration: new opportunities for whey fractionation, International Dairy Journal 8 (1998) 243-250.

[10] K. Marshall, Therapeutic applications of whey proteins, Altern. Med. Rev. 9 (2004) 136–156.

[11] G.I. Imafidon, N.Y. Farkye, A. Spanier, Isolation, purification, and alteration of some functional groups of major milk proteins: a review, Crit. Rev. Food Sci. Nutr. 37 (1997) 663–689.

[12] J.K. Actor, S. A. Hwang, M.L. Kruzel, Lactoferrin as a natural immune modulator, Curr. Pharm. Des. 15 (2009) 1956–1973.

[13] A.C.M. van Hooijdonk, K.D. Kussendrager, J.M. Steijns, In vivo antimicrobial and antiviral activity of components in bovine milk and colostrum involved in nonspecific defence, Br. J. Nutr. 84 (2000) 127–134.

[14] B. Ekstrand, Antimicrobial factors in milk - A review, Food Technology, 3 (1989) 105-126.

[15] S. Goodall, A.S. Grandison, P.J. Jauregi, J. Price, Selective separation of the major whey proteins using ion exchange membranes, Journal of Dairy Science 91 (2008) 1-10.

[16] E.N. Lightfoot, Speeding the design of bioseparations: A heuristic approach to engineering design, Ind. Eng. Chem. Res. 38 (1999) 3628-3634.

[17] D.H.G. Pelegrine, C.A. Gasparetto, Whey proteins solubility as function of temperature and pH, Food Sci. Technol. 38 (2005) 77–80.

[18] I. Ali, H.Y. Aboul-Enein, P. Singh, R. Singh, B. Sharma, Separation of biological proteins by liquid chromatography: review article, Saudi Pharm. J. 18 (2010) 59–73.

[19] S. Bhattacharjee, C. Bhattacharjee, S. Datta, Studies on the fractionation of β-lactoglobulin from casein whey using ultrafiltration and ion-exchange membrane chromatography, J. Membr. Sci. 275 (2006) 141–150.

[20] S. Goodall, A.S. Grandison, P.J. Jauregi, J. Price, Selective separation of the major whey proteins using ion exchange membranes, J. Dairy Sci. 91 (2008) 1–10.

[21] M.R. Drioli, Progress and new perspectives on integrated membrane operations for sustainable industrial growth, Ind. Eng. Chem. 40 (2001) 1277–1300.

[22] R. Ulber, K. Plate, T. Demmer, H. Buchholz, T. Scheper, Downstream processing of bovine lactoferrin from sweet whey, Acta Biotechnol. 21 (2001) 27–34.

[23] C. Selkirk, Ion-exchange chromatography, Methods Mol. Biol. 244 (2004) 125–131.

[24] C.R. Lowe, A.R. Lowe, G. Gupta, New developments in affinity chromatography with potential application in the production of biopharmaceuticals, Journal of Biochemical and Biophysical Methods 49 (2001) 561-574.

[25] K.A. Thiel, Biomanufacturing, from Bust to Boom ... to Bubble? Nat. Biotechnol. 22 (2004) 1365-1372.

[26] B.K. Nfor, T. Ahamed, G.v. Dedem, L.A.M.v.d. Wielen, E.J.A.X.v.d. Sandt, M. Eppink, M. Ottens, Design strategies for integrated protein purification processes: Challenges, progress and outlook, J. Chem. Technol. Biotechnol. 83 (2008) 124-132.

[27] J.A. Asenjo, B.A. Andrews, Is there a rational method to purify proteins? From expert systems to proteomics, J. Mol. Recognit. 17 (2004) 236-247.

[28] FDA, Guidance for Industry PAT - A Framework for Innovative Pharmaceutical Development, Manufacturing, and Quality Assurance, (2004).

Chapter 2

Review of Literature

2.1 Proteins

The term “protein” was proposed by Swedish chemist Jöns Jacob Berzelius in 1838. It comes from the Greek word *πρώτειος*, meaning "primary", or "foremost" as Berzelius thought protein appears to be the primitive or principal substance of animal nutrition. At the time, there were ongoing discussions about whether proteins were macromolecules or colloidal aggregates, a debate that lasted until 1930. In 1901, Hermann Emil Fischer synthesized a dipeptide, demonstrating that amino acids can be linked together, and the following year Franz Hofmeister suggested that proteins are long chains of amino acids linked by peptide bonds. The linear sequence of amino acids via peptide bonds (amide linkages) makes up the primary structure of a protein; dependent on hydrogen binding between some amino acids, two main types of secondary structure (α-helix or β-sheet) are characterized. The tertiary structure describes the configuration of α-helix and β-sheets with respect to each other on the level of one whole polypeptide chain; quaternary structure refers to the spatial conformations of more than one protein subunits (polypeptide chains). The four levels of protein structure are shown in Figure1-1 [1].

High variation in the amino acid sequence in along with protein fold up into three-dimensional structure and side chain modifications not surprisingly results in diverse protein functions. Hence, proteins serve a broad spectrum of essential functions in living organisms; they function as catalysts (enzymes), transmit nerve impulses, transport and store other molecules such as oxygen, or provide mechanical support and immune protection. In light of the various biological functions, the broad applications of proteins in food and detergent industry, medical, environmental and biomaterials are of growing interest in their production.

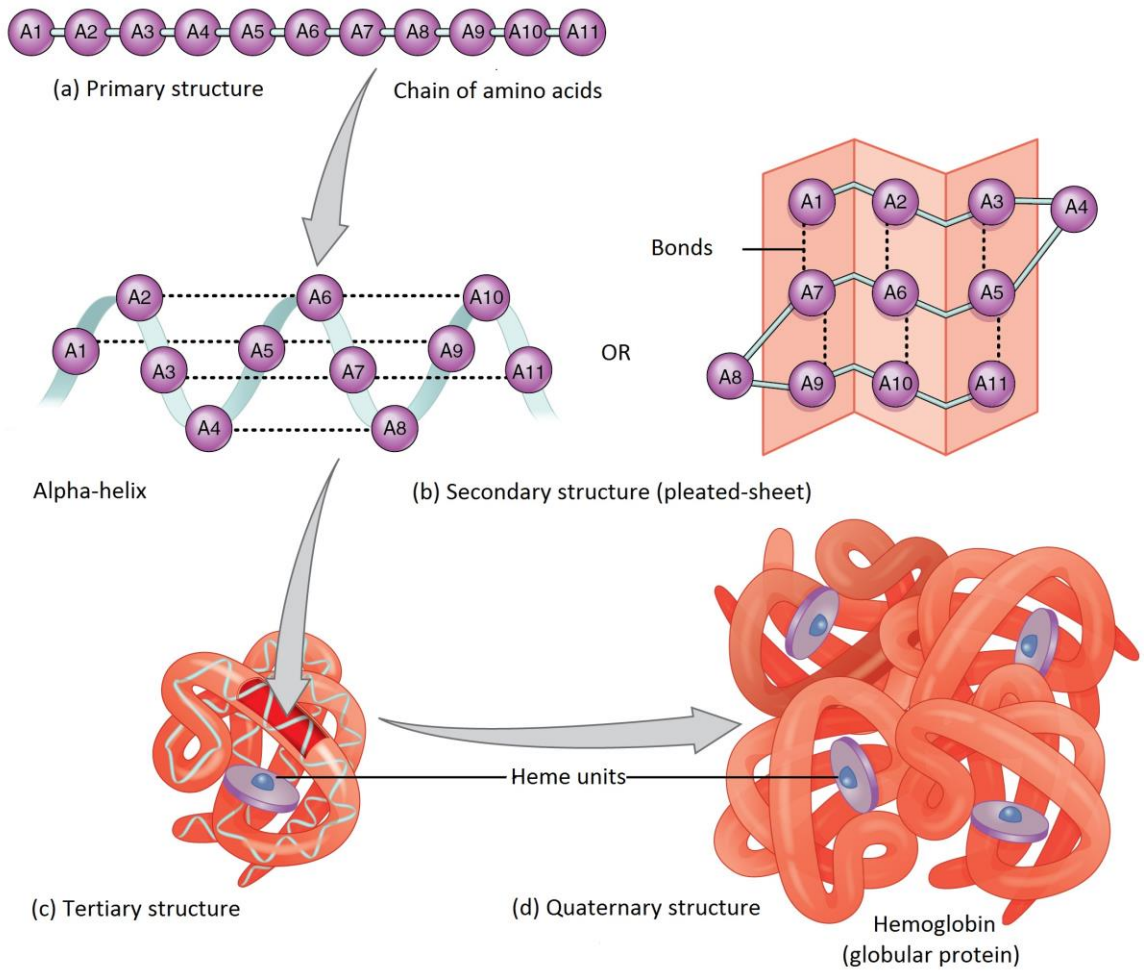

Figure 2-1 Four levels of protein structure [1]

The physical and chemical properties of a protein are established by their essential amino acids. These properties show a wide extension due to their dynamic structural variability. The physicochemical properties of the protein of interest usually decide on the multitude of possible interactions with the adsorbent and thereby on the choice of chromatography technique optimally applied for separation of a specific protein from a mixture.

The size of proteins lies within the range of 1-5 nm in diameter, significantly impacting the surface charge density. The molecular weight of most proteins lies a broad range of 15 to 200 kDa (1 Da = 1/12 mass of atom carbon-12) with one of the smallest proteins being insulin (5.8 kDa) up to multimeric glycoproteins (20,000 kDa). Hence, proteins are

rather large biomolecules and can distinctly be separated from viruses and smaller molecules such as amino acids or sugars by their size.

All proteins show maxima absorbance of ultraviolet light at 280 nm due to the strong absorbance of the two aromatic amino acids tryptophan (Trp) and tyrosine (Tyr) and, to a small extent, by the absorbance of cystine (i.e. of disulfide bonds) at this wavelength. The A_{280} varies greatly between different proteins; therefore this characteristic allows for a quantitation of the amount of protein in batch and flow through chromatography by absorption measurements in a simple spectrometer.

The charged groups on the side chains of amino acids contribute to net surface charge of proteins. The pH of the solution, the pKa-values of the side chain as well as the side chain's environment affect the charge on each side chain. The principle of ion exchange chromatography of proteins underlies on the knowledge of differences in net charge protein of interest. At a particular pH, known as the isoelectric point (pI), positively and negatively charged groups are evenly balanced and protein net surface charge equals zero.

Other properties of proteins, also crucial in downstream processing, are solubility and hydrophobicity. In general, proteins are soluble only in strongly polar solvents such as water, glycerol or formic acid. The solubility of proteins is dependent on pH and salt concentration. It is lowest at the isoelectric point and most likely precipitation will occur. Neutral salts have been known to have a two-fold effect on protein solubility; at low concentrations, they increase the solubility by suppressing the electrostatic protein–protein interaction (salting-in) and, dramatic decrease in protein solubility occurs at high salt concentrations due to ionic affinity of salt (salting-out). Solubility considerations drive biophysical processes of proteins such as phase transitions including crystallization and precipitation, but they also limit design spaces in process design for other chromatography modes. The most common methods for preparative purification of proteins all involve chromatography. The methods separate according to differences between the properties of the target protein and the properties of other components in the

sample. Examples of protein properties used in different chromatography methods are given in Table 2-1.

Hydrophobicity refers to the tendency of nonpolar amino acids residues to repel water molecules. These residues prefer to hide themselves internally in the protein 3D structure but some will be exposed to solvent to different extents. The surface charge density and distribution of residues form the basis for hydrophobic interaction chromatography (HIC). Thus, HIC suits all steps of a purification process; for instance high-yield capture, separation of active from inactive forms, and polishing monoclonal antibodies.

Table 2-1 Protein properties and their influence on selection of chromatography methods

Target protein property	Purification method
Molecular weight	Gel filtration (GF)
Specific ligand recognition/ Post translational modifications	Affinity chromatography (AF)
Charge properties	Ion exchange chromatography (IEC)
Hydrophobicity	Hydrophobic interaction chromatography (HIC), Reversed phase chromatography (RPC)

2.2 Strategies of protein purification

Protein purification has been developed in parallel with the discovery and further studies of proteins. It has a more than 200-year history; first attempts reported in 1789 by Fourcroy isolating substances from plants having similar properties to egg albumin (egg white). Up until the 20th century, the only existing separation technologies were methods such as precipitation, filtration and crystallization. In 1840, Hoppe-Seyler prepared the first hemoglobin crystalline. Ovalbumin, the first crystalline protein, was obtained by Hofmeister in 1889. During World War II, there was an urgent need for blood proteins. The Cohn plasma fractionation was developed for the purification of albumin and other proteins from serum. This procedure includes multiple precipitation steps and continues

to be used to this day. In fact, it was the onset of protein purifications in full-scale biopharmaceutical industry. In 1903, Tswett published his findings on separation of chlorophylls and carotenoids. In 1924, Svedberg (Nobel Prize, 1926) showed that centrifugation can be used to separate proteins. For the next a few decades, other major protein separation methods were developed: electrophoresis and affinity chromatography in the 1930s and size exclusion and ion exchange chromatography in the 1950s [2].

The 1950s and 1960s marked the invention of new hydrophilic chromatography matrices. The matrix is usually porous beads to which ligands are covalently coupled to obtain a chromatography medium. In 1955, starch was used to separate proteins based on differences in size. The onset of cellulose ion exchangers by Peterson and Sobers (1956), cross-linked dextrans (Sephadex) by Porath and Flodin (1959), and polyacrylamide (1961) and agarose (1964) by Hjertén, was a revolution in protein chromatography. Axén and co-workers (1967) introduced cyanogen bromide activation, which supported the development of ligand coupling in affinity chromatography. The method is accredited to Cuatrecasas et al. (1968). In the 1960s and 1970s, hydrophobic interaction chromatography (HIC), reversed phase chromatography (RPC), and immobilized metal ion affinity chromatography (IMAC) were developed [2].

The first application of protein chromatography in a large scale was insulin production in the 1970s. Protein purification is now being exploited at all scales from micrograms and milligrams in biochemistry labs to kilograms or even tonnes in industrial facilities. In some laboratories, proteins are purified in parallel, using automated chromatography systems. The common purification strategies have revolutionized protein purification by providing speed and simplicity, and this day many proteins can be readily purified. It should be noted, however, that these methods do not always provide sufficient purity, and other physicochemical-based chromatography methods, for example, GF, IEC, and HIC may accordingly have to be added to the protocol. Proteins that may be fairly easy to acquire in a pure state are not always stable under the initial conditions tested. Some proteins may be very challenging to purify in an active and stable form, for example, integral membrane proteins, unstable protein complexes, proteins expressed as insoluble aggregates, and proteins with a specific set of post-translational modifications. The

challenges in protein purification that still remain make it worthy to acquire concrete knowledge about protein purification so that the available methods can be selected and applied in an optimal mode.

IEC for the separation of biological macromolecules was introduced in the 1960s and proceeds to play a significant role in the separation and purification of biomolecules. Currently, IEC is one of the most commonly used techniques for purification of proteins, peptides, and other charged molecules, allowing for high resolution and group separations with high loading capacity. The technique is capable of separating molecular species that have only minor differences in their charge properties, such as two proteins differing by one charged amino acid. These features make IEC suitable for capture, intermediate purification or polishing steps in a purification protocol and the technique is applied from small scale purification and analysis through to purification of kilograms of product.

2.3 Model formulation in liquid chromatography

A model always opens the opportunity to ‘play’ with different ideas or to test different sets of parameters which in the end helps to argue what is possible and what is not.

Many researchers have contributed to liquid chromatography (LC) modeling. There exist a dozen or more theories with different complexities. First principles models of chromatography may have an important role to play in the systematic development and operation of industrial chromatographic bio-separations based on fundamental process understanding. However, before first principles modelling approaches are adopted by industry, a critical mass of evidence needs to be built demonstrating the unique advantages mechanistic models can give industry compared to a purely experimental approach.

Model formulation of LC consists of deriving or selecting suitable descriptive equations that mathematically describe the physical phenomena encountered in chromatographic separations. Two types of physical phenomena dominate chromatography; *movement of solutes* through the packed bed of porous particles via mass transfer mechanisms, and

adsorption based on the fundamental thermodynamic interactions between migrating solutes and the stationary phase. Equations used to describe these phenomena are discussed in sections 2.3.1 and 2.3.2, respectively.

2.3.1 Principles of mass transfer

Mass balance equations describe the movement of loaded components through the packed bed. The main factors with regard to mass transfer phenomena that contribute to this are illustrated in Figure 2-2, and include convective transport towards the particle, axial dispersion, diffusive transport of the solute molecule through the film surrounding the particle, and pore diffusion through the stagnant liquid-filled intra-particle pores. Diffusion along pore surfaces is usually unimportant and hence usually neglected [3]. The general system of equations used to describe the mass transfer phenomena consist of two sets of governing partial differential mass balance equations for each component. One defines the bulk fluid phase across the column axial dimension, and contains terms for accumulation in the mobile phase, accumulation in resin particles, convection, and dispersion. The other describes the intra-particle fluid phase across the radial particle dimension, which includes terms for accumulation in the intra-particle fluid phase, accumulation in the solid phase, and intra-particle diffusion. Along with the two differential mass balances, a kinetic expression is used to demonstrate diffusion through a stagnant film surrounding resin particles [3]. When coupled with a rate expression involving an appropriate adsorption isotherm, the model is known as a general rate model.

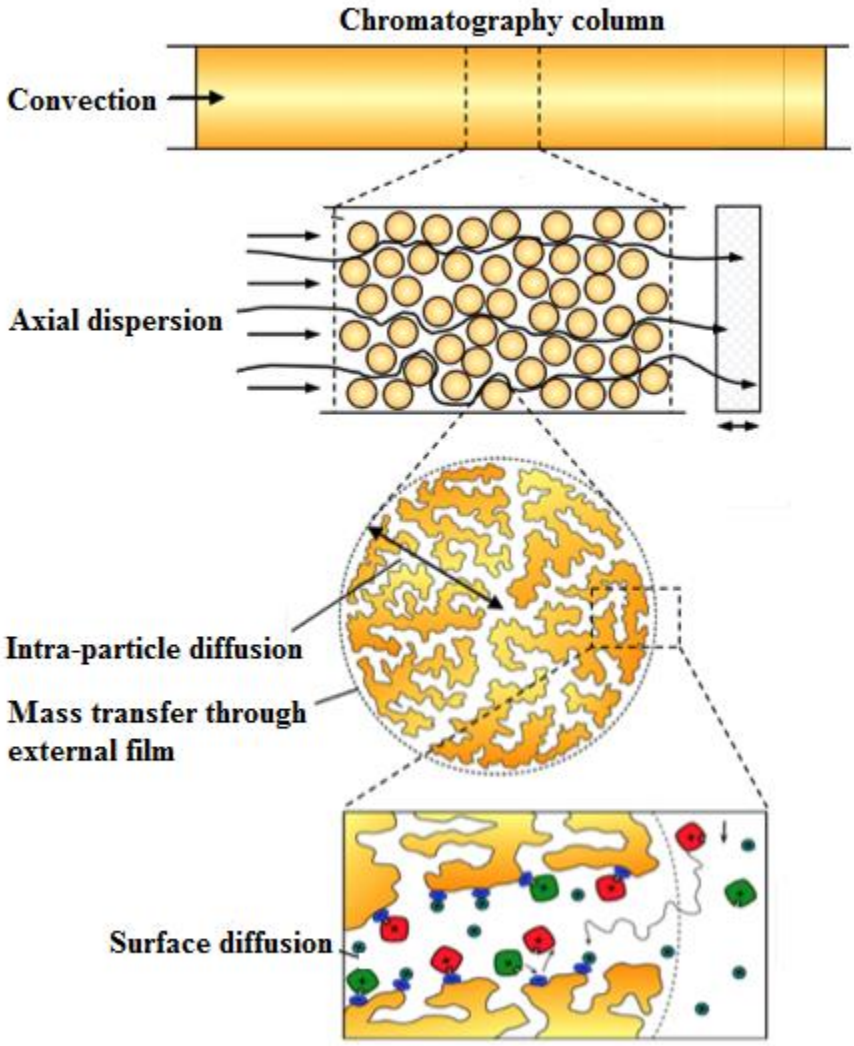

Figure 2-2 Mass transfer in chromatography column

Some basic assumptions made to formulate the mass conservation equations of the general rate model consist of the incompressibility of the mobile phase, concentration independence of the mass transfer parameters, constant mobile phase viscosity, and constant molar volumes between species in the mobile and stationary phase. These assumptions have been extensively reviewed by Guiochon et al. [3]. The column is assumed to be evenly packed with spherical, uniformly porous, uniform particles in size. As a result, the radial column dimension is usually ignored [3]. Packed beds are practically heterogeneous [4,5], and particle size varies. However, it is commonly stated that, radial or axial heterogeneity in concentration and velocity averages out when the

ratio of particle diameter to column is small (typically less than 0.03), as is valid for most analytical columns [3].

Another point of issue for bio-separations in particular, is presuming a uniformly porous resin structure. Chromatography resin particles are known to display a range of pore sizes with normal-like distribution [6,7]. In fact, this is not an issue in case species are considerably smaller than the smallest pore size, as all species have equal access to resin binding sites. However, as the size of biomolecules often falls within the pore size distribution (i.e. biomolecule and particle pore sizes are comparable), pore accessibility turns out to be dependent on component size. This can affect mass transfer performance, as there is more competition for binding sites in the larger pores which are accessible to all components, than in smaller pores where few species can enter. Moreover, as adsorbed proteins occupy a finite space, the adsorption process itself can modify the effective pore radius as bound proteins partially block pores, hindering intra-particle diffusion [8,9]. This is particularly accurate where tentacles are used inside resin pores to increase resin capacity [10]. A change of tentacle orientation (which can occur when the mobile phase composition changes) can result in big changes to pore accessibility of components. If the effect of variations to particle structure is large, then the more detailed distributed pore model can be used in order to account for the pore size distribution of the stationary phase, and pore shrinkage due to protein adsorption [10]. As an alternative, diffusion parameters can be calculated as a function of stationary phase concentration [9].

In spite of the issues cited regarding model assumptions, the predictive capability of the general rate model is well established. Earlier studies applying the general rate model focused on increasing theoretical understanding of underlying phenomena such as displacement effects [11], limited protein diffusion [8], scale up [12], intra-particle diffusion [13], and hydrophobic interaction mechanisms [14]. Next, the general rate model was used to process development tasks such as process design [15], optimization [16–18], design space analysis [19] and scale up [20], even though most often using widely known proteins. In the latest years, the general rate model has been successfully used to simulate more complicated chromatographic processes that are often nonlinear and include streams with multiple components [21–25].

2.3.2 Adsorption

Adsorption of proteins refers to the reversible adhesion of molecules from a mobile liquid phase onto the surface of stationary solid phase with which they are in contact. The adsorption phenomenon can be addressed with the fundamental thermodynamic interactions and kinetics rate that the adsorption process occurs [26]. Factors that contribute in protein adsorption can be distinguished as conformational entropy of proteins, hydrophobic and electrostatic interactions [27]. These general considerations determine the equilibrium distribution of the mixture components between two adjacent phases.

Adsorption of proteins and other macromolecules is very complicated that makes the application of theoretical models still not amenable. Factors complicating protein adsorption, as described in the review by Rabe et al. [28] include following:

1. Protein molecule contains charged and hydrophobic groups heterogeneously distributed throughout the entire protein structure; some of these groups are on the external surface while others are partially or completely located within the molecule core. Thus, on one hand, Proteins are typically asymmetric and so representing them as a sphere is unrealistic. On the other hand, Proteins often simultaneously interact with multiple binding sites, using the cooperative contributions from multiple groups. Cooperative effects from proteins that are already adsorbed means that proteins are sometimes more likely to adsorb if there are pre-adsorbed proteins.

2. Proteins often unfold and as a result the structure of bound proteins may be different from that of proteins in mobile phase.

3. Due to broad ranges of ionic strength often encountered, electrostatic force fields can vary causing the local conditions to vary.

4. In some instances, proteins have tendency to self-associate (aggregate), it can occur both in solution and the stationary phase, thus attractive or repulsive interactions between adsorbed protein molecules are important.

5. Proteins often denature in extreme conditions or due to other components, e.g. proteases.

6. Due to structural re-arrangements, overshooting effect can be observed where the adsorption kinetics passes a local or global maximum before the saturation is reached.

As result of these complications, protein adsorption equilibria are generally described by empirical or semi-empirical approaches [3]. The relationship between equilibrium concentration of adsorbed protein in the stationary phase and free protein in the mobile phase is expressed by an adsorption isotherm. There are several different adsorption isotherm models to discuss the equilibrium characteristics of the adsorption process, which can be grouped into equilibrium models and kinetic models.

Equilibrium isotherm models

Equilibrium models represent a state in which the rate of adsorption of molecules onto the surface is counter-balanced by the rate of desorption of molecules back into the mobile phase. Therefore, the isotherm is formulated on the basis of a dynamic equilibrium between the stationary phase and the mobile phase.

In the simplest equilibrium model of chromatography, it is assumed that the chromatography resin is under challenged and as a result there are a great number of free binding sites available [3]. The assumption leads to the linear relation between the concentration of the protein on the surface and in the mobile phase. The linearity of the adsorption isotherm is, however, limited to small sample concentrations. This is not likely the case in industrial bio-separations, where columns are loaded up to full capacity as possible with the aim of maximizing productivity [29]. Thus, the ideal model has only been used in a few studies, where its simplicity was synergetic in shortening time to solve optimization problems [30,31].

In practice, as the resin becomes gradually saturated, it becomes more difficult for proteins to find free binding sites. After a certain amount of protein has been loaded onto the resin, all sites will be occupied and no more protein can bind. Many different isotherm models have been developed to represent this phenomena, such as Langmuir,

steric mass action and quadratic isotherms [32]. Each isotherm makes a range of assumptions and often aims to address specific adsorption phenomena.

A model commonly used to describe protein adsorption equilibrium is Langmuir isotherm, and assumes the extent of equal probable binding sites coverage limited to one molecular layer adsorption, with no lateral interactions between adsorbed molecules, steric hindrance, or migration of adsorbed molecules on the adsorption surface [3]. In spite of the limits of these assumptions, the Langmuir isotherm still serves as a kind of starting point for the development of theoretical descriptions of protein adsorption conditions. Single component Langmuir isotherms are typically employed where simulation of a model chromatographic system is used to derive understanding of a particular feature or aspect of chromatography. For instance, Gu et al., [11] used a single component Langmuir to study optimization of desorption chromatography, and Sun and Yang [33] applied a single component Langmuir to investigate the difference between mass transport models.

The influence of mobile phase modulators on protein adsorption, such as ionic strength or pH, is often counted in adsorption models if the model is envisaged for exploring potential operating conditions during process development. The Langmuir isotherm with mobile phase modulators has been used in numerous studies for process design and optimization, examining a variety of different proteins and mechanisms of chromatographic retention (affinity, ion exchange, hydrophobic interaction and reversed phase chromatography) [15,16,20,31,34,35].

Adsorption models can also be extended to deal with more than one component, including competition between components. Multicomponent adsorption isotherms are generally less rigorous than single component isotherms, as multicomponent adsorption is not well understood [3]. For example, the multicomponent Langmuir isotherm is only thermodynamically correct when all components have identical saturation capacities, which is rarely the case for the extremely heterogeneous, multicomponent feed streams of industrial processes. Despite this limitation, the multicomponent competitive Langmuir isotherm is useful for systems with similar components, and has been used for

hydrophobic interaction chromatography of alpha chymotrypsin and alpha amylase [18], IgG capture with cation exchange chromatography [36], and the separation of monoclonal antibody variants with ion exchange chromatography [22].

The steric mass action (SMA) isotherm describes protein-salt equilibria in ion-exchange systems as a the stoichiometric exchange of mobile phase proteins and bound counter-ion [37,38], and steric shielding of binding sites [39,40]. The SMA formalism requires electroneutrality of the stationary phase to describe competitive binding by mass-action equilibrium. The multipoint binding nature of protein molecule is represented by model parameters namely characteristic charge, and the steric shielding of binding sites by adsorbed solutes by a steric factor for each component [40]. The model has been capable of successfully describing linear and nonlinear adsorption of proteins over a range of salt concentrations, containing alpha chymotrypsinogen A, ribonuclease A (RNase A), nyomysin sulphate on a cation exchange system [41], BSA on a strong anion exchanger [13], IgG, BSA and myoglobin on an anion exchanger [42], and at a recent time Lysozyme, ribonuclease A and cytochrome C on a cation exchanger [23–25].

Kinetic isotherm models

Kinetic isotherm models considers the mechanism behind protein adsorption events through rate expression which a protein is transported from the mobile phase into the adsorbent and ultimately adsorbed [43].

The kinetic Langmuir isotherm is the most commonly used kinetic model, and has been used for modeling affinity [44], ion exchange [20,45], and reversed phase chromatography processes [46]. A second order kinetic binding expression was applied to model IgG elution during affinity chromatography by Sandoval et al. [47]. To and Lenhoff [14] used a kinetic expression including a term describing conformational change on the resin surface during HIC.

Kinetic isotherms account for various factors such as physical and chemical properties of adsorbents as well as mass transfer processes; Susanto et al. [45] and Degerman et al. [46] both took this approach when using the equilibrium dispersive mass transport model.

Although these chromatography models are useful for predicting adsorption capacities and also interpreting into mass transfer relationship, the kinetic parameters do not have physical meaning [48].

2.4 Model applications

The use of a general rate model establishes an efficient study of interfering effects in LC and thereby promotes a better understanding of the primary sources of the interfering effects. The model also provides a useful tool for studying various aspects of chromatography process development, including process optimization, robustness and sensitivity analysis, and scale up. The following section reviews the most recent general developments in these fields.

2.4.1 Process optimization

There are useful examples of mathematical optimization of the chromatographic purification of therapeutic proteins using mechanistic models of chromatography, where mathematical optimization refers to minimizing or maximizing an objective function by varying decision variables subject to constraints [17,24,31]. Common factors to study in the objective function include the yield and productivity of the chromatographic separation, and the purity of the product. When considering multiple objectives, cost functions have been used which define the relative importance of each factor when optimizing a particular process [18]. Alternatively, multiple optimizations can be completed where the objective function is changed each time so that each factor is weighted in a different way. The resulting optimal values can then be used to generate a Pareto front useful for considering the trade-off between the different factors [19,49].

The yield, productivity and purity are usually included as a constraint if not included in the objective function. A wide range of decision variables are usually available in chromatographic separations. Column length, flow rate, volumes (wash, load and elution), buffer composition (e.g. ionic strength, pH) have all been considered. Osberghaus et al. [23] compared mechanistic and empirical model based approaches for the optimization of a three component separation, and concluded that for processes with

low robustness, the performance of a DoE approach was significantly inferior to the performance of a mechanistic model, resulting in inaccurate predictions and a sub optimal process. However, discussion of the advantages and disadvantages revealed useful synergies between the two approaches, which suggested process optimization should start with the traditional DoE approach in order to easily and quickly reveal important factors which will provide a basic understanding of the chromatography. Then the outcomes from this study can be used to direct the development of a mechanistic model, using data from DoE experiments for model calibration and validation. The mechanistic model can then be used for detailed process optimization, as well as other development tasks which are discussed in this section.

Despite the examples seen in the literature, mathematical optimization of the sort described above does not see regular use in industry due to the large and frequent inconsistency of inlet material, uncertainties in controlled process parameters, and frequency of non-ideal phenomena such as resin fouling which stimulates an attention on identifying the most robust operating conditions, rather than optimizing for particular scenarios.

2.4.2 Robustness and sensitivity analysis

Product development and manufacture in a chromatographic step are in alignment with robust control of process performance assuring that the process can handle bioprocess variability [50]. Maximizing process robustness and minimizing sensitivity to disturbances are main aspects of this task. A number of model based studies have been published that highlight these tasks [19,42,51]

Jakobsson et al. [42] conducted a full factorial study of six factors on the purity and yield of the ion exchange purification of BSA, myoglobin and IgG. Using the results the relative importance and effect of each process parameter was determined. Degerman et al. [34] used a model based approach to determine which process parameters were critical to control in order to assure process robustness for three case studies: (i) purification of IgG from BSA with hydrophobic interaction chromatography, (ii) purification of insulin from desamido insulin with reversed phase chromatography, and (iii) purification of IgG

from BSA and myoglobin with hydrophobic interaction chromatography. Parameters were classified corresponding to significance, and risk of batch failure was determined for each case study accounting for uncertainty in a selection of process parameters. Gétaz et al. [51] varied both process parameters (flowrate, loading, column length, feed concentrations, and buffer compositions) and model parameters (mass transfer coefficient and saturation capacity) around the standard operating conditions that had been found by process optimization. The results were used to determine critical process parameters depending on the position of operation within the design space, and to determine correlated effects. All studies described found that process disturbances significantly decrease design space size, and demonstrate the significance of process robustness in order to ensure product quality.

2.4.3 Scale up

Currently, scale-up strategies are largely based on "rule of thumb" nature with the guide of some general scale-up rules that are not essentially accurate. These rules for the most part are empirical or semi-empirical relationships about particle size, flow rate, column length, and resolution. Some of these rules are discussed Snyder and Kirkland [52], Ladisch [53], and others [3,54,55]. The correlations are more of a "trial-and-error and experience" nature when they are used for scale-up.

As an alternative of practicing these scale-up guidelines, a rate model can be applied to simulate chromatograms of a larger column a priori, i.e., beforehand it is constructed or purchased. The model uses only few experimental data from a small column with the same resin as a large column. Gerontas et al. [20] presented a model-integrated approach to scale-up using scale down columns with reduced bed height. The mechanistic model to predict process operation in columns at full bed height, as a result achieved considerable savings in terms of time and material. In spite of the simplified feed composition in comparison to complex bioprocess materials (BSA and lactoferrin were selected due to the difficulty in acquiring the very large quantities of protein needed to load the manufacturing scale columns), the study proved how a quite simple application of a

mechanistic model can be of tremendous value for industry where time and material restrictions are of great importance.

References

[1] O. College, Anatomy & Physiology, in: Anat. Physiol., OpenStax College, n.d. http://cnx.org/contents/14fb4ad7-39a1-4eee-ab6e-3ef2482e3e22.

[2] J. Curling, U. Gottschalk, Process chromatography: Five decades of innovation, BioPharm Int. 20 (2007) 70–94.

[3] G. Guiochon, A. Felinger, D.G. Shirazi, A.M. Katti, Fundamentals of preparative and nonlinear chromatography, Academic Press, San Diego, USA, 2006.

[4] T. Farkas, M.J. Sepaniak, G. Guiochon, Column radial homogeneity in high-performance liquid chromatography, J. Chromatogr. A. 740 (1996) 169–181. doi:10.1016/0021-9673(96)00107-0.

[5] R.A. Shalliker, B. Scott Broyles, G. Guiochon, Axial and radial diffusion coefficients in a liquid chromatography column and bed heterogeneity, J. Chromatogr. A. 994 (2003) 1–12. doi:10.1016/S0021-9673(03)00311-X.

[6] P. DePhillips, A.M. Lenhoff, Pore size distributions of cation-exchange adsorbents determined by inverse size-exclusion chromatography, J. Chromatogr. A. 883 (2000) 39–54. doi:10.1016/S0021-9673(00)00420-9.

[7] Y. Yao, A.M. Lenhoff, Pore size distributions of ion exchangers and relation to protein binding capacity, J. Chromatogr. A. 1126 (2006) 107–119. doi:10.1016/j.chroma.2006.06.057.

[8] P.M. Boyer, J.T. Hsu, Experimental studies of restricted protein diffusion in an agarose matrix, AIChE J. 38 (1992) 259–272. doi:10.1002/aic.690380212.

[9] A. Susanto, T. Herrmann, E. von Lieres, J. Hubbuch, Investigation of pore diffusion hindrance of monoclonal antibody in hydrophobic interaction chromatography using confocal laser scanning microscopy, J. Chromatogr. A. 1149 (2007) 178–188. doi:10.1016/j.chroma.2007.03.002.

[10] H. Thomas, B. Coquebert de Neuville, G. Storti, M. Morbidelli, M. Joehnck, M. Schulte, Role of tentacles and protein loading on pore accessibility and mass transfer in cation exchange materials for proteins, J. Chromatogr. A. 1285 (2013) 48–56. doi:10.1016/j.chroma.2013.01.104.

[11] T. Gu, G.T. Tsao, G.-J. Tsai, M.R. Ladisch, Displacement effect in multicomponent chromatography, AIChE J. 36 (1990) 1156–1162. doi:10.1002/aic.690360805.

[12] Z. Li, Y. Gu, T. Gu, Mathematical modeling and scale-up of size-exclusion chromatography, Biochem. Eng. J. 2 (1998) 145–155. doi:10.1016/S1369-703X(98)00027-8.

[13] A. Susanto, K. Wekenborg, J. Hubbuch, H. Schmidt-Traub, Developing a chromatographic column model for bovine serum albumin on strong anion-exchanger Source30Q using data from confocal laser scanning microscopy, J. Chromatogr. A. 1137 (2006) 63–75. doi:10.1016/j.chroma.2006.10.004.

[14] B.C.S. To, A.M. Lenhoff, Hydrophobic interaction chromatography of proteins, J. Chromatogr. A. 1205 (2008) 46–59. doi:10.1016/j.chroma.2008.07.079.

[15] L. Melter, A. Butté, M. Morbidelli, Preparative weak cation-exchange chromatography of monoclonal antibody variants, J. Chromatogr. A. 1200 (2008) 156–165. doi:10.1016/j.chroma.2008.05.061.

[16] D. Karlsson, N. Jakobsson, A. Axelsson, B. Nilsson, Model-based optimization of a preparative ion-exchange step for antibody purification, J. Chromatogr. A. 1055 (2004) 29–39. doi:10.1016/j.chroma.2004.08.151.

[17] M. Degerman, N. Jakobsson, B. Nilsson, Constrained optimization of a preparative ion-exchange step for antibody purification, J. Chromatogr. A. 1113 (2006) 92–100. doi:10.1016/j.chroma.2006.01.121.

[18] M.E. Lienqueo, C. Shene, J. Asenjo, Optimization of hydrophobic interaction

chromatography using a mathematical model of elution curves of a protein mixture, J. Mol. Recognit. 22 (2009) 110–120. doi:10.1002/jmr.927.

[19] M. Degerman, K. Westerberg, B. Nilsson, A Model-Based Approach to Determine the Design Space of Preparative Chromatography, Chem. Eng. Technol. 32 (2009) 1195–1202. doi:10.1002/ceat.200900102.

[20] S. Gerontas, M. Asplund, R. Hjorth, D.G. Bracewell, Integration of scale-down experimentation and general rate modelling to predict manufacturing scale chromatographic separations, J. Chromatogr. A. 1217 (2010) 6917–6926. doi:10.1016/j.chroma.2010.08.063.

[21] D. Nagrath, F. Xia, S.M. Cramer, Characterization and modeling of nonlinear hydrophobic interaction chromatographic systems, J. Chromatogr. A. 1218 (2011) 1219–1226. doi:10.1016/j.chroma.2010.12.111.

[22] B. Guélat, G. Ströhlein, M. Lattuada, L. Delegrange, P. Valax, M. Morbidelli, Simulation model for overloaded monoclonal antibody variants separations in ion-exchange chromatography, J. Chromatogr. A. 1253 (2012) 32–43. doi:10.1016/j.chroma.2012.06.081.

[23] A. Osberghaus, K. Drechsel, S. Hansen, S.K. Hepbildikler, S. Nath, M. Haindl, et al., Model-integrated process development demonstrated on the optimization of a robotic cation exchange step, Chem. Eng. Sci. 76 (2012) 129–139. doi:10.1016/j.ces.2012.04.004.

[24] A. Osberghaus, S. Hepbildikler, S. Nath, M. Haindl, E. von Lieres, J. Hubbuch, Optimizing a chromatographic three component separation: A comparison of mechanistic and empiric modeling approaches, J. Chromatogr. A. 1237 (2012) 86–95. doi:10.1016/j.chroma.2012.03.029.

[25] A. Osberghaus, S. Hepbildikler, S. Nath, M. Haindl, E. von Lieres, J. Hubbuch, Determination of parameters for the steric mass action model—A comparison between two approaches, J. Chromatogr. A. 1233 (2012) 54–65.

doi:10.1016/j.chroma.2012.02.004.

[26] J.M. Mollerup, A Review of the Thermodynamics of Protein Association to Ligands, Protein Adsorption, and Adsorption Isotherms, Chem. Eng. Technol. 31 (2008) 864–874. doi:10.1002/ceat.200800082.

[27] W. Norde, Driving forces for protein adsorption at solid surfaces, Macromol. Symp. 103 (1996) 5–18. doi:10.1002/masy.19961030104.

[28] M. Rabe, D. Verdes, S. Seeger, Understanding protein adsorption phenomena at solid surfaces, Adv. Colloid Interface Sci. 162 (2011) 87–106. doi:10.1016/j.cis.2010.12.007.

[29] N. Tugcu, D.J. Roush, K.E. Göklen, Maximizing productivity of chromatography steps for purification of monoclonal antibodies, Biotechnol. Bioeng. 99 (2008) 599–613. doi:10.1002/bit.21604.

[30] S. Chan, N. Titchener-Hooker, E. Sorensen, Optimal Economic Design and Operation of Single- and Multi-column Chromatographic Processes, Biotechnol. Prog. 24 (2008) 389–401. doi:10.1021/bp070270m.

[31] C.K.S. Ng, H. Osuna-Sanchez, E. Valéry, E. Sørensen, D.G. Bracewell, Design of high productivity antibody capture by protein A chromatography using an integrated experimental and modeling approach, J. Chromatogr. B. 899 (2012) 116–126. doi:10.1016/j.jchromb.2012.05.010.

[32] K.Y. Foo, B.H. Hameed, Insights into the modeling of adsorption isotherm systems, Chem. Eng. J. 156 (2010) 2–10. doi:10.1016/j.cej.2009.09.013.

[33] Y. SUN, K. YANG, Analysis of mass transport models based on Maxwell–Stefan theory and Fick's law for protein uptake to porous anion exchanger, Sep. Purif. Technol. 60 (2008) 180–189. doi:10.1016/j.seppur.2007.08.004.

[34] M. Degerman, K. Westerberg, B. Nilsson, Determining Critical Process Parameters and Process Robustness in Preparative Chromatography - A Model-

Based Approach, Chem. Eng. Technol. 32 (2009) 903–911. doi:10.1002/ceat.200900019.

[35] N. Borg, K. Westerberg, N. Andersson, E. von Lieres, B. Nilsson, Effects of uncertainties in experimental conditions on the estimation of adsorption model parameters in preparative chromatography, Comput. Chem. Eng. 55 (2013) 148–157. doi:10.1016/j.compchemeng.2013.04.013.

[36] T. Müller-Späth, G. Ströhlein, L. Aumann, H. Kornmann, P. Valax, L. Delegrange, et al., Model simulation and experimental verification of a cation-exchange IgG capture step in batch and continuous chromatography, J. Chromatogr. A. 1218 (2011) 5195–5204. doi:10.1016/j.chroma.2011.05.103.

[37] M.A. Rounds, F.E. Regnier, Evaluation of a retention model for high-performance ion-exchange chromatography using two different displacing salts, J. Chromatogr. A. 283 (1984) 37–45. doi:10.1016/S0021-9673(00)96240-X.

[38] F.E. Regnier, I. Mazsaroff, A Theoretical Examination of Adsorption Processes in Preparative Liquid Chromatography of Proteins, Biotechnol. Prog. 3 (1987) 22–26. doi:10.1002/btpr.5420030105.

[39] A. Velayudhan, C. Horváth, Preparative chromatography of proteins, J. Chromatogr. A. 443 (1988) 13–29. doi:10.1016/S0021-9673(00)94779-4.

[40] C. a Brooks, S.M. Cramer, Steric mass-action ion exchange: Displacement profiles and induced salt gradients, AIChE J. 38 (1992) 1969–1978.

[41] V. NATARAJAN, S. CRAMER, A Methodology for the Characterization of Ion-Exchange Resins, Sep. Sci. Technol. 35 (2000) 1719–1742. doi:10.1081/SS-100102490.

[42] N. Jakobsson, D. Karlsson, J.P. Axelsson, G. Zacchi, B. Nilsson, Using computer simulation to assist in the robustness analysis of an ion-exchange chromatography step, J. Chromatogr. A. 1063 (2005) 99–109. doi:10.1016/j.chroma.2004.11.067.

[43] T. Gu, Mathematical Modeling and Scale-Up of Liquid Chromatography, Springer International Publishing, Cham, 2015. doi:10.1007/978-3-319-16145-7.

[44] H. Bak, O.R.T. Thomas, J. Abildskov, Lumped parameter model for prediction of initial breakthrough profiles for the chromatographic capture of antibodies from a complex feedstock, J. Chromatogr. B. 848 (2007) 131–141. doi:10.1016/j.jchromb.2006.07.020.

[45] A. Susanto, E. Knieps-Grünhagen, E. von Lieres, J. Hubbuch, High Throughput Screening for the Design and Optimization of Chromatographic Processes: Assessment of Model Parameter Determination from High Throughput Compatible Data, Chem. Eng. Technol. 31 (2008) 1846–1855. doi:10.1002/ceat.200800457.

[46] M. Degerman, N. Jakobsson, B. Nilsson, Modeling and optimization of preparative reversed-phase liquid chromatography for insulin purification, J. Chromatogr. A. 1162 (2007) 41–49. doi:10.1016/j.chroma.2007.02.062.

[47] G. Sandoval, B.A. Andrews, J.A. Asenjo, Elution relationships to model affinity chromatography using a general rate model, J. Mol. Recognit. 25 (2012) 571–579. doi:10.1002/jmr.2223.

[48] K. Kaczmarski, D. Antos, H. Sajonz, P. Sajonz, G. Guiochon, Comparative modeling of breakthrough curves of bovine serum albumin in anion – exchange chromatography, J. Chromatogr. A. 925 (2001) 1–17.

[49] D. Gétaz, S.B. Hariharan, A. Butté, M. Morbidelli, Modeling of ion-pairing effect in peptide reversed-phase chromatography, J. Chromatogr. A. 1249 (2012) 92–102. doi:10.1016/j.chroma.2012.06.005.

[50] A.S. Rathore, Roadmap for implementation of quality by design (QbD) for biotechnology products, Trends Biotechnol. 27 (2009) 546–553. doi:10.1016/j.tibtech.2009.06.006.

[51] D. Gétaz, A. Butté, M. Morbidelli, Model-based design space determination of

peptide chromatographic purification processes, J. Chromatogr. A. 1284 (2013) 80–87. doi:10.1016/j.chroma.2013.01.117.

[52] L. Snyder, J. Kirkland, J. Glajch, Practical HPLC method development, Wiley, New York, 2012.

[53] M. Ladisch, Bioseparations engineering: principles, practice, and economics, Wiley, New York, 2001.

[54] D. Ruthven, Principles of adsorption and adsorption processes, Wiley, New York, 1984.

[55] A. Rathore, A. Velayudhan, Scale-up and optimization in preparative chromatography: principles and biopharmaceutical applications, CRC, Boca Raton, FL, 2002.

Chapter 3

Determination of adsorption isotherm parameters for minor whey proteins by gradient elution preparative liquid chromatography

Abstract

Ion-Exchange Chromatography (IEC) techniques have been extensively investigated in protein purification processes, due to the more selective and milder separation steps. To date, existing studies of minor whey proteins fractionation in IEC have primarily been conducted as batch uptake studies, which require more experimental search space, time and materials. In this work, the selected resin's (SP Sepharose FF) equilibrium and dynamic binding capacity were first investigated. Next, adsorption of the pure binary mixture of lactoperoxidase and lactoferrin was studied to calibrate steric mass action (SMA) model using a simplified approach with data from single column experiments. The calibrated model was then verified by performing factorial-design based experiments for various process operating conditions assessing process performance on a larger bed height column. The model predicted results demonstrated a realistic agreement with the experiments providing reproducible column elution profile and reduced experimental work. Finally, whey protein isolate was used to evaluate model parameters in real conditions. Results obtained herein are suitable for future large scale applications.

Keywords

Milk protein separation; Whey proteins; Mathematical modeling; Downstream process development; Steric mass action; Inverse method; Adsorption isotherm

3.1 Introduction

Lactoperoxdiase and lactoferrin are two minor whey proteins having unique properties for nutritional, biological, and food ingredient applications [1]. Hence, they exemplify the potential for commercial exploitation of minor, bioactive milk protein products [2], [3] and [4]. Extraction of proteins from dairy fluids by techniques such as chromatography[5], [6] and [7], precipitation and membrane-based technologies, mainly ultrafiltration and diafiltration [8], [9], [10], [11] and [12] has been extensively studied over the last few decades. However, precipitation and membrane techniques may result in undesirable consequences on changes in native structure affecting functional properties of

the whey proteins. Therefore, there has been an increasing interest in liquid chromatographic processes because of many advantages reported for this technology, such as the very rapid rate of association between target proteins and functional groups; short processing times; ease of scale-up and operation without the need for lengthy column packing procedures; no heat-treatments, extremes of pH, or chemical pre-treatment that could compromise protein structure and functionality among others [13]. Over the last few decades ion-exchange chromatographic techniques have been used to purify lactoperoxidase and lactoferrin [2], [14], [15] and [16]. For example, Fee and Chand [17] have extensively investigated the use of cation exchange chromatography for the capture of lactoperoxidase and lactoferrin from raw milk while Noppe et al. [18] were able to purify lactoferrin from skim milk using macro-porous monolithic column.

In spite of the promise of ion-exchange chromatography for effective separation and purification of proteins in many analytical, preparative and process applications, purification of high-value proteins in bio-pharmaceutical industry is still a challenging task as the existing separation methods are not applicable for large-scale operation due to inadequate understanding of the mechanistic features affecting protein adsorption. This represents an obstacle to the development of design of large-scale chromatographic separation processes for applications estimated to average above $200 million per pharmaceutical product other than based on an empirical basis [18]. The approaches for the determination of isotherm parameters solely based on batch experiments require extensive experimental work. Consequently, downstream process development incurs large overhead costs. Besides, the batch experiments do not essentially produce parameters that could be used directly to obtain precise predictions of industrial process development. Hence there is a great interest in developing more efficient and straightforward methods to recover pure protein fractions. A more cost-effective process can be accomplished through further development of knowledge of its fundamentals. A quantitative understanding of protein adsorption would, therefore, overcome the obstacle to the development of large-scale chromatographic separation processes other than based on an empirical basis [19]. It would enable to simulate the process efficiently as a tool for modern process development strategies. By this approach, the need for labor-intensive

experiments is reduced, and hence, not only shortens the time for development from laboratory to production scale but also reduces the overall cost for development.

The aim of this study is to develop a model-based method to determine steric mass action (SMA) adsorption isotherm parameters of two minor whey proteins, lactoperoxidase and lactoferrin. The isotherm parameters were determined for lactoperoxidase and lactoferrin at pH 6.7 on a 1 mL column pre-packed with the strong cation-exchange adsorbent, SP Sepharose FF. A Fast Protein Liquid Chromatography (FPLC) system was coupled to the experimental system for analysis. Subsequently, the quality of the results was evaluated on a pre-packed 4.7 mL column. Moreover, this study also incorporated the prediction of the model with respect to the target protein recovery from whey protein isolate.

3.2 Theory

3.2.1 Transport-dispersive model

A mathematical model involving convective and dispersive transport, mass transfer resistances and equations describing sorption in ion-exchange chromatography is described below. Details on the equations and the execution of their solution can be found elsewhere [20], [21] and [22]. On column level, concentration change for the i^{th} component with respect to the time and position is described by:

$$\frac{\partial c_i}{\partial t} = -u_{\text{int}} \frac{\partial c_i}{\partial x} + D_{ax} \frac{\partial^2 c_i}{\partial x^2} - \frac{1-\varepsilon_c}{\varepsilon_c} \cdot \frac{3}{r_p} k_{eff,i} \left[c_i - c_{p,i} \right] \tag{3-1}$$

The first term on the right hand side represents the convective transport through the column while the second and third term represents respectively the dispersive transport and the mass transfer to the particle surface. The symbol u_{int} indicates the interstitial velocity, ε_c the column voidage, r_p the particle radius, D_{ax} the axial dispersion representing combined effect of dispersion and diffusive processes, and $k_{eff,}i$ epitomize combined effect of both the internal and external mass transfer resistances in one lumped film diffusion coefficient. Likewise, on particle level, concentration change for the*i*th component is expressed by:

$$\frac{\partial c_{p,i}}{\partial t} = \frac{3}{\varepsilon_p r_p} k_{eff,i}[c_i - c_{p,i}] - \frac{1-\varepsilon_p}{\varepsilon_p}\frac{\partial q_i}{\partial t} \tag{3-2}$$

where q_i denotes the concentration of component *i* within the particle and ε_p the particle voidage. The first term on right hand side describes adsorption and desorption processes on particle level, i.e. the interaction between mobile and particle bound phase. The expression $\partial q_i/\partial t$ employs an isotherm equation described in the next section.

The boundary conditions used are of Danckwert's type conditions [23]:

$$\frac{\partial c_i}{\partial x}(0,t) = \frac{u_{\text{int}}}{D_{ax}}\left(c_i(0,t) - c_{inj}(t)\right) \tag{3-3}$$

$$\frac{\partial c_i}{\partial x}(L,t) = 0 \tag{3-4}$$

Method of lines was used to convert the partial differential equations (PDEs) into a system of ordinary differential equations (ODEs). The resultant ODEs along with Danckwert's boundary conditions are then solved in Matlab R2014a (The Mathworks, Natick, ME, USA).

3.2.2 Steric mass action isotherm

The steric mass action (SMA) isotherm [24] is a frequently used isotherm in IEC when one or more macromolecules with steric hindrance are involved as the case of proteins studied here. SMA isotherm is capable in replicating the influence of counter-ions on the retention behavior of protein species through the use of the proteins' characteristic charges, νi and the average number of adsorbent binding sites of the proteins based on the assumption of a monovalent salt counter-ion. SMA isotherm also considers column properties such as total ionic capacity of adsorbent, Λ, steric effect of the proteins, σ_i, as well as the average number of shielded biding sites on adsorbent surface. The dynamic SMA isotherm is given in Eq. (3-5):

$$\frac{\partial q_i}{\partial t} = k_{ads,i}\left[\Lambda - \sum_{j=1}^{k}\left(\upsilon_i - \sigma_i\right)q_i\right]^{\upsilon_i} c_i - k_{des,i}c_{salt}^{\upsilon_i}q_i \tag{3-5}$$

where q_i and c_i represent the concentration of the protein *i* in adsorbed and in solution, respectively, c_{salt} is the salt concentration of the solution, and $k_{ads,i}$ and $k_{des,i}$ are respectively the adsorption and desorption coefficients. Assuming attainment of rapid equilibrium $(\partial q_i/\partial t=0)$, Eq. (3-5) rearranges to:

$$k_{i,eq} = \left(\frac{q_i}{c_i}\right)\left(\frac{c_{salt}}{\Lambda - \sum_{i=2}^{n}(\nu_i + \sigma_i)q_i}\right)^{\nu_i} \tag{3-6}$$

where the parameter $ki_{,eq}$ is the ratio of adsorption ($k_{ads,i}$) and desorption coefficient ($k_{des,i}$).

3.2.3 Numerical solution based on inverse method

A common practice in calculating the SMA parameters are model-based inverse method. This method is often applied to determine the adsorption parameters by the best fit between experimental data and model prediction [25], [26] and [27]. An error function, $F(p)$, is defined as a sum of least square error between the experimentally measured and estimated concentration profiles from the mathematical model. The best-fit (tuned) values of the isotherm parameters are obtained by minimization of the error function:

$$F(p) = \min_{p}\sum_{i=1}^{k}\left[c_{i,ex} - c_{i,m}\right]^2 \tag{3-7}$$

The minimization of Eq. (3-7) was executed with the MatLab function *lsqnonlin*.

3.3 Materials and experimental methods

3.3.1 Materials

Commercial whey protein isolate (WPI) was acquired from PROTEINCO (Quebec, Canada). Protein standards, lactoferrin from bovine milk, approximately 95% pure (by SDS Electrophoresis), and lactoperoxidase from bovine milk, ≥90% pure were used. Reagents used for buffer preparation mono and dibasic sodium phosphate, sodium

chloride, hydrochloric acid, 95%; sodium hydroxide were all of analytical grade. All chemicals were purchased from Sigma–Aldrich (Oakville, Canada) unless otherwise specified.

3.3.2 Apparatus and software

The columns used in ion-exchange chromatography were strong cation exchanger, pre-packed HiTrap™ SP Sepharose FF 1 mL column (2.5 cm length, 0.7 cm ID) and HiScreen™ SP Sepharose FF 4.7 mL column (10.0 cm length, 0.77 cm ID) from GE Healthcare (Mississauga, Canada). The experiments were carried out on an ÄKTA purifier 100 fast protein liquid chromatography (FPLC) system equipped with Pump P-903, UV (2.0 mm path length), conductivity and pH monitor UPC-900, an auto sampler A-900 and a fraction collector Frac-950 with a system flow rate of 1 mL/min. Primary analyses of the chromatograms were performed and monitored with the control software Unicorn 5.31. All further data analysis as well as the solution of model equations and all applications connected to the model was performed with MatLab R2014a (The Mathworks, Natick, ME, USA).

3.3.3 Methods

3.3.3.1 Dead volume of the chromatographic system and void volumes of IEC columns

The ÄKTA purifier system and the two columns were characterized with 20.0 µL tracer injections according to a volumetric flow of 1.0 and 2.3 mL/min for HiTrap and HiScreen SP FF columns respectively. 1.0% (v/v) acetone (Caledon Laboratories, Canada) injections were used to determine the system dead volume. 20.0 µl injections of a filtrated 10.0 mg/mL dextran and 1.0 M NaCl solution (Sigma, St. Louis, MO, USA) onto the two columns were used to determine the voidage. Furthermore, the dextran signals at 215 nm were used to calculate the axial dispersion coefficient using UNICORN. Acid–base titration was carried out to determine the total ionic capacity, Λ, of the column. Initially, the column was washed off with a 0.5 M HCl solution until a constant UV and conductivity signal was achieved. Afterwards, the column was flushed with ultra-pure water until a constant UV and conductivity signal was reached. Then, the column was

titrated with 0.01 M NaOH solution until an increase in conductivity signal was observed. The ionic capacity of the column was calculated using the following equation:

$$\Lambda = \frac{C_{NaOH} V_{NaOH}}{V_c (1 - \varepsilon_t)} \tag{3-8}$$

with the column volume, V_c, and the NaOH concentration and volume used for titration (C_{NaOH}, V_{NaOH}). The lumped film diffusion coefficient, k_{eff}, was estimated by the inverse fitting of the model response to the experimentally measured data.

3.3.3.2 Static binding capacity

Batch experiments were conducted to measure equilibrium adsorption capacities of SP Sepharose™ FF resin. These experiments were confined to single-protein studies. Aliquots (0.2 g) of equilibrated, swelled, drained resin were quantitatively weighed into a 15-mL falcon tubes. The protein standard samples were reconstituted to 0.03–15.0 mg/mL. The tubes were left to shake overnight, at 22 ± 0.5 °C, on a rotating wheel, and then centrifuged to remove the resin for 20 min at 3000 × *g*. The supernatant solution was filtered and analyzed on a UV spectrophotometer at 280 nm. The optical density data were converted to their corresponding protein concentrations by reference to a standard calibration curve prepared with the respective protein. With the equilibrium protein concentration, *C*, so determined, the corresponding quantity of protein adsorbed onto the exchanger, *q*, was calculated by mass balance:

$$q = q_i + \frac{F_D}{W}(C_i - C) \tag{3-9}$$

where C and C_i are the equilibrium and initial protein concentrations in solution, respectively; likewise q and q_i are the equilibrium and initial concentrations on the adsorbent, and F_D and $W$are respectively the amount of feed and adsorbent.

3.3.3.3 Dynamic binding capacity

The dynamic binding capacity is the most relevant resin characteristics to dynamic adsorption; and hence, it was investigated before undertaking gradient elution

experiments. Solutions of proteins containing 0.05 mg/mL lactoperoxidase and 0.15 mg/mL lactoferrin were used as feed solutions. After equilibrating in the HiTrap™ column with 0.02 M sodium phosphate buffer at pH 6.7, the solutions were loaded onto the column at different flow velocities (2.6 and 5.2 cm/min). All the procedures were executed with ÄKTA chromatographic system. The column effluent was detected at 280 nm and recorded until it reached to 10% of the feed solution absorbance. The dynamic binding capacity, $Q_{10\%}$ was calculated using Eq. (3-10):

$$Q_{10\%} = \frac{C_0 \int_0^{V_{10\%}} (1 - \frac{C}{C_0}) dV}{V_c} \tag{3-10}$$

where C and C_0 are the protein outlet and initial concentrations, respectively, $V_{10\%}$ is the 10% breakthrough volume, and V_c is the volume of the column.

3.3.3.4 Gradient elution experiments

The running buffer used for all experiments was a 0.02 M sodium phosphate buffer at pH 6.7 while the same buffer with additional 1.0 M NaCl was employed for elution purposes. The reason behind the choice of pH 6.7 is for natural milk pH level. 2 mL of a sample containing 0.035 mg/mL lactoperoxidase and 0.11 mg/mL lactoferrin was loaded onto the HiTrap SP FF column. This step was followed by a 2-column volume (CV) flushing with running buffer to remove unbound proteins. Afterwards, linear gradients from 0% to 100% high salt buffer with 10, 15, 20 and 25 CV were carried out. The flow rate was 1.0 mL/min and the column was regenerated and re-equilibrated with 1.0 M NaOH and running buffer respectively, both steps for 5 CV. All solutions were prepared using ultra-pure water (Barnstead easy-pure RODI, Fisher Scientific). Prior to use, buffers and samples were filtered through 0.45 μm membranes, and degassed by sonification, in order to reduce air entrainment issues.

3.3.3.5 Gradient elution experiments at high column loads

The experiments were carried at a 15 CV gradient, pH 6.7 and 1.0 mL/min flow rate. Two experiments were conducted with 2.0 mL samples and higher concentrations of

protein (0.175 and 0.35 mg/mL) and (0.55 and 1.1 mg/mL) for lactoperoxidase and lactoferrin respectively. In the other two experiments, the concentration for lactoperoxidase and lactoferrin were 0.035 and 0.11 mg/mL and loaded volumes 8.0 and 16.0 mL.

3.3.3.6 Sensitivity analysis

A full factorial design of experiment was conducted to verify the estimated parameters with different gradient end concentrations, gradient lengths, sample volumes and concentrations. The reference operating point was chosen to be 20 CV gradient, 0.03 mg/mL lactoperoxidase, 0.1 mg/mL lactoferrin, 6.0 mL sample load and 1.0 M NaCl salt concentration. The factorial experiment was conducted at a variation of ±5% salt concentration, ±10% for gradient length, ±20% for the sample volume, ±30% lactoperoxidase sample concentration and ±50% lactoferrin sample concentration. Protein concentrations were studied over a broad range as it can vary with different feedstock and represent concentrations normally present in native whey [28] and [29]. Results are given in Table 3-1.

Table 3-1 The design of factorial experiment

Run	Gradient end salt concentration (M)	Gradient length (CV)	Sample volume (ml)	Protein concentration (lactoperoxidase/lactoferrin) (mg/ml)
1	1.05	18	4.8	0.02/0.05
2	0.95	18	4.8	0.02/0.05
3	1.05	22	4.8	0.02/0.05
4	0.95	22	4.8	0.02/0.05
5	1.05	18	4.8	0.05/0.2
6	0.95	18	4.8	0.05/0.2
7	1.05	22	4.8	0.05/0.2
8	0.95	22	4.8	0.05/0.2
9	1.05	18	7.2	0.02/0.05
10	0.95	18	7.2	0.02/0.05
11	1.05	22	7.2	0.02/0.05
12	0.95	22	7.2	0.02/0.05
13	1.05	18	7.2	0.05/0.2
14	0.95	18	7.2	0.05/0.2
15	1.05	22	7.2	0.05/0.2
16	0.95	22	7.2	0.05/0.2

3.3.3.7 Column model evaluation

Model predictions were experimentally assessed on HiScreen™ SP Sepharose FF with whey protein isolate as it is convenient and reproducible to simulate native whey feedstock. A solution of whey proteins was prepared by dissolving 20.0 mg/mL WPI in phosphate buffer at pH 6.7. This concentration yields individual concentrations of 0.026 mg/mL of lactoperoxidase and 0.147 mg/mL of lactoferrin, which are comparable with the total lactoperoxidase and lactoferrin concentration normally present in native whey.

3.3.3.8 Analytical determinations

Total protein concentration in WPI was determined using BCA (bicinchoninic acid) reagent. The BCA protein assay kit from Sigma (Oakville, Canada) was used, with BSA protein standard. Lactoferrin content in whey was determined by enzyme-linked immunosorbent assay (ELISA) using polyclonal antibodies purchased from Bethyl Labs., USA. Lactoperoxidase concentration in whey was determined by Lowry protein assay. Protein concentration in the eluted peaks were measured by the absorbance at 280 nm using extinction coefficient of for lactoperoxidase $\varepsilon_{1\%} = 14.9$ [30], lactoferrin $\varepsilon_{1\%} = 15.1$ [31].

A 50 µL aliquot of lactoferrin pool was applied to an Eclipse XDB-C18 (5 µm, 4.6 mm × 150 mm) on an Agilent HPLC system to determine its concentration in collected fractions during gradient experiments. A linear gradient of 25% to 75% (v/v) solvent B in solvent A (solvent A: 0.1% (v/v) TFA in water, solvent B: TFA/acetonitrile/water, 0.1/95/4.9% (v/v)) was used to elute lactoferrin at 1.0 mL/min over 20 min. Quantity of lactoferrin was estimated from the calibration curve obtained with known quantities of standard lactoferrin. The fractions from the chromatographic run were analyzed by sodium dodecyl sulfate polyacrylamide gel electrophoresis (SDS–PAGE) using a Mini-PROTEAN system (Bio-Rad). It was performed on a 12% separating gel and a 4% stacking gel according to ref. [32]. After running the electrophoresis, the gels were stained with Coomassie Brilliant Blue R-250.

3.3.3.9 Parameter estimation

The SMA isotherm parameters, k_{eq} and ν, were estimated from the linear gradient elution data. The estimation of parameters was accomplished by determining the shielding parameter σ from high column load gradient elution experiments. The 280 nm plotted over time, exported with UNICORN, have been imported into Matlab with respect to the FPLC's dead volume. The inverse method was used to the best fit of chromatographic experimental data to the mathematical model response.

3.4 Results and discussion

3.4.1 Column characterization

The volume between the UV cell and the conductivity cell was found to be 0.13 mL. The dead volume between the mixing valve and the column was 4.41 mL in total. All data were corrected with respect to this dead volume. The column voidage was estimated by pulse injections of dextran as a non-binding, non-pore-penetrating, and NaCl as non-binding, pore-penetrating tracers. The total ionic capacity was determined by acid–base titration. The calculated voidage and capacities are given in Table 3-2.

Table 3-2 Column parameters calculated

		HiTrap™ SP FF	HiScreen™ SP FF
Column voidage	ε_c	0.301	0.296
Particle voidage	ε_p	0.893	0.893
Total voidage	ε_t	0.925	0.917
Total ionic capacity (M)	Λ	1.770	1.510
Axial dispersion coefficient (mm^2/s)	D_{ax}	0.058	0.059

3.4.2 Adsorption studies

3.4.2.1 Static binding capacity

Protein batch uptake on the SP Sepharose FF resin were investigated and the experimental data (Figure 3-1) showed that maximum binding capacity is around 90 mg lactoperoxidase and lactoferrin per g resin which is comparable to the manufacturer's claim for ribonuclease A of 70 mg/mL medium [33]. The observed isotherm shape likely means that there is a strong protein-surface attraction, giving a steep isotherm slope for solution concentrations up to approximately 2 mg/mL, where protein–protein repulsion is minimal. Above this concentration, though, strong protein–protein repulsion may significantly limit adsorption, accounting for the modest increase in adsorption with increased protein concentration, the fact that the SP FF capacity at low ionic strength is now high enough. The curves for both lactoperoxidase and lactoferrin on SP FF reflect significant retention, even at high ionic strengths. This behavior may be due to the presence of highly charged patch on one lobe of the protein such that relatively high salt concentrations would be needed to screen the electrostatic attraction between that patch and the oppositely charged resin effectively.

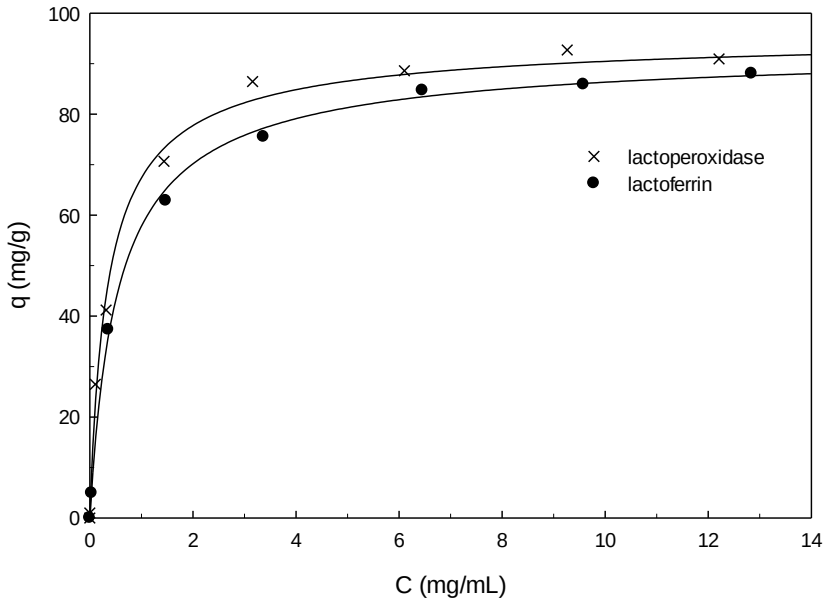

Figure 3-1 Equilibrium adsorption data of SP FF resins for lactoperoxidase and lactoferrin after 24 h

3.4.2.2 Dynamic binding capacity

Frontal analysis of the breakthrough curve was used to determine the dynamic binding capacity in HiTrap™ SP FF. At linear velocities of 2.6 and 3.25 cm/min, the dynamic binding capacity $Q_{10\%}$ could reach 1.49 and 1.17 mg/mL of adsorbent for lactoperoxidase and 19.26 and 15.27 mg/mL of adsorbent for lactoferrin, respectively (Figure 3-2). The total dynamic capacity is, therefore, about 20.75 and 16.44 mg/mL under these conditions. As the flow velocity increased, the retention time of protein in the column was reduced, resulting to a decrease of the dynamic binding capacity.

3.4.3 Model-based adsorption parameter estimation

Estimation of the isotherm parameters were carried out using inverse method by minimizing the global error between experimental and simulated concentration profiles by solving the isothermal and the column model simultaneously. Gradient elution data at a low protein concentration was used to estimate equilibrium constant, k_{eq}, and characteristic charge, υ. The steric factor had no significant effect on the peak position;

however, it affected peak shape on high column loadings. This phenomenon was captured by estimating the steric factor from the various column loads experiments. Least squares fits of the mechanistic model to the chromatograms at 10, 15, 20, and 25 CV for two-component mixture are shown in Figure 3-3. The scatter plot displays the experimental data, whereas the dotted line shows the model response for simulation with SMA parameter estimations. The first eluting component is lactoperoxidase followed by lactoferrin. This order of elution agrees with published studies [34] and [35]. The elution peaks slightly overlap. Obviously, an increase in elution gradient length increases the gap between the retention time of lactoperoxidase and the lactoferrin. All experiments were replicated three times and checked for reproducibility (Figure 3-4).

A

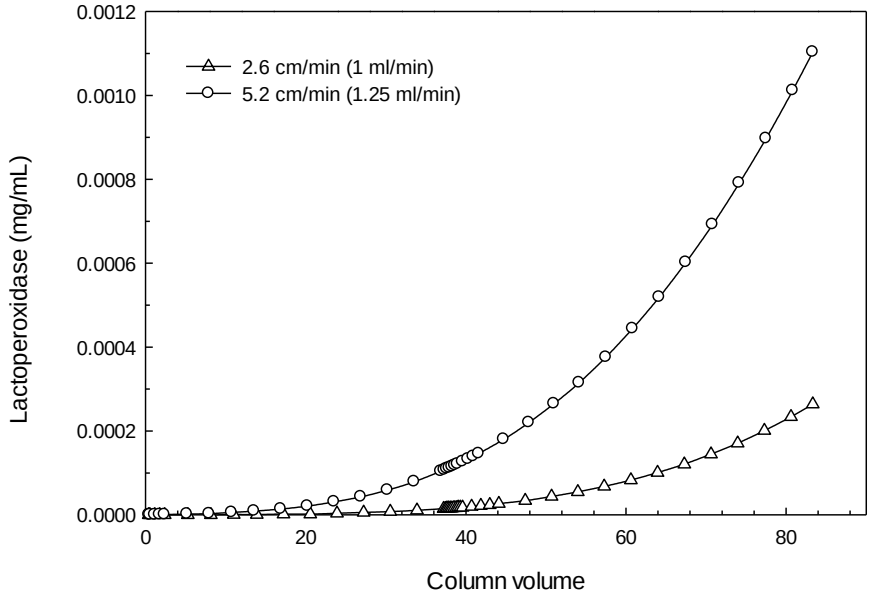

B

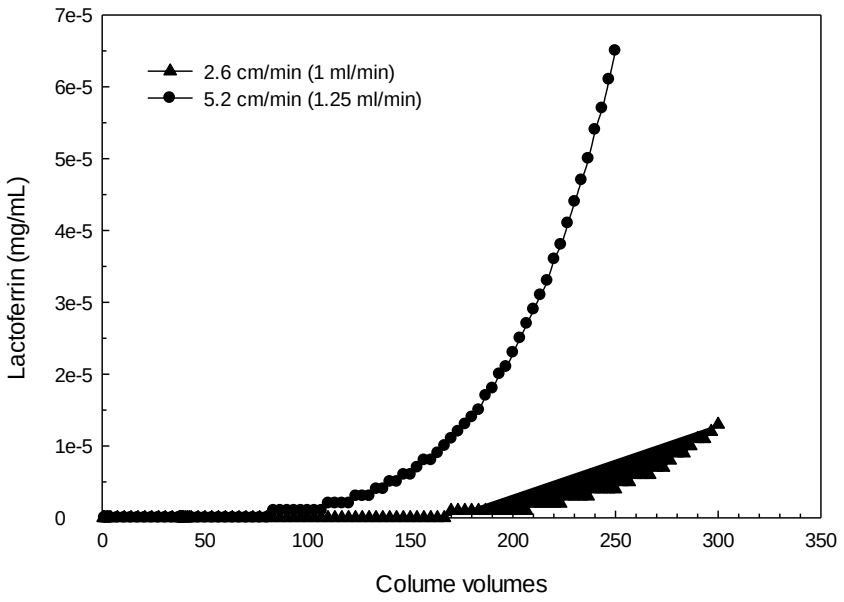

Figure 3-2 Breakthrough curve of lactoperoxidase **A** and lactoferrin **B** to SP FF at different flow velocities

As shown in Figure 3-3, the model-predicted concentration profiles of lactoperoxidase and lactoferrin deviate slightly from the gradient elution with 10 CV. It can be attributed to a phenomenon that has been observed in ion-exchange chromatography by Jansen et al.[36]. At low salt concentration, only the counter-ions herein proteins enter the adsorbent and are exchanged, whereas the co-ions herein sodium ions are repulsed. However, at increased salt concentration, the entire salt molecule is taken up as a result of the electrical shielding effects. A sharp increase of salt concentration in the mobile phase intensifies this phenomenon, leading to relative weaker protein–adsorbent interactions and faster elution of proteins than model prediction. Nonetheless, the simulation results agree very well with the experimental elution profiles of longer gradient lengths. The SMA parameters determined by the inverse method are given in Table 3-3. High adsorption rate for lactoferrin confirms the fact that it has strong interactions with the adsorbent which leads to elute at high salt concentration (~1.0 M NaCl) compared to lactoperoxidase as expected. The charge factors for both lactoperoxidase and lactoferrin are fairly low due to working pH close to their isoelectric points (pI ~8). Lactoperoxidase

shows prominently higher shielding factor than lactoferrin although they have very close molecular weights. One explanation could be the configuration of lactoperoxidase interacting with the adsorbent. It might cover larger surface of the adsorbent due to its 3D structure and prevents other protein molecules to bind to the matrix. However, it does not affect lactoferrin adsorption; according to the adsorption studies we did in previous section, lactoferrin with higher concentration, has greater binding capacity.

A

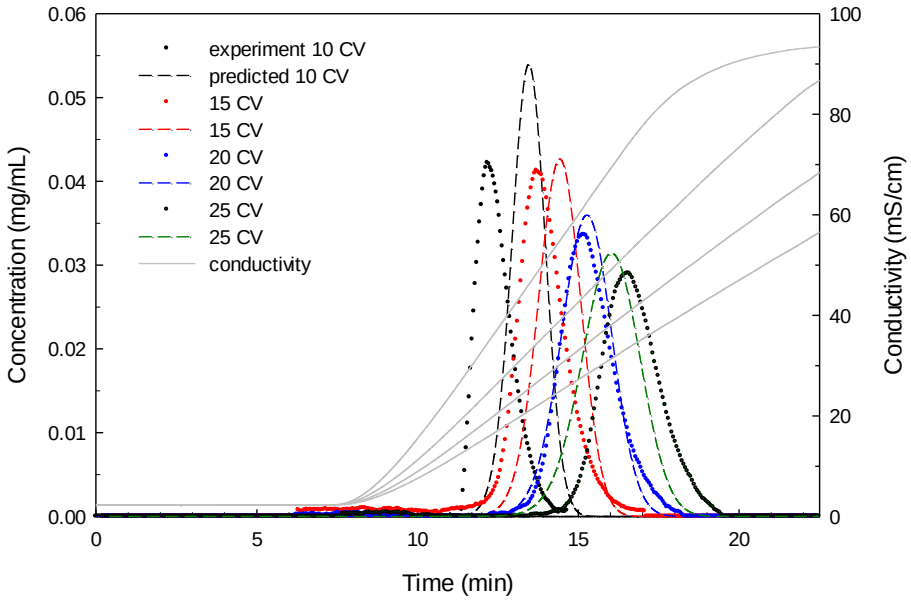

B

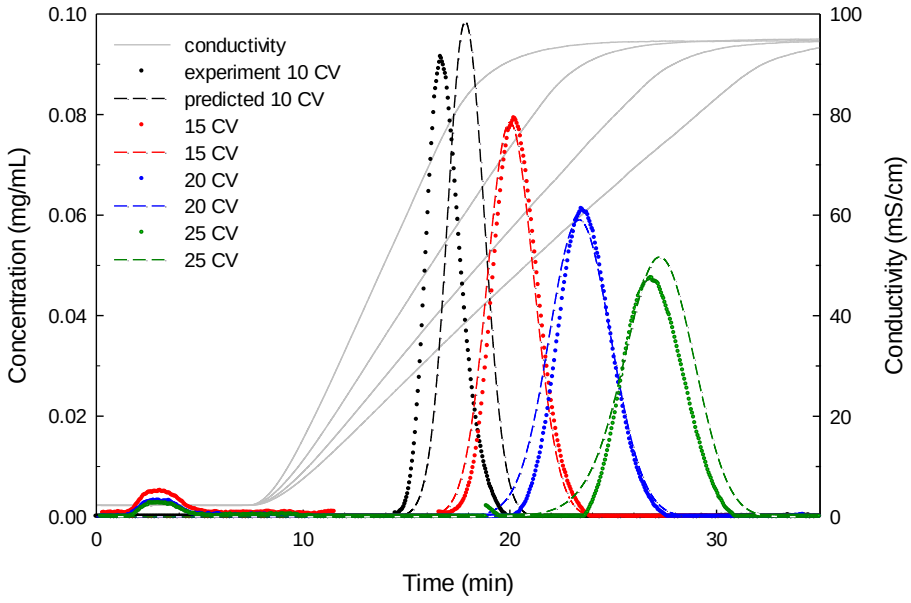

Figure 3-3 Experiments (solid line) and predicted (dashed line) elution profiles of mixtures of standard lactoperoxidase **A** and lactoferrin **B** at different gradient column volumes

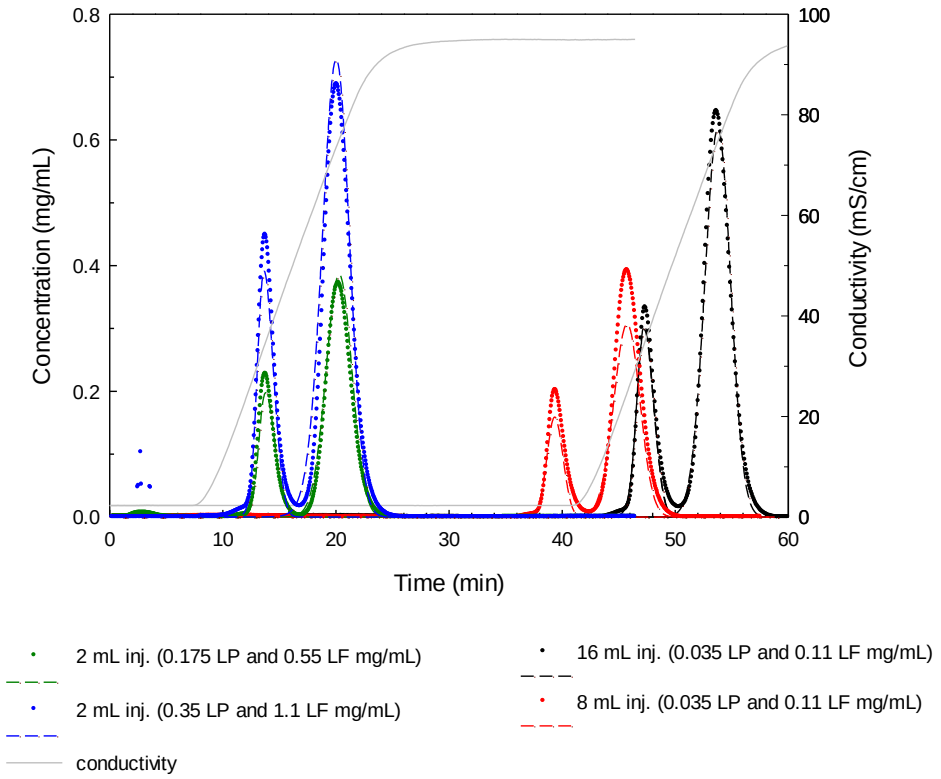

Figure 3-4 Experiments (solid line) and predicted (dashed line) elution profiles of mixtures of standard lactoperoxidase and lactoferrin at different column loadings eluted with a salt gradient ranging from 0 to 1 M NaCl

Table 3-3 Isotherm parameters for lactoperoxidase and lactoferrin on SP Sepharose FF column

Parameter	
Lactoperoxidase	
k_{eq}	1.00
ν	1.86
σ	1283
k_{des}	2.25
Lactoferrin	
k_{eq}	12.84
ν	1.62
σ	0.16
k_{des}	0.98

3.4.4 Parameter verification

The estimated isotherm parameters were verified by a full factorial design of experiment in which salt concentration, gradient, sample size and concentration were selected as process variables and the yield of lactoferrin was used as the evaluated response. The results of simulated and experimental yields under different operating conditions are given in Table 3-4. As seen from Table 3-4, the simulated values for yield of lactoferrin are in good agreement with the experimental results except for Run 2. The experimental yield of Run 2 is inconceivable higher. Such a deviation between simulation and experiment for Run 2 is most probably due to the incomplete desorption of lactoferrin from the adsorbent in previous runs, in other words the adsorbent was not completely regenerated, thus resulting in a yield higher than 1.0. However, the model agrees well with the experimentally determined yield indicating adequate to be considered for future work.

Table 3-4 The results of predicted and experimental yield of lactoferrin for factorial experiment

Run	Predicted yield of lactoferrin (%)	Experimental yield of lactoferrin (%)
1	99.7	100
2	**99.7**	**112**
3	99.7	100
4	99.7	100
5	99.9	99.5
6	99.9	100
7	99.8	99.3
8	99.9	93.7
9	100	100
10	100	100
11	99.9	100
12	100	102
13	99.8	100
14	99.8	106
15	100	100
16	99.8	96.3

3.4.5 Model validation

The validity of the estimated isotherm parameters was further examined experimentally by feeding WPI to semi-preparative HiScreen SP FF column. As depicted in Figure 3-5, experimental and predicted chromatograms were generally in good agreement. Observed deviations could be attributed to the calibrated model inaccuracies. One reason for uncertainties in parameter estimation is due to different column characteristics. Two columns with different sizes were used in this study even though same adsorbent used in both columns, they showed slightly different ionic capacity and voidage. Another reason could be the retention time shifts caused by time-lag noises. For example, sample injection by system pump associated with change in system tubing configuration. A

comprehensive sensitivity analysis of parameter estimation would be preferred but the intention of this work was focused on parameter estimation.

The results were further analyzed by gel electrophoresis as it can be seen in Figure 3-5. Lane S corresponds to the whey protein isolate sample; no bands could be visualized for lactoferrin and lactoperoxidase. This was expected as these proteins in total constitute about 4% of the total whey proteins, thus an extremely small amount to be detected by SDS–PAGE. Fractions F1 and F2 contain significant amount of lactoferrin and lactoperoxidase with a molecular weight of around 77 kDa confirming their identity.

3.5 Conclusions

In this study, the calibrated model succeeds in predicting the separation of two proteins, lactoperoxidase and lactoferrin. Considering the significance of adsorption isotherm, the objective for SMA parameter determination is to investigate a much wider space of operating variables while reducing experimentation work, process development time and material usage.

The procedure is simply applicable using a few single column experiments and requires relatively small amounts of material. The obtained isotherm parameters demonstrate highly effective potential to predict elution profiles for higher loading volumes or different protein concentrations which enables the model to be applied for different whey protein feed-stocks. The model is also used to predict the performance of the process in terms of product concentration and yield. With respect to protein yield and concentration, the calibrated model proves to predict the performance with high accuracy (error $\leq$10%), making it a useful tool to investigate the sensitivity of process performance to variations in process parameters such as salt concentrations and column load as well as for scale-up. Thus, based on the findings in this manuscript, obtained SMA parameters can be employed for fast process development of minor whey proteins separation.

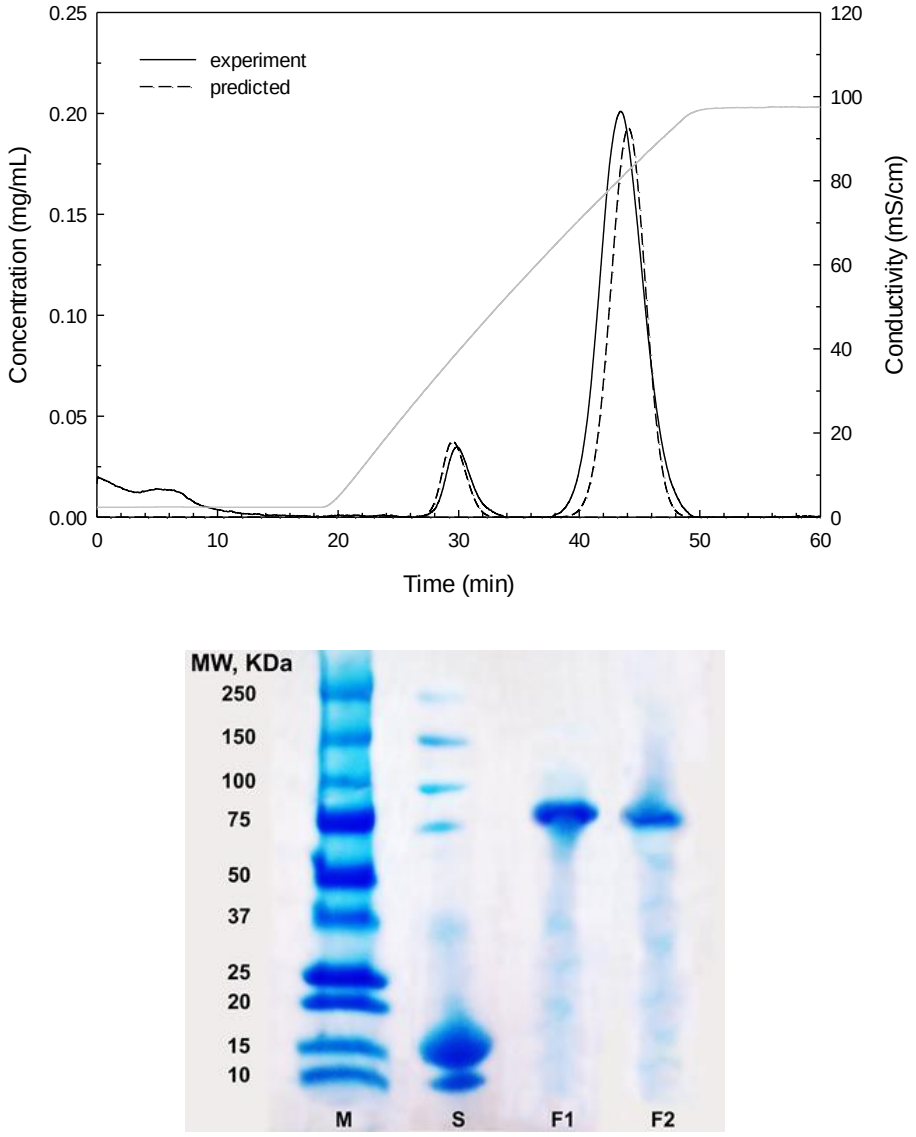

Figure 3-5 Elution profile of the WPI (20 mg/mL) eluted with a salt gradient ranging from 0 to 1 M NaCl and SDS–PAGE of WPI and fractions collected during elution. M: Bio-Rad marker (molecular weights in kDa), S: sample of WPI, F1 and F2: Fraction of lactoferri

References

[1] Smithers, G. W., Ballard, F. J., Copeland, A. D., De Silva, K. J., Dionysius, D. A., Francis, G. L., Regester, G. O. 1996. New opportunities from the isolation and utilization of whey proteins. *J. Dairy Sci.*, *79*(8), 1454–9.

[2] Tomita, M., Wakabayashi, H., Yamauchi, K., Teraguchi, S., Hayasawa, H. 2002. Bovine lactoferrin and lactoferricin derived from milk: production and applications. *Biochem Cell Biol*., *80*(1), 109–12.

[3] Uchida, T., Sato, K., Kawasaki, Y., and Dosako, S. 1996. Separation of lactoperoxidase, secretory component and lactoferrin from milk or whey with a cation exchange resin. US 5 516 675

[4] Zydney, A. L. 1998. Protein Separations Using Membrane Filtration: New Opportunities for Whey Fractionation. *Int. Dairy J.*, *8*(3), 243–250.

[5] Conrado, L. S., Veredas, V., Nóbrega, E. S., Santana, C. C. 2005. Concentration of alpha-lactalbumin from cow milk whey through expanded bed adsorption using a hydrophobic resin. *Braz. J. Chem. Eng.*, *22*(4), 501–509.

[6] Heebøll-Nielsen, A., Justesen, S. F. L., & Thomas, O. R. T. 2004. Fractionation of whey proteins with high-capacity superparamagnetic ion-exchangers. *J. Biotechnol.* *113*(1-3), 247–262.

[7] Liang, M., Chen, V. Y. T., Chen, H.-L., Chen, W. 2006. A simple and direct isolation of whey components from raw milk by gel filtration chromatography and structural characterization by Fourier transform Raman spectroscopy. *Talanta*, *69*(5), 1269–77.

[8] Avramescu, M-E., Gironès, M., Borneman, Z., & Wessling, M. 2003. Preparation of mixed matrix adsorber membranes for protein recovery. J. Membr. Sci., 218(1-2), 219–233.

[9] Kawai, T., Saito, K., & Lee, W. 2003. Protein binding to polymer brush, based on ion-exchange, hydrophobic, and affinity interactions. J. Chromatogr. B, 790(1-2),

131–142.

[10] Langlotz, P., & Kroner, K. H. 1992. Surface-modified membranes as a matrix for protein purification. J. Chromatogr. A, 591(1-2), 107–113.

[11] Plate, K., Beutel, S., Buchholz, H., Demmer, W., Fischer-Frühholz, S., Reif, O., Scheper, T. 2006. Isolation of bovine lactoferrin, lactoperoxidase and enzymatically prepared lactoferricin from proteolytic digestion of bovine lactoferrin using adsorptive membrane chromatography. J. Chromatogr. A, 1117(1), 81–86.

[12] Zou, H., Luo, Q., Zhou, D. 2001. Affinity membrane chromatography for the analysis and purification of proteins. J.Biochem. Bioph. Meth., 49(1-3), 199–240.

[13] Drioli, M. Romano, 2001. Progress and new perspectives on integrated membrane operations for sustainable industrial growth, Ind. Eng. Chem., 40, 1277–1300.

[14] Saufi, S. M.; Fee, C. J. 2011. Recovery of lactoferrin from whey using cross-flow cation exchange mixed matrix membrane chromatography. Separation and Purification Technology, 77(1), 68−75.

[15] Doultani S, Turhan KN, Etzel MR. 2004. Fractionation of proteins from whey using cation exchange chromatography. Process Biochemistry, 39(11), 1737-1743.

[16] Du QY., Lin DQ, Xiong ZS, Yao SJ. 2013. One-Step purification of lactoferrin from crude sweet whey using cation-exchange expanded bed adsorption. Ind. Eng. Chem. Res., 52(7), 2693–2699

[17] Fee CJ, Chand A. 2005. Direct capture of lactoferrin and lactoperoxidase from raw whole milk by cation exchange chromatography. Separation and Purification Science, 48, 143-149.

[18] Noppe W, Plieva FM, Galaev IY, Vanhoorelbeke K, Mattiasson B, Deckmyn H. 2006. Immobilised peptide displaying phages as affinity ligands: Purification of lactoferrin from defatted milk. J. Chromatogr. A, 1101(1-2), 79-85.

[19] Lawlis VB, Heinsohn H. 1993. BIOSEPARATIONS - INDUSTRIAL PERSPECTIVES ON THE ROLE OF CHROMATOGRAPHY IN THE PURIFICATION OF BIOLOGICAL MOLECULES. LC GC, 10(11), 720.

[20] Guiochon, G., Felinger, A., Shirazi, D. G., Katti, A. M. 2006. Fundamentals of Preparative and Nonlinear Chromatography. San Diego, USA: Elsevier Academic Press.

[21] Schmidt-Traub, H. 2006. Preparative Chromatography of Fine Chemicals and Pharmaceutical Agents. Weinheim, Germany: WILEY-VCH.

[22] Von Lieres E., Andersson J. 2010. A fast and accurate solver for the general rate model of column liquid chromatography. Comput. Chem. Eng., 34(8), 1180–1191.

[23] Danckwerts, P. V. 1953. Continuous flow systems. Chem. Eng. Sci., 2(1), 1–13.

[24] Brooks, C. A., Cramer, S. M. 1992. Steric mass-action ion exchange: Displacement profiles and induced salt gradients. AIChE J., 38(12), 1969–1978.

[25] Kempe H., Axelsson A., Nilsson B., Zacchi G. 1999. Simulation of chromatographic processes applied to separation of proteins. J. Chromatogr. A, 846(1–2) 1-12.

[26] Chan S., Titchener-Hooker N., Bracewell DG, Sørensen E. 2008. A systematic approach for modeling chromatographic processes—Application to protein purification. AIChE J., 54(4), 965-977.

[27] Beckley K., Verhaert P., van der Wielen L., Hubbuch J., Ottens M. 2009. Opinion: Rational and systematic protein purification process development: the next generation. Trends Biotechnol., 27(12), 673-679.

[28] Hahn, R., Schulz, P ., Schaupp, C., Jungbauer, A. 1998. Bovine whey fractionation based on cation-exchange chromatography. J. Chromatogr. A, 795(2), 277–287.

[29] Korhonen, H., Pihlanto-Leppälä, A., Rantamäki, P., Tupasela, T. 1998. The

functional and biological properties of whey proteins: Prospects for the development of functional foods. Agric. Food Sci., 7(2), 283–296.

[30] Carlström, A. 1965. The heterogeneity of lactoperoxidase. Acta Chem. Scand., 19, 2387–2394.

[31] Groves, M. L. 1960. The Isolation of a Red Protein from Milk 2. J. Am. Chem. Soc. , 82(13), 3345–3350.

[32] Laemmli UK. 1970. Cleavage of structural proteins during the assembly of the head of bacteriophage T4, Nature, 221, 680–685.

[33] GE Healthcare Technologies. 2014. SepharoseTM Fast Flow: Ion exchange chromatography, Data file 18-1177-22 AE.

[34] Yoshida S., Xiuyun Y. 1991b. Isolation of lactoperoxidase and lactoferrins from bovine milk rennet whey and acid whey by sulphopropyl cation exchange chromatography. Netherlands Milk Dairy Journal, (45), 273-280.

[35] Etzel MR, Liten AD, Moore PM. 1998. Chromatographic capture of proteins from milk. 2nd International Conference On Expanded Bed Adsorption, Napa Valley, California, USA.

Chapter 4

Optimization of Lactoperoxidase and Lactoferrin Separation on an Ion-Exchange Chromatography Step

Abstract

Lactoperoxidase (LP), which is a high-value minor whey protein, has recently drawn extensive attention from research scientists and industry due to its multifunction and potential therapeutic applications. In this study, the separation and optimization of two similar-sized proteins, LP and lactoferrin (LF) were investigated using strong cation exchange column chromatography. Optimization was started with central composite design based experiments to characterize the importance of different decision variables. The three variables used in the optimization were flow rate, length of gradient and final salt concentration in the linear elution gradient step. The obtained empiric functional model represented the effect of the significant factors on the yield as the objective function. Afterwards, the calibrated mechanistic model was employed to predict accurate optimal set of variables. The optimal operating points were found and the results were compared with validation experiments. Predictions respecting yield confirmed a very good agreement with experimental results while keeping purity, a product quality characteristic, equal or above to a predefined value.

Keywords

Cation exchange chromatography, Minor milk protein, Response surface modeling, Simulation, Steric mass action (SMA), Optimization

4.1 Introduction

Today, the purification of high-value proteins from waste food streams has attracted a great attention. Due to the high number of potential applications of protein isolates, a few chromatographic processes have been developed to isolate high-purity protein fractions [1]. Ion-exchange chromatography (IEC) is one of the most powerful techniques to

overcome biomolecules purifying challenges and is commonly applied in downstream processes.

Milk whey is a mixture of a variety of proteins. The mixture displays a wide range of chemical, physical, and functional properties [2]. Whey proteins have been adequately separated into different fractions; the isolation of the major and minor proteins [3–7]; however, the efficient purification of high-value minor proteins of similar molecular weights such as lactoperoxidase (LP) and lactoferrin (LF) still remains as a challenge. LP has an approximate molecular weight of 77.5 kDa [8] with an isoelectric point approaching 9.5. Molecular weight of LF is 78.0 kDa with an isoelectric point around 8.7. In addition, proteins exhibit susceptible structure that alters their functionality, thus these macromolecules should be processed as quickly as possible and in as few steps as possible. In biotechnology industry, yield and bioactivity are directly associated to efficient processing [9,10]. Despite of the significant effort that has been applied toward developing downstream processes, there are still issues that need further considerations before an industrial application will be viable. Some of these challenges include labor-intensive experimental work, rule of thumbs and consequently optimization of downstream processes can cover up to 50–80% of total production costs [11]. Growing demands for high quality products result in more complexity of processes and analytics, thus increasing the costs for product work-up. Process analytical technology (PAT) [12], introduced in the guidelines of the US Food and Drug Administration, emphasizes on better understanding of a process, as well as sensitivity and robustness analyses that ultimately leads to reduce overall process development cost and time from laboratory to production scale.

This is the main motivation for extreme attempts to assist the development and optimize chromatography processes, mostly industrial preparative processes, aiming for higher productivity, yield, and purity of the protein of interest. Successful approaches to the optimization of chromatographic separations always include a detailed consideration of the physicochemical properties of involved components as well as interactions between the proteins and the adsorbent phase. To the best of our knowledge, no model-integrated approach has been applied to optimize minor milk proteins separation in IEC, making it a

topic worthy of investigation. The present work aims to study optimization of method development to maximize yield of lactoperoxidase with respect to a constraint on purity. A statistical study was first conducted to examine the influence of the operation variables (concentration of salt at the end of gradient, length of gradient and velocity). Subsequently productive information was used to assist the mechanistic model to gain more insight into the optimization of IEC. In this work, purity was defined as a nonlinear constraint in the optimization procedure to meet equal or above to a preset requisite at the operating point.

4.2 Theory

4.2.1 Response surface modeling and design of experiments

Response surface methodology (RSM), a collection of mathematical-statistical technique based on design of experiments (DoE), has been successfully used for optimization studies of different bio-separation processes [13]. RSM has been widely adopted to investigate the effects of several design factors influencing a response by varying them simultaneously in a limited set of experiments. The concept of DoE-techniques outlines various statistical approaches to maximize specific information in an experimental planning and after all determine the most favorable direction to move in order to find a true optimum. Central composite design (CCD) is an ideal choice as a symmetrical experimental design for sequential experimentation and allows reasonable information to calculate model lack of fit while reducing the number of design points. In general, CCD is the more known class of quadratic design that consists of: (1) a factorial (or cubic) design; (2) an additional design often a star design with all points set to an equal distance from the center and (3) at least one center point [14]. Therefore, full uniformly routable central composite designs involve the total number of $N = k^2 + 2k + c_p$ points, where k is the number of the factors, and c_p is the number of the replicate runs performed at the center point. In this design, the distance α from the center point depends on the number of the factors and can be calculated by $\alpha = 2^{(k-p)/4}$. All factors have to be adjusted at five levels (-α,−1,0,+1,+α) [20]. The quadratic polynomial model for the measured values of the results from experiments variable, Y with k factors is given by:

$$Y = \beta_0 + \sum_{i=1}^{k} \beta_i x_i + \sum_{i=1}^{k} \beta_{ii} x_i^2 + \sum_{1 \le i \le j}^{k} \beta_{ij} x_i x_j + \varepsilon \quad (4\text{-}1)$$

where x_i and x_j are the design factors in coded values, β_0 is the constant parameter, β_i , β_{ij} ,and β_{ii} are the coefficient of the linear, interaction, and quadratic terms of the model, respectively. The coefficients of Eq. (4-1) are estimated using statistical software packages (e.g., Minitab, Design Expert, SPSS).

4.2.2 Mechanistic modeling of chromatography

A mechanistic model is used to describe the physical phenomena based on a set of mathematical equations. Two types of physical phenomena dominate chromatography; movement of solutes through the packed bed of porous particles via mass transfer mechanisms, and adsorption based on the fundamental thermodynamic interactions between migrating solutes and the stationary phase. The general system of equations used to describe the mass transfer phenomena consist of two sets of partial differential mass conservation equations. The general rate model for a chromatographic process includes convective and diffusive flows through porous particles on the column level and imitates mass transfer resistances and surface interactions on particle level. In IEC, an external film surrounding adsorbent particles is commonly presumed to model the movement of components from column to particle level; the sorption of protein on the particle surface can be described by the steric mass-action (SMA) model, developed by [15] and generally used for the modeling of salt gradient elution in IEC, for example in [16].

On column level, concentration change for the i^{th} component with respect to the time and position, is described by:

$$\frac{\partial c_i}{\partial t} = -u_{\text{int}} \frac{\partial c_i}{\partial x} + D_{ax} \frac{\partial^2 c_i}{\partial x^2} - \frac{1-\varepsilon_c}{\varepsilon_c} \cdot \frac{3}{r_p} k_{eff,i} \left[c_i - c_{p,i} \right] \quad (4\text{-}2)$$

The first term on the right hand side represents the convective transport through the column while the second and third term represents respectively the dispersive transport and the mass transfer to the particle surface. The symbol u_{int} indicates the interstitial

velocity, ε_c the column voidage, r_p the particle radius, D_{ax} the axial dispersion representing combined effect of dispersion and diffusive processes, and $k_{eff,i}$ epitomize combined effect of both the internal and external mass transfer resistances in one lumped film diffusion coefficient. Analogously, on particle level, concentration change for the i^{th} component is expressed by:

$$\frac{\partial c_{p,i}}{\partial t} = \frac{3}{\varepsilon_p r_p} k_{eff,i}[c_i - c_{p,i}] - \frac{1-\varepsilon_p}{\varepsilon_p}\frac{\partial q_i}{\partial t} \tag{4-3}$$

where q_i denotes the concentration of component i within the particle and ε_p the particle voidage. The first term on right hand side describes adsorption and desorption processes on particle level, i.e. the interaction between mobile and particle bound phase.

For the description of sorption kinetics, the steric mass-action (SMA) isotherm developed by Brooks and Cramer [17] was embedded into the mechanistic model and has been successfully used to describe protein adsorption in IEC. Based upon the stoichiometric exchange of charges and steric hindrance of binding sites, the isotherm can be described by the reaction:

$$c_i + \nu_i \bar{q}_{salt} \Leftrightarrow q_i + \nu_i c_{salt}$$

The parameter ν_i is the characteristic charge of protein, which represents the average number of ligands, or binding sites, interacting during adsorption. $\bar{q}_{salt}$ is the concentration of adsorbed salt counter-ions that are available for exchange, c_{salt} is the salt concentration of the bulk.

$$\bar{q}_{salt} = \Lambda - \sum_{i=2}^{n+1}(\nu_i + \sigma_i)q_i \tag{4-4}$$

where the parameter Λ is the ionic capacity of the adsorbent and σ_i is the steric factor, which represents the average number of counter-ions shielded per adsorbed protein molecule.

SMA isotherm in its kinetic form can be expressed as:

$$\frac{\partial q_i}{\partial t} = k_{ads,i}\left[\Lambda - \sum_{j=1}^{k}\left(\nu_j - \sigma_j\right)q_j\right]^{\upsilon_i} c_i - k_{des,i}c_{salt}^{\nu_i}q_i \tag{4-5}$$

$k_{ads,i}$ and $k_{des,i}$ respectively denote the adsorption and desorption rates.

4.2.3 Optimization

Optimization maximizes/minimizes an objective function, by varying one or more variables, called decision variables to obtain an optimal purification step. A chromatographic purification step involves of many decision variables such as loading, washing and elution times, salt concentration, the flow rate in the different steps, column length, column diameter, and the gradient in the elution step. The decision variables can be narrowed down by including lower and upper boundaries. To limit the optimization further, constraints can also be added as equality or inequality functions. The most typical objective functions used in a preparative chromatographic purification step are production rate and yield. In this work, the objective function studied was the yield, and the inequality constraints set on the optimization was purity.

The yield is calculated as the fraction of the target component captured:

$$Y = \frac{\int c_{caputered,i}dV}{V_{load} \times c_{load}} \tag{4-6}$$

where $c_{\text{captured},i}$ is the concentration of the target component i leaving the column during the elution.

The purity is defined as

$$Pu_i = \frac{m_{captured,i}}{\sum_j m_{captured,j}} \tag{4-7}$$

where $m_{\text{captured},i}$ is the amount of substance captured of component i.

4.3 Materials and methods

4.3.1 Materials, column and software

The study aims at an optimal separation of lactoperoxidase on the adsorbent SP Sepharose FF by linear gradients. Lactoperoxidase from bovine milk, ≥ 90% pure and Lactoferrin from bovine milk, approximately 95% pure were used. Sodium monobasic phosphate, sodium dibasic phosphate and sodium chloride for buffers preparation were purchased from Sigma-Aldrich (Oakville, Canada). NaOH was used for pH-adjustment. The running buffer in all experiments was 0.02 M sodium phosphate buffer at pH 6.7. The buffer for elution purposes contained additional NaCl. Proteins were diluted into phosphate buffers by slowly stirring to prevent any foam formation. Afterward, the protein solution was filtered through a 0.22 μm polyethersulfone hydrophilic Millex-GP filter unit (Millipore, France) to remove any fine particles. The chromatographic setup consisted of a prepacked HiScreen SP Sepharose FF 4.7 ml column (10.0 cm length, 0.77 cm ID) and an ÄKTA purifier 100 system, both purchased from GE Healthcare (Mississauga, Canada). The software Minitab® 17 (State College, Pennsylvania, USA) was used as a statistical tool for handling response surface methodology. The software MATLAB R2014a was used to execute the mechanistic model.

4.3.2 Experimental methods

In all experimental setups the column was at first equilibrated with running buffer for 5 column volumes (CV). This step was followed by an automated sample load of 2 mL protein mixture. Then the column was flushed for another 2 CV to remove unbound proteins, before initiating a linear elution gradient. The elution gradient was applied from 0% to 100% high salt elution buffer, followed by a 5 CV high salt wash step and regenerated and re-equilibrated with 1 M NaOH and running buffer respectively. Conductivity and UV-absorbance were measured online at column outlet. The data collected from these measurements was further analyzed and taken into account to estimate SMA parameter by the inverse method. Three design factors were employed to describe the gradient profile:

- final concentration of salt in elution step [M].
- length of linear elution gradient [CV].
- superficial velocity [cm/min]

The experimental ranges used for these factors included (0.35-1.35 M) for final concentration of salt in elution step, (1.11-5.98 cm/min) for flow velocity, and (9.88–35.1 CV) for length of gradient. All the buffers were prepared using ultra-pure water (Barnstead easy-pure RODI, Fisher Scientific), filtered with a 0.45 µm membrane and degassed prior to use.

4.3.2.1 Protein quantification

Lactoperoxidase concentration was determined by Lowry protein assay. The collected fractions of lactoperoxidase were analyzed using measurement of absorbance at 280 nm (extinction coefficient of lactoperoxidase $\varepsilon_{1\%}$ = 14.9 [18]) and 412 nm. Lactoperoxidase absorbs radiation at 280 nm as well as 412 nm; it has maximum absorbance at 412 nm [19] and its purity is estimated as a ratio of A_{412}/A_{280}. The BCA (bicinchoninic acid) protein assay kit from Sigma (Oakville, Canada) with BSA protein standard was used to further analysis of protein fractions from ÄKTA.

4.3.3 Mathematical method

4.3.3.1 Screening experiments to determine importance of design factors

Concentration of salt was studied over a broad range as for the elution step a lower salt concentration can result in a lower purity for lactoperoxidase and less lactoperoxidase will elute in the elution step. On the other hand, a higher salt concentration in the elution step is less critical as lactoferrin is far from eluting at lower conductivities. Flow rate is remarked to be easy to control and was investigated over a narrower range, with upper bound recommended by the manufacturer. Initial operating conditions to maximize chromatography performance were determined by means of a functional relationship between the experimental designs combined with response surface modeling. To assure the consistency of prediction error, the value (α) was adjusted as 1.68 ($\sqrt[4]{8}$), and it was assumed all points with the equal distance from the design center have the constant prediction variance. Table 4-1 shows design factors in their coded and un-coded

(experimental) forms, in an experimental design performed in a random order to avoid systematic error. As seen in Table 4-1, the design experiments had 20 runs in total. The analysis of variance (ANOVA) was used to test the significance of the fit of the empiric model. The significance level of 0.05 was chosen to establish the statistical significance in all results.

4.3.3.2 SMA model calibration and validation

The inverse method [20] was used to calibrate the model parameters to experimental data. SMA parameters were estimated based on 20 chromatograms seeking to achieve a best fit between model response and measured chromatogram data. The optimal set of the parameter values, $\{\nu, k_{ads}, k_{des}, \sigma\}$, can be generated by minimizing the error function $F(p)$ defined as following:

$$F(p) = \min_{\theta} \sum_{i=1}^{p} (c_{i,ex} - c_{i,m})^2, \qquad \theta = \{\nu, k_{ads}, k_{des}, \sigma\} \tag{4-8}$$

where p is the total number of the experimental data. The minimization of Eq. (4-8) was performed with the MATLAB function *lsqnonlin*.

Method of lines (MoL) [21] was used to discretize the column in space dimension. The boundary conditions of the column were Danckwert's boundary conditions [22]. The discretized model was solved with a stiff ordinary differential equation solver (*ode15s*) using variable-order method in MATLAB [23].

For estimating the dispersion coefficient's dependency on flow rate, the mean particle Peclet number (*Pe*) estimated to be 0.5 [24], the dispersion coefficient was calculated from:

$$D_{ax} = \frac{u_{\text{int}} d_p}{Pe} \tag{4-9}$$

The film mass transfer coefficient k_f can be estimated from the correlation [25]:

$$Sh = (7 - 10\varepsilon_c + 5\varepsilon_c^2)(1 + 0.7\,\mathrm{Re}^{0.2}\,Sc^{1/3}) + (1.33 - 2.4\varepsilon_c + 1.2\varepsilon_c^2)\,\mathrm{Re}^{0.7}\,Sc^{1/3} \quad (4\text{-}10)$$

where $Sh = k_{eff}\,d_p/D_m$ is the Sherwood number, $Re = u_0\rho d_p/\eta$ is the Reynolds number and $Sc = \eta/\rho D_m$ is the Schmidt number.

To ascertain that the model is correct, the confidence interval of the parameters calculated from the Jacobian and the residual. The model is then compared to the validation experiments, and if the simulation fits the experiments, the model is valid. The validity region can now be determined as the union between the calibration region and the validation experiments.

4.3.3.3 Optimization method

The calibrated mechanistic model was then employed for optimization with respect to an objective function. In this study, yield as the fraction of target protein eluted was defined the objective function. The purity of lactoperoxidase was used as the nonlinear inequality constraint with the requirement of 85%. The parameters such as concentration of the feed and pH are determined by the composition of natural milk. Other parameters such as buffer, eluting salt and stationary phase material were kept the same during the optimization step. The main decision variables were determined according to the results of the DoE-RSM; length of gradient has no significant effect on yield thus the response to variation of the final salt concentration in the elution and mobile phase flow velocity was studied by computer simulation. The optimization problem with respect to the objective was solved using *fmincon* in MATLAB. FMINCON finds the optimum of an objective function Y with defined lower and upper boundaries on the decision variables. The optimization problem can be defined as:

$$Y_{max} = \max_{\substack{velocity \\ salt\ concentration\ at\ the\ end\ of\ gradient}} (Y)$$

$$LB \leq x \leq UB$$

subject to purity ≥ purity requirement

Table 4-1 Coded and un-coded values of the process factors in screening experiments of central composite design

Run	Coded			Un-coded		
	Salt	Length of gradient	Flow velocity	Salt (M)	Length of gradient (CV)	Flow velocity (cm/min)
1	-1	-1	-1	0.35	15	2.1
2	1	-1	-1	1.1	15	2.1
3	-1	1	-1	0.35	30	2.1
4	1	1	-1	1.1	30	2.1
5	-1	-1	1	0.35	15	4.998
6	1	-1	1	1.1	15	4.998
7	-1	1	1	0.35	30	4.998
8	1	1	1	1.1	30	4.998
9	-1.681	0	0	0.094	22.5	3.549
10	1.681	0	0	1.355	22.5	3.549
11	0	-1.681	0	0.725	9.88	3.549
12	0	1.681	0	0.725	35.1	3.549
13	0	0	-1.681	0.725	22.5	1.112
14	0	0	1.681	0.725	22.5	5.985
15	0	0	0	0.725	22.5	3.549
16	0	0	0	0.725	22.5	3.549
17	0	0	0	0.725	22.5	3.549
18	0	0	0	0.725	22.5	3.549
19	0	0	0	0.725	22.5	3.549
20	0	0	0	0.725	22.5	3.549

4.4 Results and discussion

4.4.1 Results of Response surface modeling

In this study, the best-fitting response surface provided a functional relationship between the objective function yield and the gradient explanatory factors salt concentration, length of gradient and flow velocity. The normal probability plot of the residuals from the analysis was normally distributed; indicating no evidence of non-normality, skewness,

outliers, or unidentified variables exist. An R^2 of 0.89 is probably due to the variations in the experiments at the six center points.

According to the analysis of variance (ANOVA), the calculated probability (p-value) of a test statistic was less than 0.005 for the term final concentration of salt which translates its significance within 95% confidence interval; whereas the p-values of gradient length and flow velocity justifies that the coefficients are zero. The mixed effects/interaction terms of each two factors were also quantified and revealed no considerable effect in the response model. The coefficient plot (Figure 4-1) shows the scaled and centered coefficients for the most important factors and their influence on the objective function. The height and direction of the bars illustrate the corresponding significance of each factor. In addition, the coefficient plot displays relatively large confidence intervals for the coefficients. The broad confidence intervals are probably due to variations in the experimental equipment as the six center points show fairly large variance. Another explanation could be the fact that the investigated system reveals non-linear performance that the statistical model cannot describe.

Analysis of the model response shows that gradient final salt concentration is an important factor for yield. This is to be expected as salt will displace protein as elution proceeds, and as a result more protein will be present in the collected fractions. It suggests that gradients with a high salt concentration at gradient end were most successful with respect to the separation problem.

The variation in the two factors gradient length and flow velocity were not high enough to cause an effect on the separation of lactoperoxidase in the process. It assures that at higher flow rates, there is no broadening effect or leakage in the loading step. The significance of the coefficient for velocity×velocity term with regard to the p-value predicted by the model indicates that the hypersurface exhibits a curvature meaning that there is a maximum/or minimum somewhere in the direction of flow velocity (Figure 4-2).

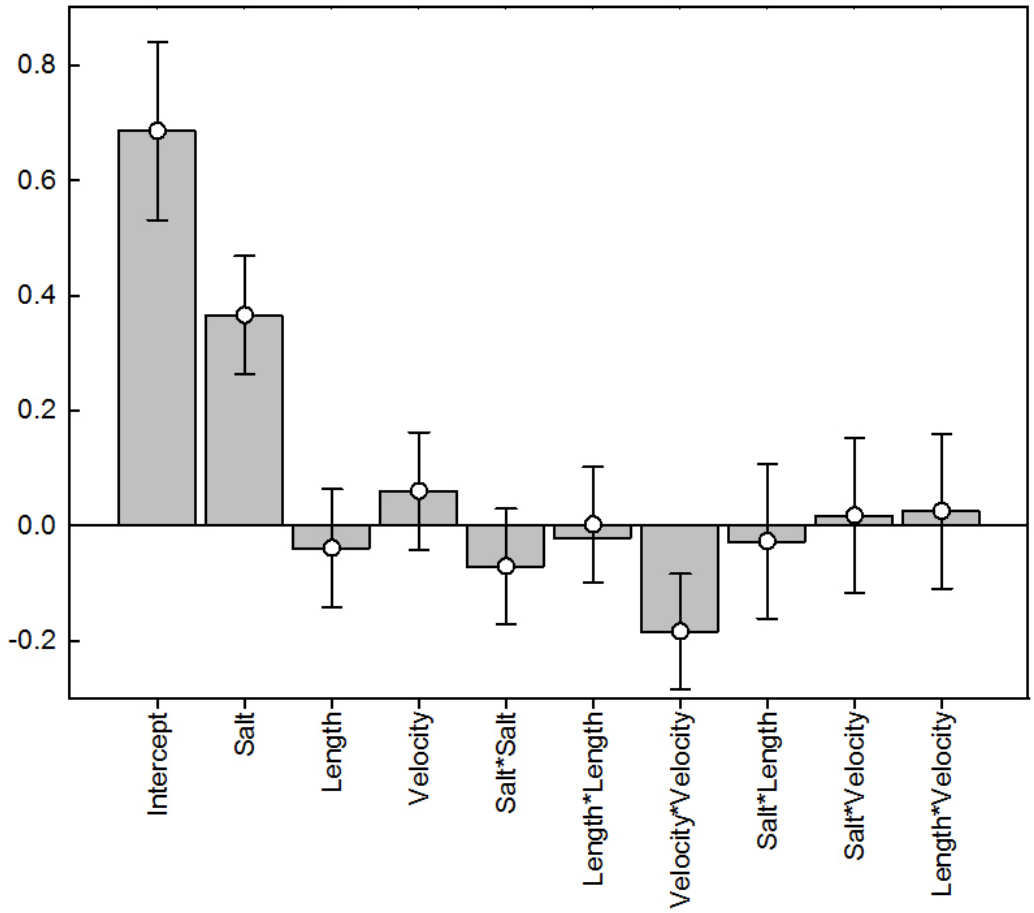

Figure 4-1 The coefficient plot resulting from the response surface regression of the screening experiments. The coefficient are scaled and centered and the height and direction of the bars show the relative importance of each factor.

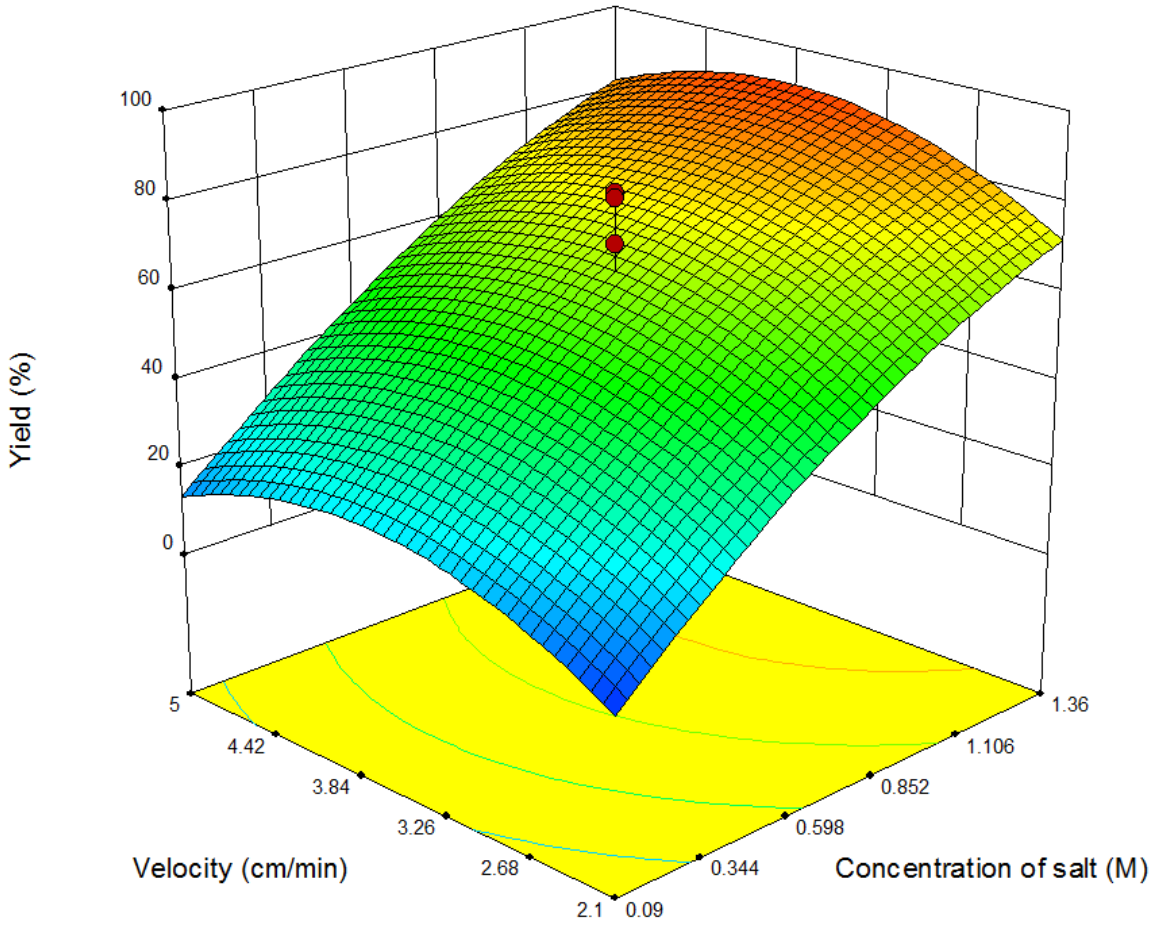

Figure 4-2 3D surface plot based on the CCD method

The Figure 4-3 illustrates the projection of the response surface as a two dimensional plane for three levels of the factor length of gradient 15, 22.5 and 30 CV. As can be seen in Figure 4-3, the maximum velocity of around 3.8 cm/min with highest concentration of salt in elution buffer is predicted to achieve maximum protein yield to for all gradient lengths. The optimal region is quiet large and the concentration of salt within the contour plot is steep. This indicates that small changes in the concentration of salt in elution buffer will have significant effects on the product quality of the investigated process.

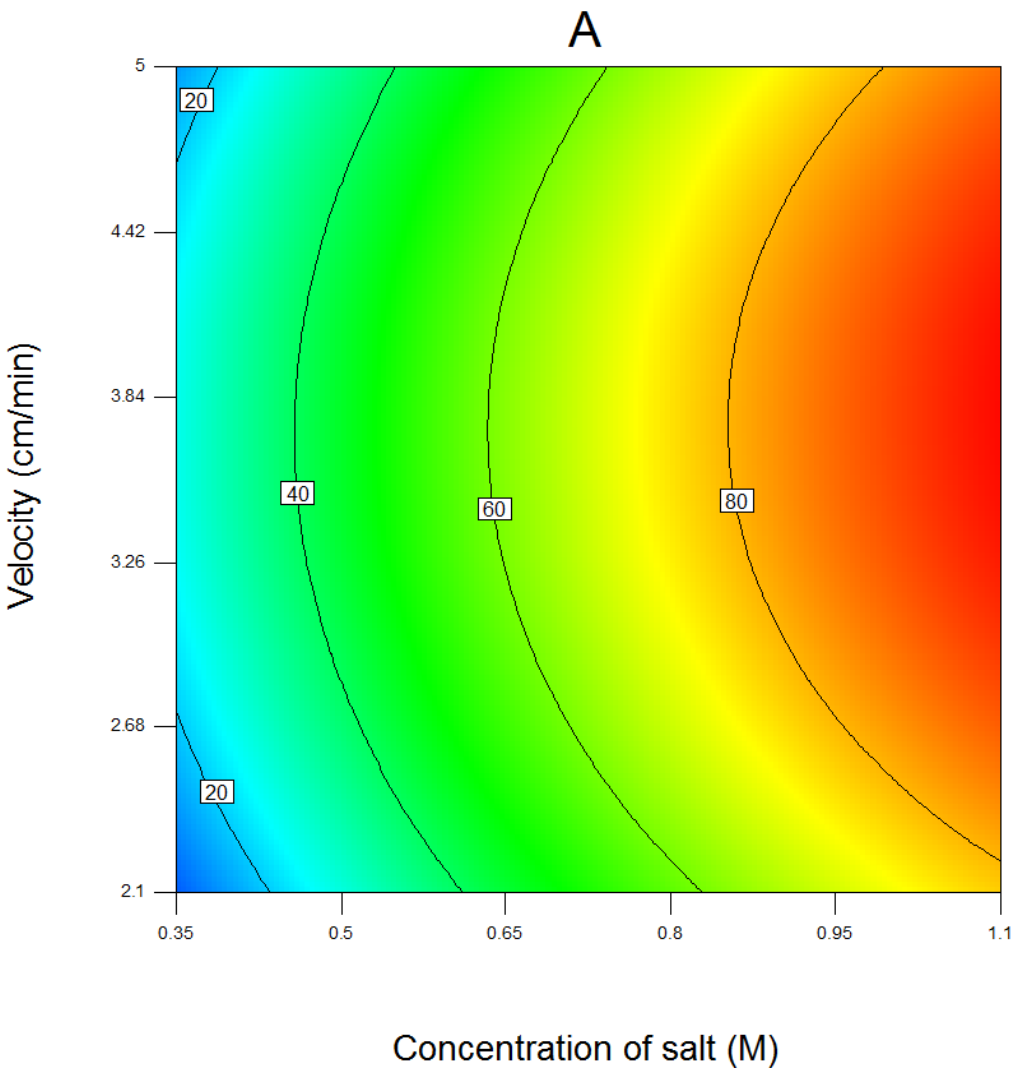
A
Velocity (cm/min)
5
4.42
3.84
3.26
2.68
2.1
20
40
60
80
20
0.35
0.5
0.65
0.8
0.95
1.1
Concentration of salt (M)

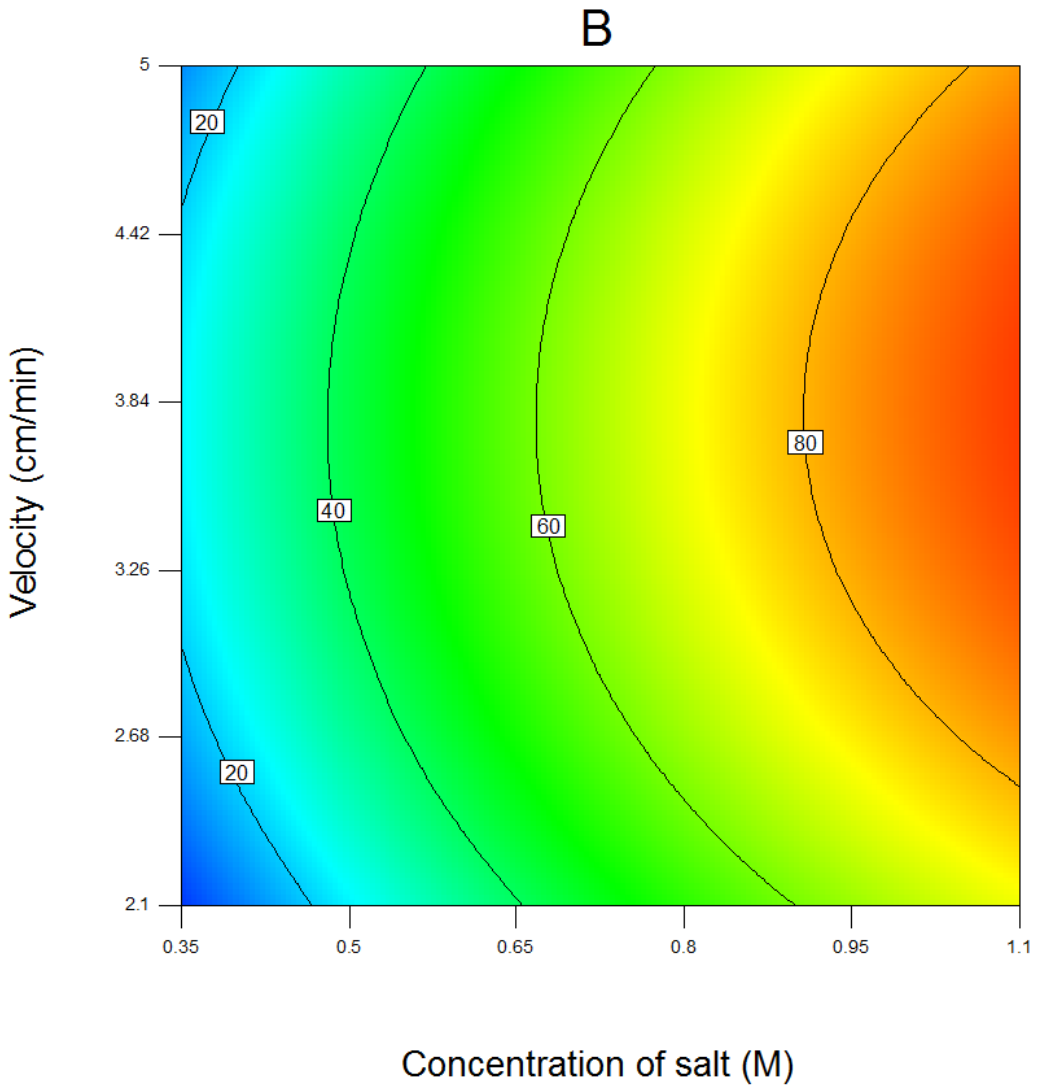
B
Velocity (cm/min)
5
4.42
3.84
3.26
2.68
2.1
20
40
60
80
20
0.35
0.5
0.65
0.8
0.95
1.1
Concentration of salt (M)

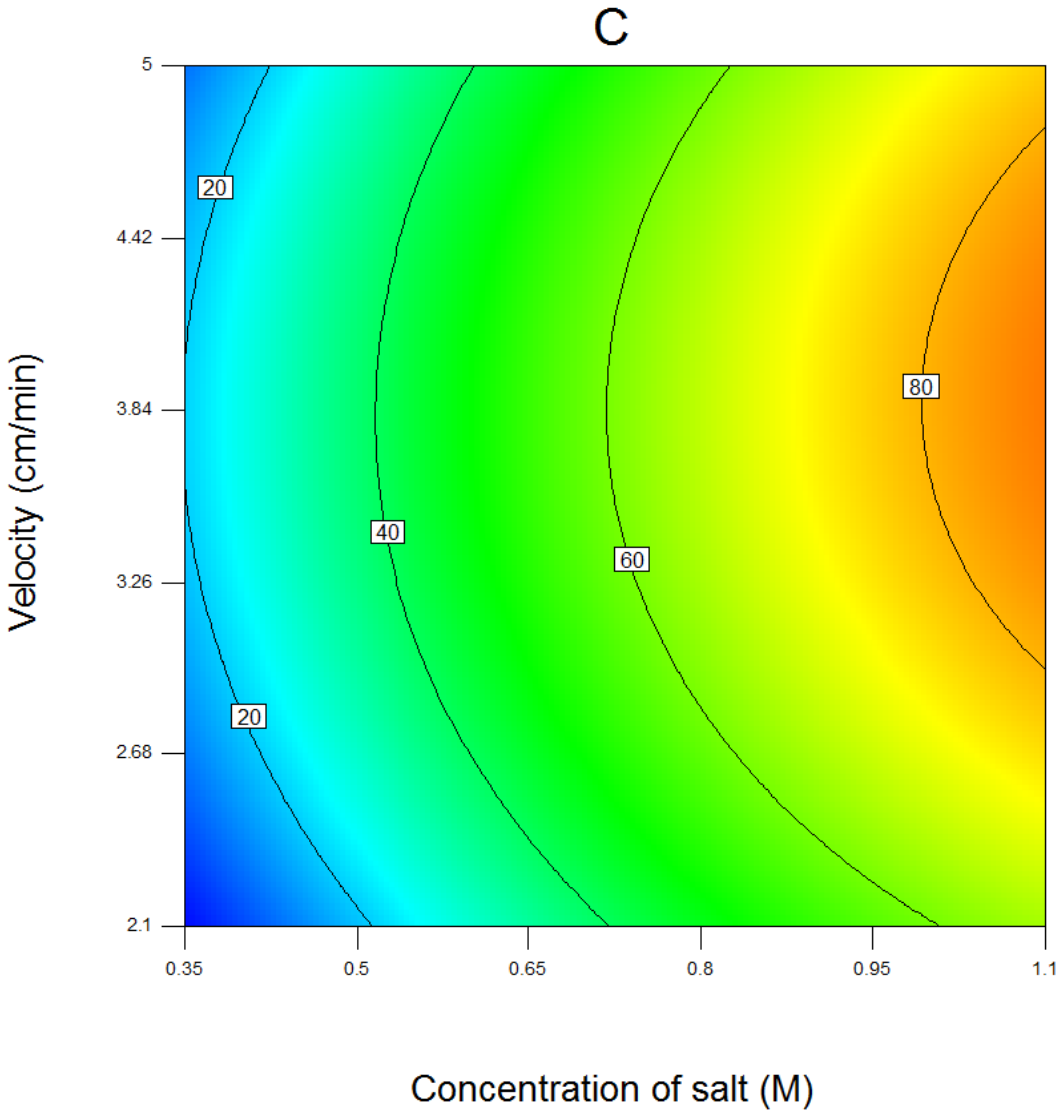

Figure 4-3 Surface contour plots based on 20 experiments. The factors Final concentration of salt and Flow velocity span the space, the factor Length is depicted in three levels: 15, 22.5, 30 CV. The contour lines illustrate the predicted values for the yield of lactoperoxidase

Based on this empiric model function and the modeling surfaces, the factor setups for maximum qualities of separation with respect to yield were predicted (see Table 4-2), experiments to evaluate the model predicted results were performed. The comparison between experimental results and the empiric model predictions shows low predictability

of the RSM model. As it can be seen in Figure 4-4, the predicted coefficient of determination, pred-R^2 of about 0.66, indicates a narrow predictability. In other words, quadratic RSM can only describe 66% of the variety in the experimental data.

Table 4-2 Optimum factor set for maximum yield of lactoperoxidase based on the DoE–RSM approach

Concentration of salt (M)	1.10
Flow velocity (cm/min)	3.77
Gradient length (CV)	15
Predicted yield (%)	96.41
Experimental yield (%)	78.04

4.4.2 Results of the mechanistic model

4.4.2.1 Model calibration and validation

In this section, the bed parameters of a 4.7 mL prepacked HiScreen™ SP Sepharose FF column characterized in [26] were set into the mechanistic model. The adsorption parameters with their confidence intervals are presented in Table 4-3. The parameters were estimated based on DoE experiments in section 4.4.1 to keep the predictions over the similar design space. The steric factor (σ) had negligible influence on the fitting result; thus it was fixed during the optimization of Eq. (4-8) to previously calibrated values in [26]. Broad statistical range in the determination of σ has been reported before in [15] and [27].

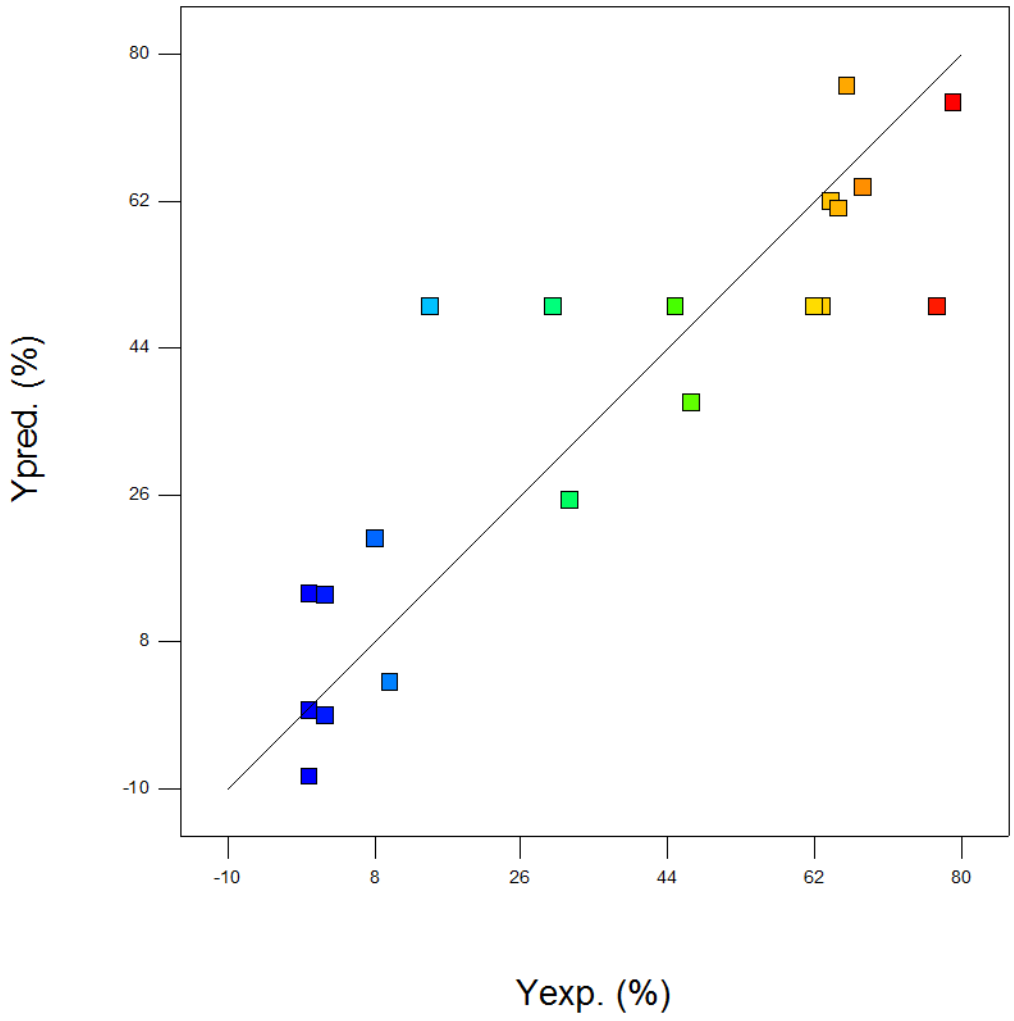

Figure 4-4 Experimental and predicted yield of lactoperoxidase. The predicted IEC yield was obtained using empirical functional relation

The successful predictions based on the calibrated and verified mechanistic model is a key associated to a model-integrated process development. The validation experiments were carried out as a gradient elution experiment with higher protein concentrations that were not used in the model calibration. The model fitted the validation experiment with relatively good accuracy; in Figure (4-6) an example chromatogram for the gradient elution experiments with 3.55 cm/min flow velocity an elution gradient volume of 22.5 CV at 0.26 and 1.47 mg/ml for LP and LF concentrations is shown. The elution gradient with started after 50 minutes and continued for around 50 minutes, at which point 100%

high salt buffer with a salt concentration of 0.725M NaCl was reached. The first breakthrough is LP and the second is LF. In the washing step, some of the LP and LF were washed out; the model did not capture this amount of protein loss, causing the lack of fit in the elution step at the chromatogram. The relative error between simulated and experimental chromatogram is only 2.9% for LP and 8.6% for LF protein. If a more accurate solution is sought, the model should be recalibrated based on a new set of DoE experiments in this region.

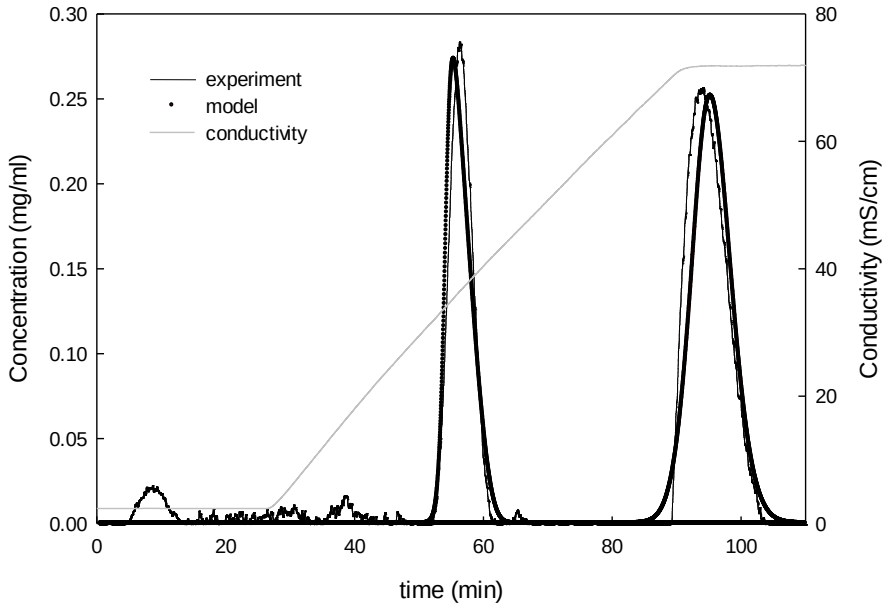

Figure 4-5 The validation experiment with an elution gradient of 22.5 CV

4.4.2.2 Optimization predictions based on the mechanistic model

The elution gradient was numerically optimized with respect to the objective function. On Table 4-4, the prediction for the optimal gradient based on SMA parameters derived from chromatograms of the 4.7 mL column on the ÄKTA system is given in numbers. To quantitatively evaluate the optimizing performance of the calibrated model, the experimental validation was performed with the corresponding data; chromatogram was beforehand transformed from the UV absorbance measurements on the ÄKTA system to mg/ml of protein using extinction coefficient. However, the experimental yield is close to

the predictions with a good precision and describes the mechanistic model to be successful and predictive.

Table 4-3 SMA parameters for lactoperoxidase and lactoferrin on HiScreen™ SP FF column

	k_{eq}	ν	k_{des}	σ
lactoperoxidase	0.22±0.005	3.07±0.014	19.89±0.071	1283
lactoferrin	11.65±0.003	2.73±0.006	0.98±0.22	0.98

The predictions for the yield of lactoperoxidase with respect to optimal operating conditions deviate slightly; one explanation for this deviation can be the dynamic effects that the model cannot handle; for instance pH-variations caused by increasing high salt buffer in the system as suggested in [17]. However, as the constraint on purity ($\geq 85\%$) was acceptably satisfied in the optimization step, thus deviation in the yield of protein can be ignored. The lowest expected purity can be determined by means of the confidence intervals of the process parameters.

Table 4-4 Optimum factor sets for maximum yield of lactoperoxidase based on the mechanistic modeling approach

Concentration of salt (M)	0.82
Flow velocity (cm/min)	4.32
Gradient length (CV)	16.28
Predicted yield (%)	89.92
Experimental yield (%)	86.73

4.5 Conclusion

The method presented in this manuscript constitutes data from factorial design of experiment approach to quickly identify the significance of process parameters on the objective function as well as complexity of the system. The empiric multi-variate model revealed a low capability to predict the behavior in the IEC column with respect to optimal operating settings for separation as a result of lack of fit and limitations in robustness of linear gradient elution process. Nevertheless, it was reasonably accurate to prove the significant factors. In the next step, mechanistic model was calibrated based on the DoE-planned experiments by the inverse method. The calibrated model with reduced number of variables was then applied to find the optimal operating conditions and provide insight into the knowledge of process performance with respect to yield of lactoperoxidase and more accurate predictions with respect to process variations. The optimal operation was successfully predicted, yet the prediction of yield was slightly deviates from the experimental results. It can be related to some effects such as random configuration of protein interacting with binding sites of the adsorbent or slight changes in pH during salt gradient elution step that the model was unable to take into account.

In summary, model-integrated process development proved to be efficient with regard to the objective for the optimization of process and led to find the true optimum process parameters of flow velocity and concentration of salt at the end of gradient.

References

[1] B. Ekstrand, Antimicrobial factors in milk - a review, Food Biotechnol. 3 (1989) 105–126.

[2] C.A. Barth, S. E., Milk proteins: nutritional, clinical, functional and technological aspects, Darmstadt, 1988.

[3] L. Pedersen, J. Mollerup, E. Hansen, A. Jungbauer, Whey proteins as a model system for chromatographic separation of proteins, J. Chromatogr. B. 790 (2003) 161–173.

[4] S.. Gerberding, C.. Byers, Preparative ion-exchange chromatography of proteins from dairy whey, J. Chromatogr. A. 808 (1998) 141–151

[5] R. Hahn, P.. Schulz, C. Schaupp, A. Jungbauer, Bovine whey fractionation based on cation-exchange chromatography, J. Chromatogr. A. 795 (1998) 277–287.

[6] M.M.H. El-Sayed, H.A. Chase, Purification of the two major proteins from whey concentrate using a cation-exchange selective adsorption process, Biotechnol. Prog. (2009) NA–NA.

[7] C.J. Fee, A. Chand, Capture of lactoferrin and lactoperoxidase from raw whole milk by cation exchange chromatography, Sep. Purif. Technol. 48 (2006) 143–149.

[8] W.A. Rombauts, W.A. Schroeder, M. Morrison, Bovine Lactoperoxidase. Partial Characterization of the Further Purified Protein, Biochemistry. 6 (1967) 2965–2977..

[9] M.R. Ladisch, Bioseparations Engineering: Principles, Practice, and Economics, John Wiley & Sons, New York, 2001.

[10] H.G. Harrison, P. Todd, S.R. Rudge, P.P. Demetri, Bioseparations and Engineering, Oxford University Press, Oxford, 2003.

[11] P. Knight, Chromatography: 1989 Report, Bio/Technnology. 7 (1989) 243–249.

[12] F.D.A.U.S. Department of Health and Human Services, Guidance for Industry PAT – A Framework for Innovative Pharmaceutical Manufacturing and Quality Assurance., (2004).

[13] C.F. Mandenius, A. Brundin, Bioprocess optimization using design-of-experiments methodology, Biotechnol. Prog. 24 (2008) 1191–1203.

[14] M.A. Bezerra, R.E. Santelli, E.P. Oliveira, L.S. Villar, L.A. Escaleira, Response surface methodology (RSM) as a tool for optimization in analytical chemistry, Talanta. 76 (2008) 965–977.

[15] H. Iyer, S. Tapper, P. Lester, B. Wolk, R. van Reis, Use of the steric mass action model in ion-exchange chromatographic process development, J. Chromatogr. A. 832 (1999) 1–9.

[16] A.A. Shukla, S.S. Bae, J.A. Moore, K.A. Barnthouse, S.M. Cramer, Synthesis and Characterization of High-Affinity, Low Molecular Weight Displacers for Cation-Exchange Chromatography, Ind. Eng. Chem. Res. 37 (1998) 4090–4098.

[17] C.A. Brooks, S.M. Cramer, Steric mass-action ion exchange: Displacement profiles and induced salt gradients, AIChE J. 38 (1992) 1969–1978.

[18] A. Carlström, The heterogeneity of lactoperoxidase, Acta Chem. Scand. 19 (1965) 2387–2394.

[19] W.G. Bardsley, Steady-state kinetics of lactoperoxidase-catalyzed reactions., Immunol. Ser. 27 (1985) 55–87.

[20] G. Guiochon, A. Felinger, D.G. Shirazi, A.M. Katti, Fundamentals of preparative and nonlinear chromatography, Academic Press, San Diego, USA, 2006.

[21] M.E. Davis, Numerical Methods and Modeling for Chemical Engineers, John Wiley & Sons, New York, 1984.

[22] P.V. Danckwerts, Continuous flow systems, Chem. Eng. Sci. 2 (1953) 1–13.

[23] L.F. Shampine, M.W. Reichelt, The MATLAB ODE Suite, SIAM J. Sci. Comput. 18 (1997) 1–22.

[24] T.K. Sherwood, R.L. Pigford, C.R. Wilke, Mass Transfer, McGraw-Hill, 1975.

[25] D.J. Gunn, Axial and radial dispersion in fixed beds, Chem. Eng. Sci. 42 (1987) 363–373.

[26] N. Faraji, Y. Zhang, A.K. Ray, Determination of adsorption isotherm parameters for minor whey proteins by gradient elution preparative liquid chromatography, J. Chromatogr. A. 1412 (2015) 67–74.

[27] A.A. Shukla, S.S. Bae, J.A. Moore, K.A. Barnthouse, S.M. Cramer, Synthesis and Characterization of High-Affinity, Low Molecular Weight Displacers for Cation-Exchange Chromatography, 5885 (1998) 4090–4098.

[28] A. Osberghaus, S. Hepbildikler, S. Nath, M. Haindl, E. von Lieres, J. Hubbuch, Optimizing a chromatographic three component separation: A comparison of mechanistic and empiric modeling approaches, J. Chromatogr. A. 1237 (2012) 86–95.

Chapter 5

Impact of operating conditions on chromatography column performance- Experimental study of high-value minor whey proteins adsorption

Abstract

Over the last decades, ion-exchange chromatography (IEC) has been extensively developed for protein purification at both small and large scales. Despite several IEC columns are commercialized, the physical phenomena underlying the adsorption of proteins on ion-exchange columns performance has not been completely investigated. In this work, the influence of operating conditions on the adsorption of lactoperoxidase (LP) and lactoferrin (LF) on cation exchange chromatography adsorbent is experimentally studied in order to disclose clues to the relevant mechanisms. Analysis was carried out in columns with different I.D. (7.7 and 16 mm), packed for 100 mm with 90 μm particle size polymer-grafted cation exchanger. The flow distribution was measured using acetone as a non-binding tracer. An evaluation of van Deemter plots was done as well as LP breakthrough curves at different flow rates and LP loading concentrations. The results were compared with two columns in terms of efficiency and the LP binding capacity. The dynamic binding capacity at 10% breakthrough was found to be independent of the applied flow rate. Surprisingly in both systems, LP breakthrough takes place later at higher loading concentrations which is in contrast to IEC. The results propose a major presence of non-ideal effects as steric shielding and charge repulsion of protein in the adsorption. In addition, the accessibility of binding sites for protein at higher concentrations seems more available than sodium counter-ions in buffer.

Keywords

Ion-exchange chromatography, Breakthrough curve, Dynamic binding capacity, Column efficiency, Lactoperoxidase

5.1 Introduction

Ion-exchange chromatography was introduced in the mid-1940s as a separation technique based on charge properties of molecular species [1]. Within the last few decades, there has been an increasing interest in liquid chromatographic processes because of the

developing biotechnology scope and demands from the pharmaceutical and chemical industries for extremely particular and productive separation methods. Today, IEC is being employed for purification of proteins, peptides, nucleic acids and other charged biomolecules. IEC technique is well-suited for capture, intermediate purification or polishing steps in a purification protocol. IEC columns are commercially available from several suppliers, ranging from microscale purification and analysis through to purification of kilograms of product.

With increased commercial usage, in-depth understanding of different mechanisms within chromatography columns is desirable in order to achieve optimum performance. Regardless of application may be intended, operators seek a common set of performance characteristics such as high capacity and recovery, lot-to-lot reproducibility, purification factor and a high degree of process control. Method development for protein purification processes is preferably done at small scale typically to obtain a robust, scalable process with the highest possible performance at the lowest cost without compromising with the product quality. This has stimulated much research to study the principles of preparative chromatography and the important subject of scale up.

The performance of a chromatography column rests on elements of design and operational factors. Several studies have been focused on the determination of the experimental settings and column design parameters of separations in preparative chromatography. Atamna et al. [2] studied effect of column diameter on resolution and efficiency with four different diameters using constant length columns. Gritti and Guichon [3] explained the theoretical and experimental investigations of the impact of the column diameter to the average particle size on the column performance that manufacturers of narrow-bore and/or capillary columns with small bed aspect ratio are facing.

Rathore and Velayudhan [4,5] presented an overview of the fundamentals and practices of scale-up in preparative chromatography. Modes of interaction and modes of operation are defined to clarify the choices available in the course of scale-up. The scaling up of ion-exchange processes for protein separation has been reported in several studies. For

example, Levison et al. [6] investigated an ovalbumin separation from hen egg-white on the anion exchange with a 1000-fold scale-up. Fibrous cellulose-based ion-exchangers were operated at high flow rates in a process-scale system demonstrating no loss of capacity or binding efficiency for the target proteins. Gerberding and Byers [7] described a preparative anion exchange processing of proteins from dairy whey scaling from 5 cm to 140 cm column diameter to an economically optimized production level operation. According to the theory, an effective scale-up can be achieved by holding the retention time of the components inside the column constant [8–10]. This means that the flow rate, loading and gradient length are scaled to the column volume. Thus, one has to decide as respects column dimension and the column aspect ratio. The column aspect ratio has an impact on the pressure drop over the chromatographic bed and consequently on the bed compaction. The key point in scale-up is the concept of time scales. The time scales involved are the time scales for flow, mass transfer, and dispersion. When scaling up or scaling down, processes of similarity will be processes, which have identical time scales [11].

It should be emphasized that many of the comparative issues and scale-up challenges are associated with momentum and mass-transfer problems in a large-scale production process. The combined effects of convection, axial dispersion, mass transfer within the particle pores, and sorption rate limitations reduce the performance [12-15]. Column performance can also be affected by other factors such as protein denaturation [16] and extra-column effects [17]. Depending on specific conditions, one or more of these mechanisms may dominate contributions to band broadening and peak asymmetry (fronting and tailing) or distortions [12,18], which can considerably affect separation effectiveness [19]. Some process procedures can be difficult to control, may suffer from a lack of reproducibility and involve significant losses of product. The feasibility and successful application of ion-exchange chromatography in the purification of proteins at pilot and process scale remains to be demonstrated.

A preparative chromatography study was conducted to investigate the effect of operation conditions on the dynamic adsorptive behavior of proteins in a commercialized strong cation ion-exchange SP Sepharose Fast Flow (SP FF). As separation efficiency relies on

the flow properties of the column, the flow distribution was first observed under a non-binding condition loading an acetone solution. Prior to carry out the scale-up calculations, it is essentially necessary to figure out which mass transfer mechanism is controlling the ion-exchange process. The diffusion mechanism is often dominated mass transfer resistance for protein chromatography. To check if this hypothesis was the case for minor whey proteins and in particular lactoperoxidase, the height equivalent to plate number (HETP) and breakthrough profiles were determined for two columns with different diameters. The bed height was kept the same to maintain kinetic and dynamic equivalence. We investigated HETP as a function of velocity for LP and LF under non-binding conditions. LP breakthrough curves were then obtained at different flow rates and LP loading concentrations. The dynamic binding capacity at 10% breakthrough was calculated and compared for the both columns. Finally, the column efficiency in terms of HETP as well as dynamic binding capacity of the column performance for two different scales was evaluated.

5.2 Materials and methods

5.2.1 Materials

Lactoperoxidase and lactoferrin from bovine milk both ≥ 90% purity were used. For elution under non-retained conditions, the elution buffer was prepared from 20 mM solution of Na2HPO4 and NaH2PO4, by adding 1 M NaCl adjusted to pH 6.7. For breakthrough studies under retained conditions, the running buffer was phosphate buffer saline (PBS), adjusted to pH 6.7. All chemical reagents used in the present work were purchased from Sigma-Aldrich (Oakville, Canada), except acetone and HCl from Caledon. Ultra-pure water was obtained using a Milli-Q system (Barnstead easy-pure RODI equipped with 0.2 µm filter, Fisher Scientific). Prior to use, all buffer solutions were filtered through a hydrophilic polypropylene membrane filter with a 0.2 µm pore size (PALL life Sciences, Canada) and de-gassed.

Table 5-1 Characteristics of the columns used in experiments

Parameter	HiScreen™ SP FF	HiPrep™ SP FF
Column length (mm)	100	100
Column i.d. (mm)	7.7	16
Median particle size (μm)	90	90
Column voidage	0.296	0.273
Particle voidage	0.893	0.856
Total voidage	0.917	0.895

5.2.2 Columns and instrument

The 90 μm SP Sepharose prepacked HiScreen™ and HiPrep™ columns (7.7 mm × 100 mm and 16 mm×100 mm) were used from GE Healthcare (Mississauga, Canada). The experiments were carried out on the ÄKTA purifier 100 system (GE Healthcare Life Sciences, Canada), which includes two system pumps, a fraction collector and monitors for multi-wavelength UV absorption, pH, and conductivity. UNICORN™ 5.31 software was used for data acquisition and system control. The flow rate accuracy was checked by directly collecting the mobile phase in the absence of column at room temperature and displayed the long-term accuracy. The dead volume of the experimental device and void volumes of two columns were estimated from the elution volumes of acetone and dextran respectively corrected for the extra-column contribution.

5.2.3 Breakthrough curves under non-binding conditions

The system dispersion curve was measured using a phosphate buffer containing 3% (v/v) acetone. The non-binding breakthrough data were fitted to Eq. 1 to determine the Péclet number (Pe) using least squares regression [20]. For mass transfer, the dimensionless number Pe describes the relative rate of convective and diffusion. In Eq. (5-1), c is the

outlet effluent concentration, c_0 is the solute loading concentration, $V_{loading}$ is the volume of acetone solution loaded, and V_{50} is the loaded volume when c/c0= 0.50.

$$\frac{c}{c_0} = \frac{1}{2}\left\{1 + erf\left(\frac{Pe^{1/2}(V_{loading} - V_{50})}{2(V_{loading}V_{50})^{1/2}}\right)\right\} \quad (5\text{-}1)$$

5.2.4 Measurement of the HETP data under non-retained condition

A concentration of 0.2 mg/ml for each protein was used. The experimental protocol is as follows: 1% CV of each protein solution is injected into the column which the buffer solution is flowing through. Similarly to non-binding breakthrough, the binding experiments were monitored by recording the UV absorbance of protein at 280 nm at the column exit. Each experiment was conducted at different flow rates between 0.8-3.5 mL/min and 1.68-5.8 mL/min corresponding to linear velocities of 1.74-7.52 cm/min for HiScreen™ and 1.74-2.90 cm/min HiPrep™ columns respectively. All experiments were carried out at room temperature. Table 5-2 summarizes the experimental conditions used. It should be noted that volumes of 47 µL and 200 µL of protein samples (equivalent to 1% CV) were injected into the 7.7 mm×100 mm and the 16 mm×100 mm in order to maintain constant sample loading per unit of column cross-section area.

Table 5-2 Experimental conditions for height equivalent to theoretical plate measurement in elution chromatography of proteins

Protein	LP and LF
Concentration (mg/mL)	0.2
Injection volume (µL)	47*, 200**
Flow velocity (cm/min)	1.74, 2.50, 3.33, 4.50, 5.82, 6.67, 7.52*
	0.84, 1.00, 1.74, 2.00, 2.50, 2.88**
Buffer	20 mM NaH_2SO_4+Na_2HPO_4, 1 M NaCl pH 6.7
Temperature (^oC)	22-22.5

*HiScreen™ column

**HiPrep™ column

5.2.5 Breakthrough curves for protein adsorption on SP Sepharose FF media

Only LP was used for these studies. The breakthrough curves were measured at different LP concentrations (0.02, 0.06, 0.1, 0.5 and 1 mg/mL) and flow velocities (1.74, 2.00, 2.50, 2.90 cm/min). The loading step with the protein solution was stopped after the outlet concentration of the column reached to the feed solution absorbance, afterwards the column was washed using 20 mM sodium phosphate + 1 M NaCl solution for 5 CV, followed by phosphate buffers for 5 CV of each. To compare the adsorption performance on two columns, the dynamic binding capacity at 10% breakthrough (DBC10%) was calculated using Eq. (5-2), where c is the LP outlet concentration, c_0 is the LP loading concentration, V10% is the loading volume of LP solution when $c/c_0 = 0.10$ and V_c is the volume of the column.

$$DBC_{10\%} = \frac{c_0 \int_0^{V_{10\%}} (1 - \frac{c}{c_0}) dV_{loading}}{V_c} \quad (5\text{-}2)$$

All experiments were carried out at room temperature. Conditions are reported in Table 5-3.

Table 5-3 Experimental conditions for breakthrough studies on SP FF

Protein	LP
Concentration (mg/ml)	0.02, 0.03, 0.06, 0.1, 0.5, 1
Flow velocity (cm/min)	1.74, 2, 2.50, 2.80
Buffer	20 mM NaH_2SO_4+Na_2HPO_4, pH 6.7
Temperature (^oC)	22-22.5

5.3 Results and discussion

5.3.1 Analysis of flow distribution

Due to low Reynolds number (*Re*) typical in protein chromatography, physical insights on the flow distribution are particularly important for understanding and predicting the transport of molecules through the column. For each column, the acetone breakthrough curve was measured under non-binding conditions. As can be seen in Figure 5-1, the typical breakthrough curves obtained for both columns are identical. In all following breakthrough profiles for HiPrep™ SP FF takes place later due to its larger void volume. The Pe number values were estimated from Eq. (5-1) and summarized in Table 5-4. The Pe values are comparatively identical for each column; the higher *Pe* numbers are preferred as they correspond to a uniform distribution of flow to the inlet surface of the column as well as uniform distribution of the binding site properties. At higher *Pe* values, the breakthrough curve tends to approach ideality and breakthrough corresponds to the capacity of the media. Indeed, higher efficiency due to less back mixing and shorter required time for diffusion can be achieved with higher flow rates.

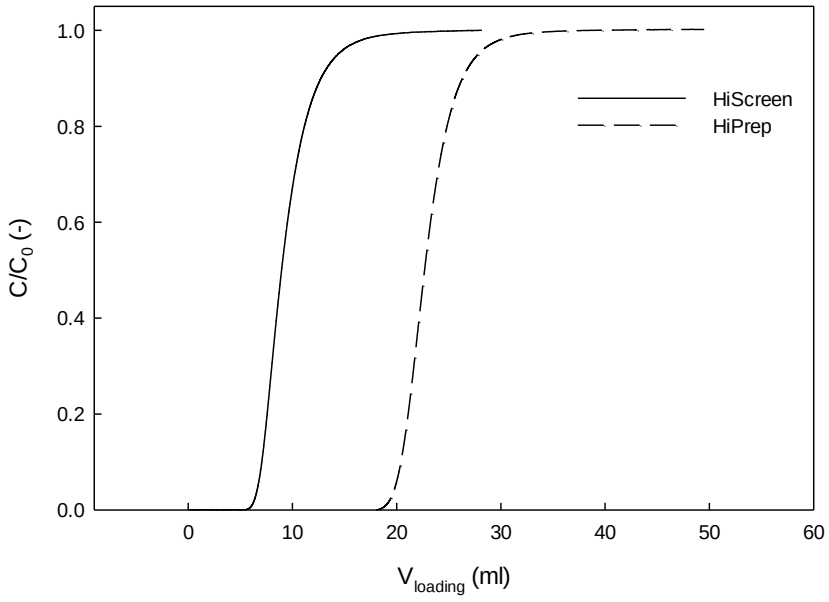

Figure 5-1 Non-binding breakthrough curves for HiScreen™ and HiPrep™ columns at a flow velocity of 2.5 cm/min and acetone loading concentration of 3% (v/v)

Table 5-4 Péclet numbers measured under a non-binding condition with 3% (v/v) of acetone

Chromatography column	HiScreen™ SP FF				HiPrep™ SP FF			
Velocity (cm/min)	3.333	4.946	5.828	7.527	0.836	2.488	2.985	3.333
Pe (–)	35.01±0.87	38.59±0.91	37.49±0.9	38.14±0.97	190.3±5.2	204.9±4.6	196.7±4.7	189±5.4

5.3.2 Operational Pressure

In laminar flow, the pressure drop ΔP across a bed of length L packed with particles of diameter d_p is given by Darcy's law:

$$\Delta P = \eta u_0 L / B_b \tag{5-3}$$

where η is the dynamic viscosity and $B_b = \varepsilon_c^3 d_p^2 / 150(1-\varepsilon_c)^2$ is the bed permeability which depends on bed structure properties. This parameter is closely associated to resistance to mass transfer. For the HiScreen™, bed permeability is calculated to be $B_b = 2.83\times10^{-8}$ and for HiPrep™ $B_b = 3.01\times10^{-8}\, cm^2/s$. Using these permeability values, the pressure drop ΔP can be estimated as a function of linear velocity u_0 (Figure 5-2). The pressures were lower than 0.7 bars for HiScreen™ and HiPrep™ columns, respectively. The large SP FF media pore size around 45-145 μm is a possible cause of this low backpressure which is an advantage for the operation. Both geometries show similar pressure values specifically at lower velocities due to their identical column height (10 cm). However as can be seen in Figure 5-2, the pressure was slightly higher with HiScreen™ column for the reason that it has smaller cross-section area.

It should be noted that the instrumentation employed in this study was not equipped with a pressure detector. Thus, the column pressure drop was only estimated and compared for the two columns.

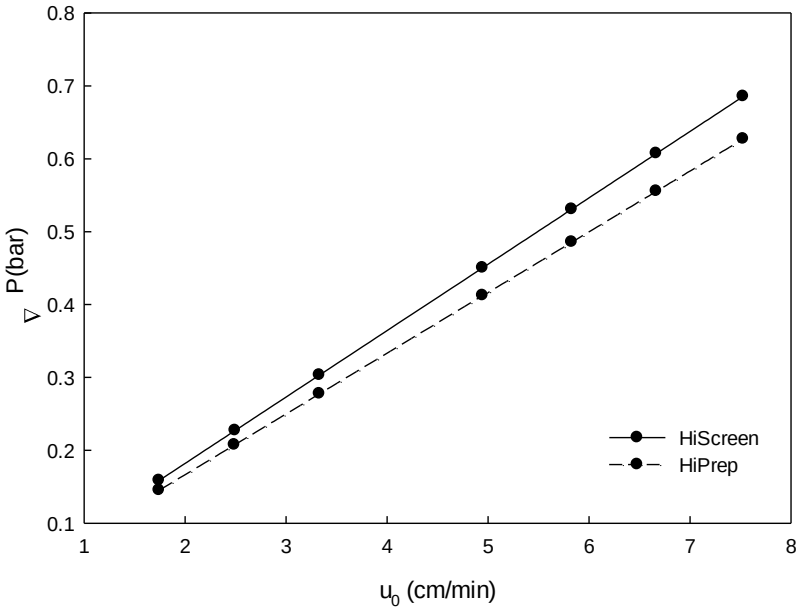

Figure 5-2 Operational pressures at different superficial velocities for the two scales of columns

5.3.3 Elution chromatography of proteins under non-retained conditions

The peak responses were recorded at a wavelength of 280 nm for both LP and LF. For each of these flow rates and for each sample, the extra column contributions to the retention volume and to the band broadening of probes were measured by replacing the chromatographic column with a ZDV union connector.

The experimental HETP data measured for the columns were corrected for the contribution of the ÄKTA FPLC system. The extra-column and the total band variances were measured according the numerical integration method. In this method, the data points (t_i,c_i) were considered and the true first and second central moments were calculated as follows:

$$\mu_1 = \frac{\int_0^t c(t)tdt}{\int_0^t c(t)dt} \tag{5-4}$$

$$\mu_2 = \frac{\int_0^t c(t)(t-\mu_1)^2 dt}{\int_0^t c(t)dt} \tag{5-5}$$

The moments were calculated based on the decomposition of the peak area into a series of elementary trapezes. The corrected reduced HETP, $h = HETP / d_p$, was given by:

$$h = \frac{L}{d_p}\frac{\mu_2 - \mu_{2,ex}}{(\mu_1 - \mu_{1,ex})^2} \tag{5-6}$$

where $\mu_{1,ex}$ and $\mu_{2,ex}$ are the first and second central moments of the extra column band profiles.

Chromatographic peaks for the two proteins (LP and LF) obtained at various flow rates on SP FF medium are shown respectively in Figure 5-3.

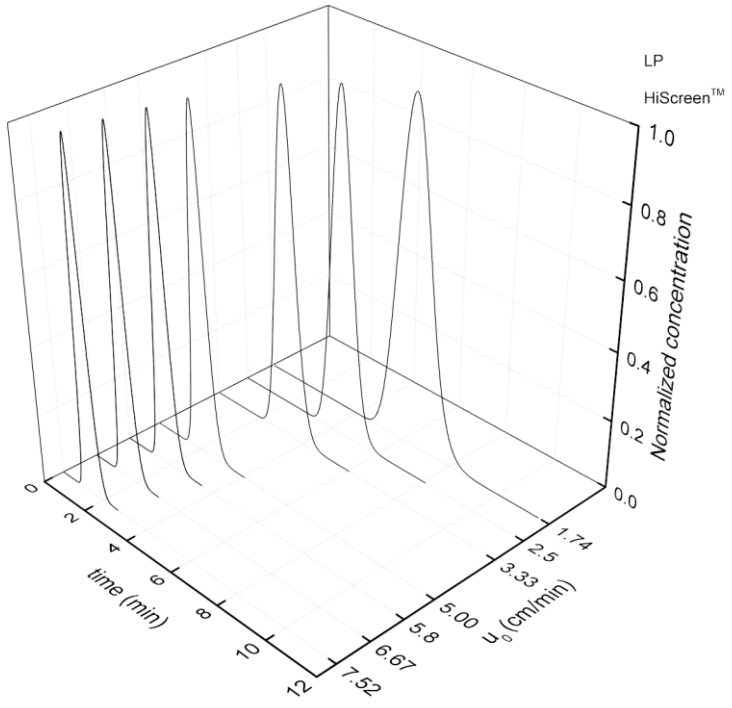
LP
HiScreen™
1.0
0.8
0.6
0.4
0.2
0.0
Normalized concentration
0
2
4
6
8
10
12
time (min)
1.74
2.5
3.33
5.00
5.8
6.67
7.52
u_0 (cm/min)

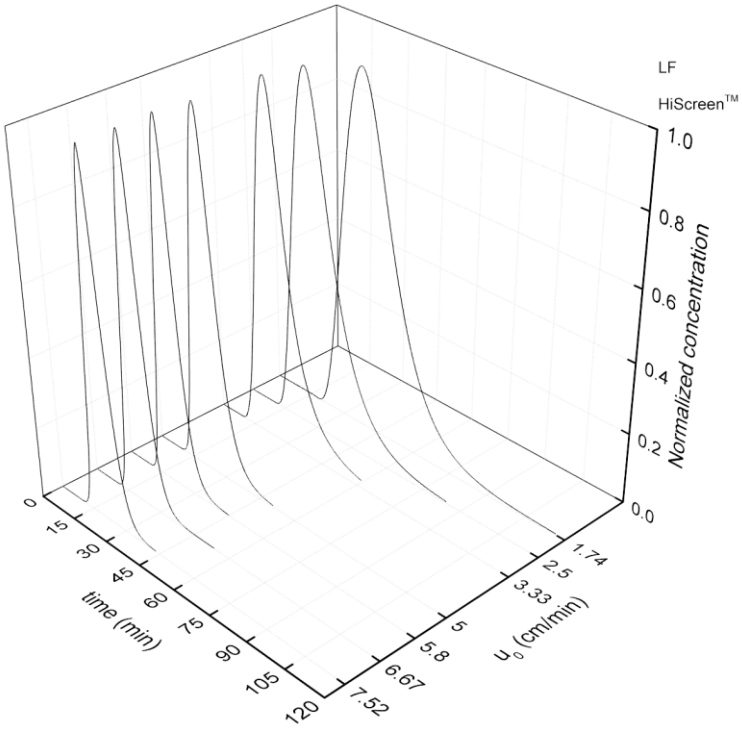
LF
HiScreen™
1.0
0.8
0.6
0.4
0.2
0.0
Normalized concentration
0
15
30
45
60
75
90
105
120
time (min)
1.74
2.5
3.33
5
5.8
6.67
7.52
u_0 (cm/min)

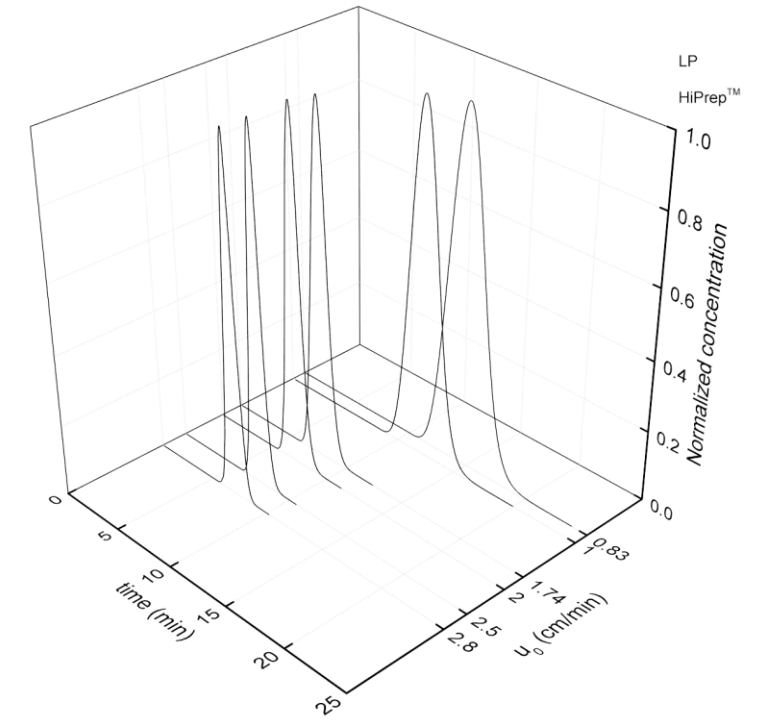
LP
HiPrep™
1.0
0.8
0.6
0.4
0.2
0.0
Normalized concentration
0
5
10
15
20
25
time (min)
0.83
1
1.74
2
2.5
2.8
u_0 (cm/min)

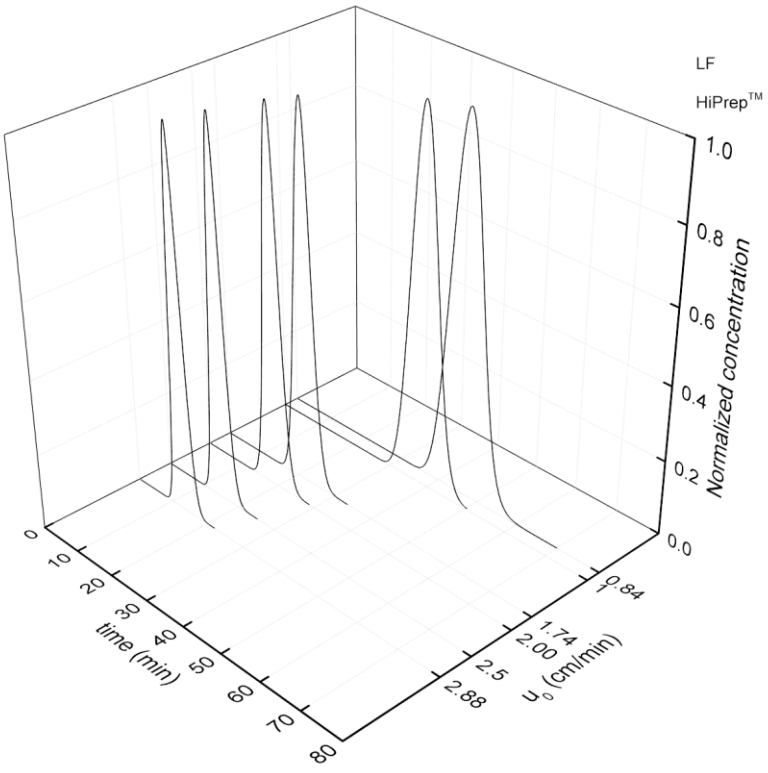
LF
HiPrep™
1.0
0.8
0.6
0.4
0.2
0.0
Normalized concentration
0
10
20
30
40
50
60
70
80
time (min)
0.84
1.74
2.00
2.5
2.88
u_0 (cm/min)

Figure 5-3 Elution chromatography of proteins on SP FF HiScreen™ and HiPrep™ columns under non-retained conditions LP and LF

5.3.3.1 HETP and Efficiency of chromatographic columns

A useful approach for the empirical characterization of column efficiency is based on van Deemter plot [21], which is used to assess the relative importance of dispersive and mass transfer kinetics. The experimental peaks for each protein in elution chromatography (Figure 5-3) were used to calculate HETP at various flow rates according to the numerical integration method described in previous section. The modified van Deemter equation adapted from [22] describes the effects of perfusion in a packed column:

$$H = A + \frac{B}{u_0} + Cf(\lambda)u_0 \tag{5-7}$$

In practical HPLC applications, $A = 2d_p$ and $B = 2D_m$; since the order of molecular diffusivity (D_m) is of $10^{-7}\ cm^2/s$ for proteins, the second term in Eq. (5-7) becomes negligibly small. The contribution of intra-particle convection becomes one at low flow rates. Thus, the slope of HETP vs. u_0 is simply and in terms of reduced HETP, i.e. $h = H / d_p$, can be written as:

$$\frac{dh}{du_0} = C = \frac{1}{30}\frac{\nu}{(1+\nu)^2}\frac{\varepsilon_p}{\varepsilon_c}\frac{d_p}{D_e} \tag{5-8}$$

where ε_c column voidage, ε_p particle voidage and ν is $((1-\varepsilon_c)/\varepsilon_c)\varepsilon_p$.

After initial rapid increase in HETP, the plot tends to a plateau at higher velocities expressed by Eq. (5-9). As u_0 increases, the slope of HETP plot changes and mass transport becomes dominated by intra-particle convection [23].

$$h_{plateau} = A + \frac{3}{5}\frac{\nu}{(1+\nu)^2}\frac{\varepsilon_p}{\varepsilon_c}\frac{B_b}{B_p} \tag{5-9}$$

Figure 5-4 illustrates the reduced HETP as a function of the superficial velocity that increases linearly with velocity for both proteins. The shape of HETP indicates the association with pore diffusion as the controlling mechanism of mass transport. It is essentially true as protein transport is restricted by diffusional hindrance due to large molecular configuration. This effect is even more remarkable for the two proteins of interest in this study. Indeed, as in our previous study, lactoperoxidase showed a high shielding factor indicating its hindrance impact on mass transport mechanism.

To check reproducibility, two separate columns for each diameter were used and evaluated. For analysis, a single modified van Deemter plot is fitted to the two separate column data sets for each I.D. The data points collected for two columns at each column diameter were virtually superimposable. Rather than averaging the end results of two separate columns, the data from each column was combined for a single modified van Deemter fit. The fitted parameters of A and C were calculated by using SigmaPlot from Systat Software Inc. The values for reduced A term were found to be 0.016 and 0.023 for the studied columns. These values are in a good agreement with the estimation of A which equals 0.018 for SP FF. The reduced plate height for the test columns slightly increased with the slope (C term) of 6.02 and 6.90 for 7.7 and 16 mm I.D. column, respectively. A similar trend was observed by Patel et al. [24]. They reported that the van Deemter A term and C term coefficient exhibited an increase with increasing column diameter. The results clearly show that both columns offer a similar chromatographic performance for studied proteins.

For our experiments, the maximum linear velocity never exceeded 8 cm/min primarily due to pressure limitation of the columns. Thus, for the applied range of study no plateau was observed.

A

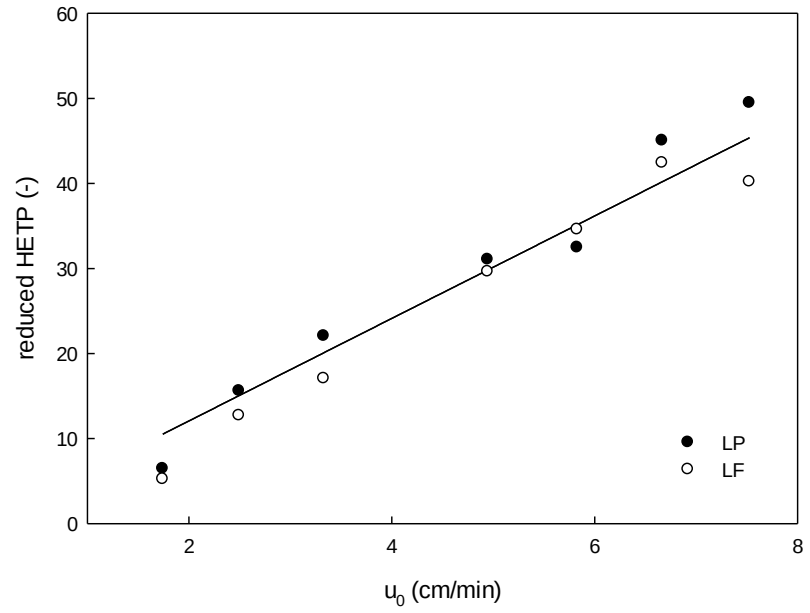

B

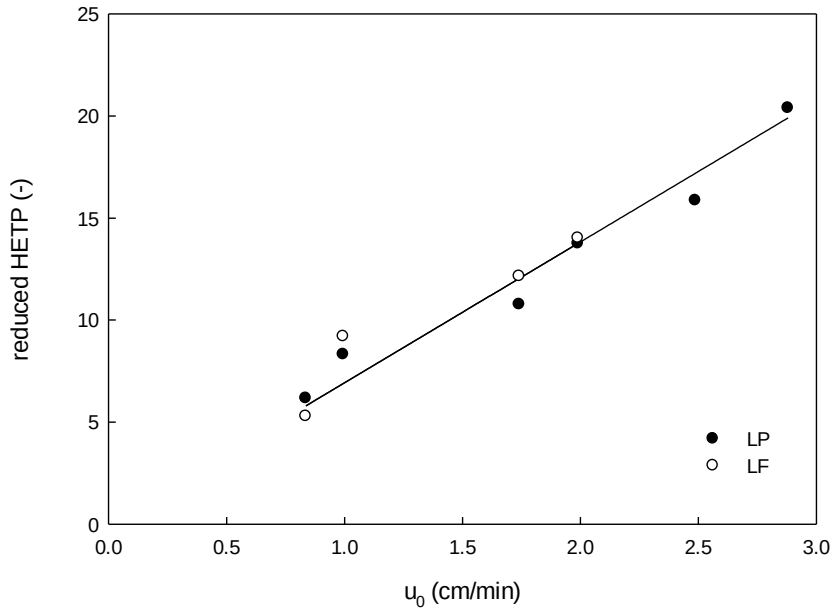

Figure 5-4 reduced HETP vs. flow velocity u_0 in elution chromatography on HiScreen™ A and HiPrep™ B columns

5.3.4 LP breakthrough curves at different operating conditions

Chromatography columns are often characterized by the shape of their breakthrough curves. The breakthrough curve shape is governed by transport processes, heat effects, and adsorption kinetics within the functionalized adsorbent and by fluid hydrodynamics in the hold-up volumes of the columns. Commercial chromatography columns are optimized such as to obtain breakthrough curves that are as sharp as possible, in order to minimize buffer consumption and to maximize the utilized adsorbent capacity.

As the operating conditions having major influence on the performance of the adsorbent are the flow rate of the mobile phase and the protein loading concentration in the feed, the effect of these two operating conditions is experimentally studied.

The obtained breakthrough curves for LP exhibited sharp breakthrough curves in most cases with both columns. The shape of the LP breakthrough curves was not rectangular, as seen for an ideal adsorbent [25]; yet symmetric in terms of the stoichiometric breakthrough time. One explanation for such a behavior could be the contribution of non-ideal effects such as dispersion effects due to pore size and length distribution. Another explanation could be the protein adsorption kinetic on the sulphopropyl (SP) strong cation exchange groups on the adsorbent surface. At high protein loadings, accessibility to the binding sites are further reduced and therefore diffusive transport limitations will be increased.

5.3.4.1 LP Adsorption at different flow rates

To study the impact of flow rate on the adsorption of LP on SP FF columns with two different diameters, dynamic adsorption experiments were carried out at flow rate between 1.74 cm/min and 2.80 cm/min. The flow rate was adjusted in order to obtain about the same linear velocity. The LP loading concentration was held constant at 0.03 mg/ml. The experimental breakthrough curves were plotted against the corrected LP loading volume ($V_{loading}$-V_0) divided by CV (Figure 5-5). For both geometries, the breakthrough curves were unchanged at the operating range of flow rate. This confirms that it is likely to maintain the quality of the separation and to avoid any product stability issues at small scale and directly apply to the larger column with no flow rate effect. The

obtained residence time of the loading acetone solution as a non-interacting tracer in the void volume was similar for both columns, i.e. at the flow velocity of 4.9 cm/min was equal to 1.88 and 1.80 min for HiScreen™ and HiPrep™ columns respectively. This generally indicates that the mass transfer mechanism is limited to diffusive transport.

A

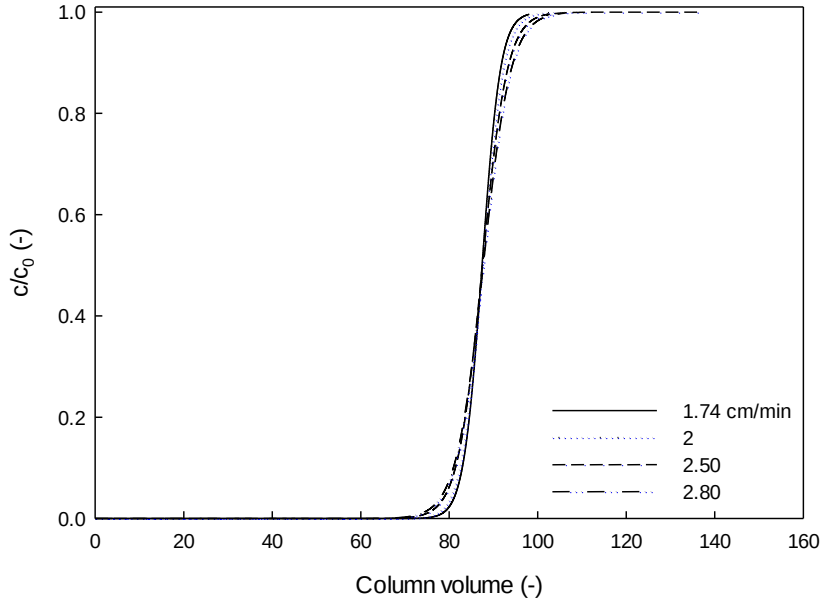

B

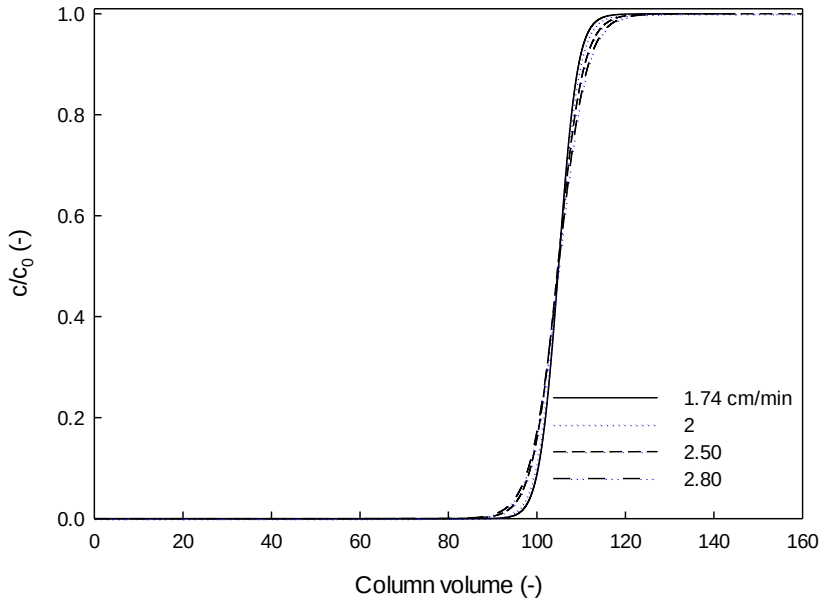

Figure 5-5 LP breakthrough curves of the column HiScreen™ A and HiPrep™ B at different flow rates ml/min

5.3.4.2 LP adsorption at different loading concentrations

The influence of feed loading concentration on breakthrough behaviour of LP was investigated at 0.02, 0.06, 0.1, 0.5 and 1 mg/mL LP for a flow velocity of 2.5 cm/min. The breakthrough curves were compared by plotting c/c_0 as a function of the corrected loading volume of LP solution multiplied by the inlet concentration (c_0) and divided by CV. Figure 5-6 illustrates the LP breakthrough curves at different LP loading concentrations for HiScreen™ and HiPrep™ columns respectively. For both columns, the profile of the breakthrough curves was uninfluenced by the feed concentration. However, the breakthrough occurs unexpectedly earlier at lower loading concentrations. This non-traditional behaviour may be due to an exclusion mechanism introduced by Harinarayan et al. [26] whereby protein binds to the outer pore regions and electrostatically hinders next protein molecules to transport into the pores. In addition, the SP functional group of cation exchange has a great preference for sodium ions. With increasing LP concentration at a low ionic strength condition as in this part of study, the preference for LP over sodium ions takes turn leading in a later breakthrough and higher dynamic capacity. van Beijeren et al. [25] also reported an increasing in binding capacity with increasing protein loading concentration for cation exchange membrane chromatography.

A

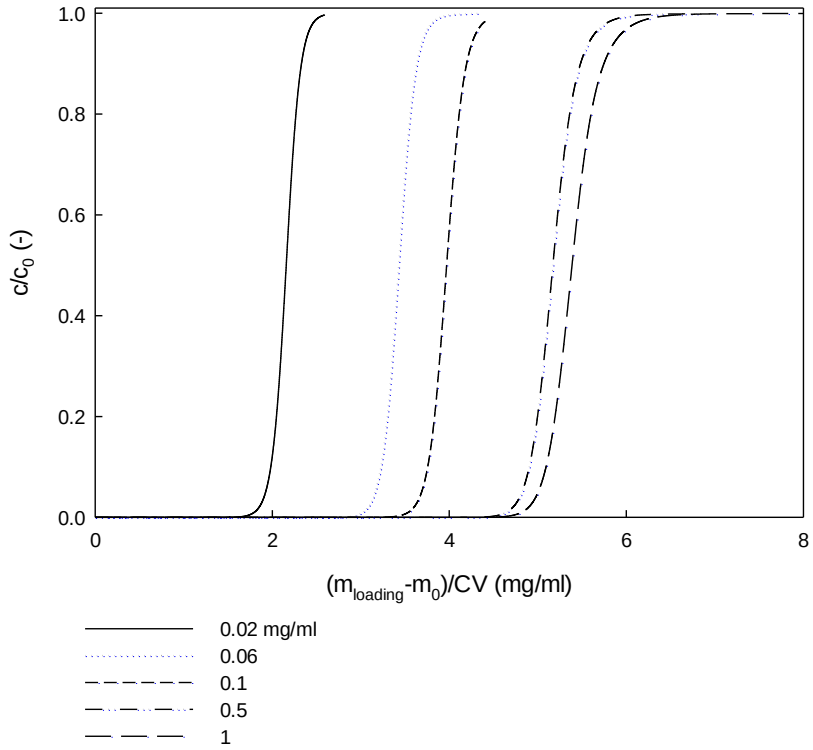
1.0
0.8
0.6
0.4
0.2
0.0
c/c0 (-)
0
2
4
6
8
(mloading-m0)/CV (mg/ml)
0.02 mg/ml
0.06
0.1
0.5
1

B

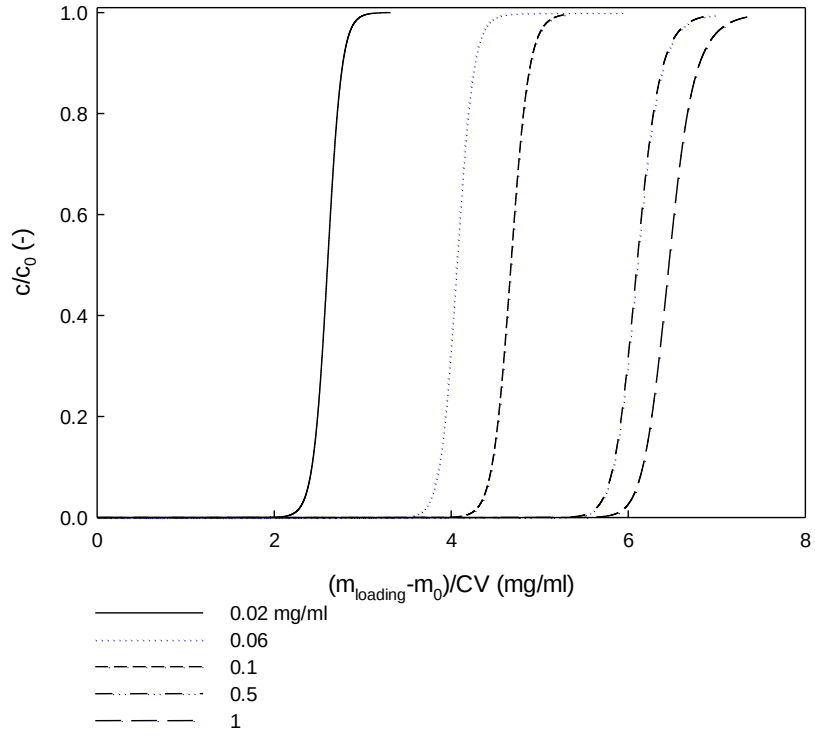

Figure 5-6 Experimental breakthrough curves of LP under different loading concentrations HiScreen™ column A and HiPrep™ column B

Dynamic binding capacity (DBC) clarifies the impact of mass transfer limitations that may occur as flow rate is increased; it is much more useful in predicting real process performance. DBC is measured under operating conditions to obtain information on what the maximum load of the target protein to the column should be in order to prevent additional loss.

For each column, the dynamic binding capacities at 10% breakthrough ($DBC_{10\%}$) were determined from the breakthrough curves attained at different flow rates. $DBC_{10\%}$ was plotted as a function of superficial velocity in Figure 5-7. A negligible decrease with increased feed flow velocity can be observed, i.e. the dynamic binding capacity at 2.5 cm/min feed flow velocity being only 1.5% lower than that at 1.74 cm/min. In fact, less

dependency of DBC on velocity is in agreement with results of HETP implying that protein uptake is controlled by pore diffusion. A decrease in dynamic binding capacity at increased flowrate for the adsorption of proteins on cation exchange was also, for example, observed for LF by Billakanti et al. [27], who found 15% decrease in DBC upon an increase of flow rate by a factor of five.

In this study, the highest $DBC_{10\%}$ was obtained for the column with the larger column. For the 20 ml column, the LP binding capacity per unit of adsorbent volume was found around 20% higher than the one obtained with the 4.7 ml column. It is likely due to better flow distribution leading to deeper penetration of protein into the particles throughout the HiPrep™ column, which ultimately results in increasing binding capacity.

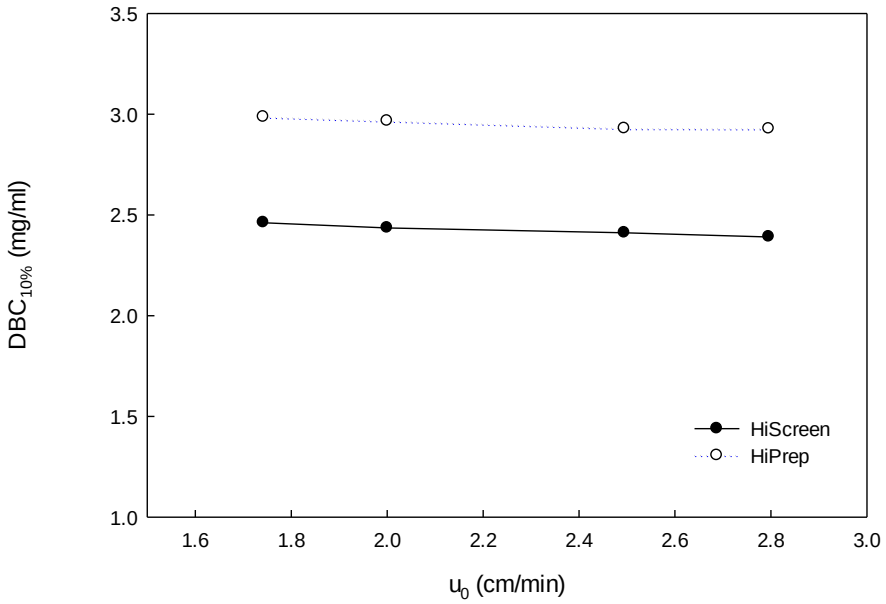

Figure 5-7 Dynamic binding capacity at 10% of breakthrough as a function of superficial flow velocity

The dynamic binding capacity was also determined as a function of LP loading concentration. Figure 5-8 shows the concentration effect for both columns. Each column shows comparable results in the $DBC_{10\%}$ with increasing the LP loading concentration. The $DBC_{10\%}$ at 0.02 mg/ml was 1.96 and 2.40 mg/ml for HiScreen™ and HiPrep™

columns, respectively. As the inlet concentration increased to 1 mg/ml, these values increased to 5.04 and 6.12 mg/ml, corresponding to 1.57 and 1.55 fold increase in binding capacity. As previously described, this phenomenon might be due to the charge repulsion between proteins in the mobile phase and proteins adsorbed on the adsorbent and/or higher LP concentration. In addition, the obtained breakthrough curve beforehand at a concentration of 0.03 mg/ml and 2.5 cm/min is consistent with the result observed at the loading concentration range between 0.02 and 1 mg/ml. At these various loading concentrations, the binding capacities were lower with the HiScreen™ column, due to its smaller column diameter.

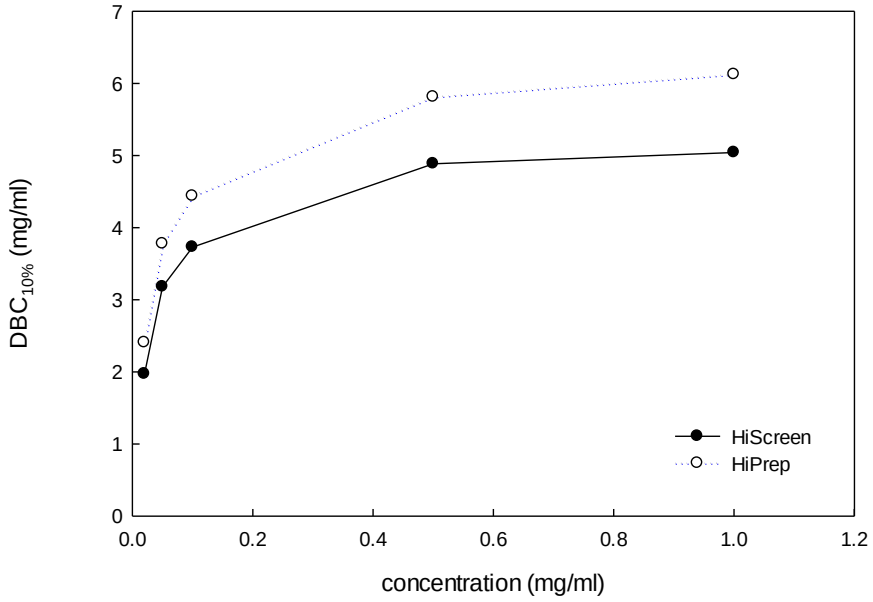

Figure 5-8 Effect of LP loading concentration on the dynamic binding capacity at 10% of breakthrough ($DBC_{10\%}$)

5.4 Conclusion

In this study, the influence of operating conditions on the adsorption of LP and LF on cation exchange adsorbent was experimentally investigated. In theory, the profiles should

be similar due to the fact that the bed height, i.e., the flow path length through the column was kept equal. It was observed that under the same bed height at both scales comparable results of back pressure and breakthrough profiles can be obtained. The process efficiency in terms of the height equivalent to a theoretical plate (HETP) as well as the dynamic binding capacity was evaluated. Trends of HETP as a function of reduced velocity were consistent with two columns representing almost a constant efficiency for the increased column dimension. This indicates that efficiency could be expected to remain unchanged in scale-up step. The LP breakthrough curves were measured at various flow rates and loading concentrations. It was observed that the LP dynamic binding capacity at 10% breakthrough capacity was independent of the applied flow rate for two geometries. This proves the advantage of column chromatography, for which high flow rates can be used without decreasing the dynamic binding capacity in larger scales. Moreover, the dynamic binding capacity decreased at higher LP concentrations, which may be as a result of non-ideal effects like steric hindrance and/or competitive adsorption between phosphate ions and protein. A profound understanding of the impact of non-ideal effects particularly at high protein loadings on the rate of mass transport and adsorption is required for further optimization of ion-exchange adsorbent materials.

Overall, according to reproducibility and comparable results at larger scale in this study, scale-up of minor whey proteins separation can be accomplished by increasing column diameter while maintaining a constant column bed length and linear velocity. Although it leads to lower flow velocities, this approach has the advantage of reduced non-ideal flow distribution compared to small scale.

References

[1] Fritz J.S. 2004. Early milestones in the development of ion-exchange chromatography: a personal account. J Chromatogr A., 1039 (1-2), 3-12.

[2] Atamna I.Z., Muschick G.M. and Issaq H.J. 1989. The effect of column diameter on HPLC separations using constant length columns. Journal of liquid chromatography, 12(3), 258-298.

[3] Gritti F., Guiochon G. 2012. Theoretical and experimental impact of the bed aspect ratio on the axial dispersion coefficient of columns packed with 2.5 μm particles. J. Chromatogr. A, 1262, 107– 121.

[4] Rathore S.A., Velayudhan A. 2002. An overview of scale-up in preparative chromatography in: scale-Up and optimization in preparative chromatography: principles and biopharmaceutical applications, Marcel Dekker, New York.

[5] Rathore A.S. and Velayudhan A. 2003. Scale-up guidelines for preparative chromatography. BioPharm, 34-42.

[6] Levison P.R., Badger S.E. and Toome D.W. 1992. Economic considerations important in the scale-up of an ovalbumin separation from hen egg-white on the anion exchange cellulose DE92. J. Chromatogr., 590, 49-58.

[7] Gerberding S.J., Byers C.H. 1998. Preparative ion-exchange chromatography of proteins from dairy whey. J. Chromatogr. A, 808(1-2), 141–151.

[8] Pedersen L., Mollerup J., Scale-up of chromatographic separations in ion-exchange chromatography. Poster presented at ISPPP 2000. Ljubljana, 5–8 November 2000, Slovenia.

[9] Pedersen L., Mollerup J., Scale-up of chromatographic separations in ion-exchange chromatography. Poster presented at PREP' 2001. Washington, DC, 26–29 May 2001, USA.

[10] Pedersen L., Mollerup J., Hansen E., Jungbauer A. 2003. Whey proteins as a model system for chromatographic separation of proteins. J. Chromatogr. B, 790(1-2), 161-173.

[11] Lightfoot E.N. 1999. Speeding the design of bioseparations: A heuristic approach to engineering design. Ind. Eng. Chem. Res,. 38(10), 3628-3634.

[12] Lenhoff A.M. 1987. Significance and estimation of chromatographic parameters. J. Chromatogr., 384, 285-299.

[13] Stanley B.J., Savage T.L., Geraghty J., 1998. Calculation of the hydrodynamic contribution to peak asymmetry in high-perfomance liquid chromatography using the equilibrium-dispersive model. Anal. Chem., 70(8), 1610-1617.

[14] Levison P.R. 2003. Large-scale ion-exchange column chromatography of proteins comparison of different formats. J. Chromatogr. B, 790(1-2), 17-33.

[15] Guiochon G., Felinger A., Shirazi D.G., Katti A.M. 2006. Fundamentals of preparative and nonlinear chromatography, 2nd ed., Elsevier Academic Press, New York.

[16] Whitley R.D., Zhang X., Wang N.H.L. 1994. Protein denaturation in nonlinear isocratic and gradient elution chromatography. AIChE J., 40(6), 1067-1081.

[17] Kaltenbrunner O., Jungbauer A., Yamamoto S. 1997. Prediction of the preparative chromatography performance with a very small column. J. Chromatogr. A, 760(1), 41-53.

[18] Li P., Xiu G., Rodrigues A.E. 2004a. Modeling breakthough and elution curves in fixed bed of inert core adsorbents: analytical and approximate solutions. Chem. Eng. Sci., 59(15), 3091-3103.

[19] Jacobson N., Degerman M., Stenborg E., Nilsson B. 2007. Model based robustness analysis of an ion-exchange chromatography step. J. Chromatogr. A, 1138(1-2), 109-119.

[20] Schneiderman S., Varadaraju H., Zhang L., Fong H., Menkhaus T.J. 2011. Mathematical model using non-uniform flow distribution for dynamic protein breakthrough with membrane adsorption media. J. Chromatogr. A, 1218(51), 9121–9127.

[21] van Deemter J.J., Zuiderweg F.J., Klinkenberg A. 1956. Longitudinal diffusion and resistance to mass transfer as causes of nonideality in chromatography. Chem. Eng. Sci., 5, 271-289.

[22] Rodrigues A.E. 1993. An extended van Deemter equation (Rodrigues equation) for performing chromatographic processes using large-pore, permeable particles. LC-GC, 6(1), 20.

[23] Rodrigues A.E., Loureiro J.M., Chenou C. 1995. Rendueles de la Vega M. Short communication: Bioseparations with permeable particles . J. Chromatogr. B, 664(1), 233-240.

[24] Patel K.D., Jerkovich A.D., Link J.C., Jorgenson J.W. 2004. In-depth characterization of slurry packed capillary columns with 1.0-µm nonporous Particles using reversed-phase isocratic Ultrahigh-pressure liquid chromatography. Anal. Chem., 76(19), 5777-5786.

[25] van Beijeren P., Kreis P., Zeiner T. 2012. Ion exchange membrane adsorption of bovine serum albumin—Impact of operating and buffer conditions on breakthrough curves. J. Membr. Sci., 415–416, 568–576.

[26] Harinarayan C., Mueller J., Ljunglöf A., Fahrner R., van Alstine J., van Reis R. 2006. An exclusion mechanism in ion exchange chromatography. Biotechnology and bioengineering, 95 (5), 775-787.

[27] Billakanti J.M., Fee C.J. 2009. Characterization of cryogel monoliths for extraction of minor proteins from milk by cation exchange. Biotechnology and Bioengineering, 103(6), 1155-1163.

Chapter 6

Concluding Remarks and Outlook

6.1 Review of objectives

The general aim of this thesis was to develop fundamental process understanding of specific chromatographic separation via the application of mechanistic chromatography models. The goal was to use the models as a powerful tool for the development and optimization of the separation process and increase the robustness of protein purification processes.

6.1.1 Determination of adsorption isotherm parameters

Chapter 3 developed a predictive approach for the separation of lactoperoxidase and lactoferrin with focusing on the cation exchange platform at an early stage of process development. This key step in the purification process provides mechanistic insights into various chromatographic subjects, such as retention, adsorption capacity whilst reducing experimental effort, process development time and cost. Most particularly, the analysis of proteins interaction is distinct from other works in providing useful intuitions into the underlying physics rather than fitting experimental data without verifying the model assumptions. The use of a mechanistic-based isotherm model allows interpreting the adsorption of single-component and binary mixtures quantitatively. The key findings from an interaction point of view are:

- The SMA isotherm parameters demonstrate the trends of the protein-adsorbent surface interactions (k_{ads},k_{des}) which largely affect adsorption patterns, indicating the dominant role of protein-adsorbent interactions in controlling isotherm profiles;

- Steric protein interactions can have a significant effect on adsorption. Depending on the protein properties, the contribution of intermolecular interactions between adsorbed protein molecules can be fairly subtle or distinct in determining the general adsorption behavior.

6.1.2 Model-based process optimization

Chapter 5 considered the development and further application of mechanistic model of chromatography in process optimization. The chapter considered the optimal purification of LP protein on IEC process. It has been difficult to quantify the variability in protein adsorption between experiments. The purified LP had to meet product quality specification, but was experiencing unacceptable performance probably due to its sensitivity to the salt concentration.

In chapter 5, process optimization started with the DoE approach in order to quickly reveal significant decision variables and produce a basic understanding of the process. Next, the outcomes from this study were used to the development of a mechanistic model, using data from DoE experiments for model calibration and validation. The model showed that it is highly predictive not only in the primary experiments but also for conditions out of the examined design space.

6.1.3 Effects of scale up and operating condition

The focus of chapter 5 was on the column studies of elution and frontal loading chromatography performed for binary systems and single component, respectively. The contributions of the mass transfer and the adsorption to overall column behavior were discussed. The convective dispersion contribution relative to diffusion was characterized and evaluated based on the fitting breakthrough profile of non-binding component. Additionally, the modified van Deemter plot qualitatively indicated the negligible role of dispersion in chromatographic efficiency under the examined conditions in this chapter. Dynamic binding capacity at 10% breakthrough capacity showed no dependency on the applied flow rate. This demonstrates applying high flow rates in column chromatography with no reduce in dynamic binding capacity for large scales. On the other hand, dynamic binding capacity unexpectedly decreased at higher protein concentrations due to non-ideal effects such as steric hindrance and/or competitive adsorption between phosphate ions and lactoperoxidase.

The key point of the study was to experimentally assess column behaviour at lab scale due to relatively smaller requirements of material as well as the ease of performing

different runs; thus assisting to determine the limiting mass transfer mechanisms that should be reflected in scale up considerations. Some issues in large columns such as forming accurate and reproducible gradients and channeling in the column that leads to peak broadening or peak splitting can be challenging. It is difficult to achieve uniform flow distribution; failure to do so can lead to peak tailing. The large column follows the same pattern in elution and breakthrough profiles as the small one does and demonstrates satisfactory performance. These observations indicates that scale-up of minor whey proteins separation can be accomplished by increasing column diameter while maintaining a constant column bed length and linear velocity. Although it leads to lower flow velocities, this approach has the advantage of reduced non-ideal flow distribution compared to small scale.

6.2 Recommendations for future work

It is inevitable from this thesis that mechanistic models of chromatography provide significant advantages to downstream process development. However, there are still some aspects to be reviewed before models are used in practice. In this section, potential outlooks for future work related to use of mechanistic chromatography models are briefly expressed.

Future work can focus on the SMA parameters determination to provide more detailed descriptions of mass transport and adsorption phenomena. The difficulty of modeling complex adsorption behavior using the proposed mechanism may be due to the simplifications in interaction calculations, protein geometry and charge distribution. Due to the dependence of protein interactions on particle size [1], large proteins and viruses generally have stronger interactions than small proteins. The adsorption of these large biomolecules may show a larger contribution of lateral interactions and lead to more different adsorption patterns [2]. The comprehensive study of protein conformation and binding positions for different conditions with the aid of powerful microscopic techniques such as molecular dynamic simulation would be of particular interest. The connection between mechanistic modeling and molecular dynamic simulations could therefore lead to an even more predictive and mechanistic model for sorption processes.

In addition, it will be informative to examine the approach for more complex protein mixtures. It is useful to investigate the underlying mechanisms and to find if there exists an inherent relation between single- and multi-component protein adsorption behaviors.

Reference

[1] Yuan, Y., Oberholzer, M.R. Lenhoff, A.M. 2000. Size Does Matter: Electrostatically Determined Surface Coverage Trends in Protein and Colloid Adsorption. *Coll. Surf. A* 165(1-3) 125-141.

[2] Trilisky, E.I., Lenhoff, A.M. 2007. Sorption Processes in Ion-Exchange Chromatography of Viruses. *J. Chromatogr. A* 1142(1) 2-12.

Appendices

Appendix A: General Rate Model

In the general rate model for IEC, a differential mass balance for the bulk-fluid phase and particle phase in the column considers convection through the column, axial dispersion and transport through the external film at the particle surface and intra-particle diffusion. The dimensionless governing equations are shown below for the bulk-fluid phase and the particle phase, respectively:

$$-\frac{1}{Pe_{Li}}\frac{\partial^2 C_{bi}}{\partial z^2}+\frac{\partial C_{bi}}{\partial z}+\frac{\partial C_{bi}}{\partial \tau}+\zeta_i(C_{bi}-C_{pi,r=1})=0$$

$$(1-\varepsilon_p)\frac{\partial q_i}{\partial \tau}+\varepsilon_p\frac{\partial C_{pi}}{\partial \tau}-\eta_i\frac{1}{r^2}\frac{\partial}{\partial r}(r^2\frac{\partial C_{pi}}{\partial r})=0$$

where C_{bi} is the concentration of component i in the bulk-fluid phase, C_{pi} is the concentration of component i in the stagnant fluid phase inside particle macropores, q_i is used to describe particle phase concentration. z is dimensionless axial coordinate, Z/L, r is dimensionless radial coordinate for particle, R/R_p, and τ is dimensionless time, t(v/L). ε_b bed void fraction and ε_p particle porosity. Pe_{Li} is Péclet number of axial dispersion for component i, vL/D_{bi}, ξ_i is dimensionless constant for component i, $3Bi_i\ \eta_i(1-\varepsilon_b)/\varepsilon_b$, and η_i dimensionless constant for component i, $\varepsilon_p D_{pi}L/(R_p v)$.

$\frac{\partial C_{bi}}{\partial \tau}$ is the rate per unit volume of accumulation of component i in the mobile phase

$(1-\varepsilon_b)\frac{\partial q_i}{\partial \tau}$ is the rate per unit volume of accumulation of component i in the stationary phase, $\frac{\partial C_{bi}}{\partial z}$ is the rate per unit volume of mass transfer by convection down the column, and $-\frac{1}{Pe_{Li}}\frac{\partial^2 C_{bi}}{\partial z^2}$ is the rate per unit volume of mass transfer by dispersion and particle mass transfer kinetics lumped into one term.

With the following boundary conditions:

$$z = 0, \frac{\partial C_{bi}}{\partial z} = Pe\left[C_{bi} - C_{fi}(\tau)\right];$$
$$z = L, \frac{\partial C_{bi}}{\partial z} = 0;$$
$$r = 0, \frac{\partial C_{pi}}{\partial r} = 0$$
$$r = 1, \frac{\partial C_{pi}}{\partial r} = Bi_i(C_{pi} - C_{pi,r=1})$$

The dimensionless feed profile $C_{fi}(\tau)$ for the modulator (i=1, the first component) in this gradient elution IEC model determines what kind of elution profile is used, including isocratic elution, step-change displacement, or gradient elution.

Convection through the column

$$-\frac{1}{Pe_{Li}}\frac{\partial^2 C_{bi}}{\partial z^2}+\frac{\partial C_{bi}}{\partial z}+\frac{\partial C_{bi}}{\partial \tau}+\zeta_i(C_{bi}-C_{pi,r=1})=0$$

Boundary condition at z=0

$$z=0,\frac{\partial C_{bi}}{\partial z}=Pe\left[C_{bi}-C_{fi}(\tau)\right]$$

Boundary condition at z=L

$$z=L,\frac{\partial C_{bi}}{\partial z}=0$$

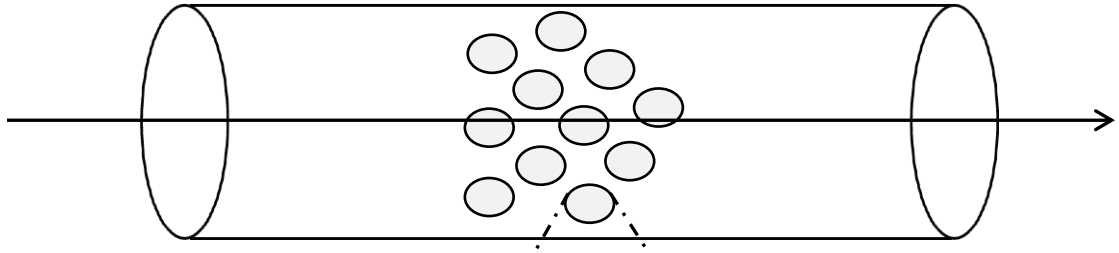

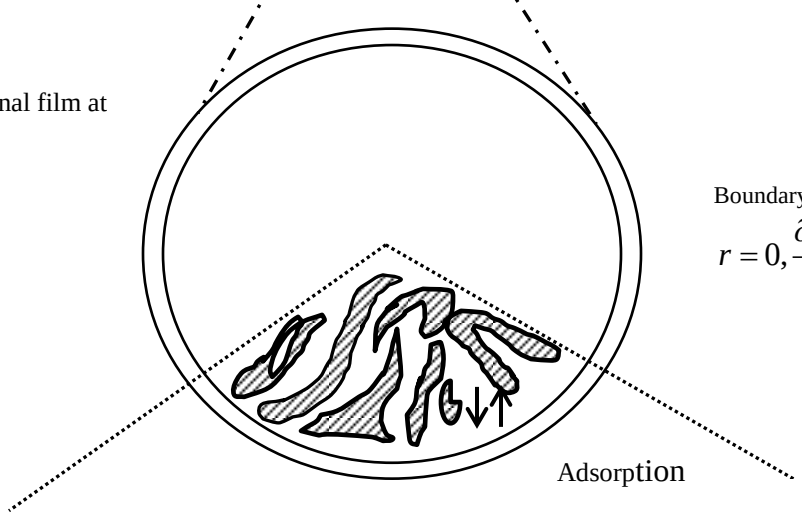

Mass transport through the external film at the particle surface

Boundary condition at r=0

$$r=0,\frac{\partial C_{pi}}{\partial r}=0$$

Adsorption

Boundary condition at $r=R_p$

$$r=R_p,\frac{\partial C_{pi}}{\partial r}=Bi_i(C_{pi}-C_{pi,r=R_p})$$

Mass transfer through particle pores

$$(1-\varepsilon_p)\frac{\partial q_i}{\partial \tau}+\varepsilon_p\frac{\partial C_{pi}}{\partial \tau}-\eta_i\frac{1}{r^2}\frac{\partial}{\partial r}(r^2\frac{\partial C_{pi}}{\partial r})=0$$

Curriculum Vitae

Name: Naeimeh Faraji

Post-secondary Education and Degrees:

Sharif University of Technology
Tehran, Iran
2001-2006 B.Sc.

Sharif University of Technology
Tehran, Iran
2006-2009 M.Sc.

The University of Western Ontario
London, Ontario, Canada
2012-2016 Ph.D.

Honours and Awards:

Ross and Jean Clark Scholarship
2014

Related Work Experience

Teaching Assistant
University of Western Ontario
2012-2016

Research Assistant
University of Western Ontario
2012-2016

Publications & Conferences:

Faraji, N., Zhang, Y., Ray A.K. 2015. *J. Chromatogr. A 1412*, 67-74

Faraji N., Ray A.K. 65th Canadian Chemical Engineering Conference, Calgary, AB October 4-7 2015

Faraji N., Ray A.K. , PREP 2015-28th International Symposium on Preparative and Process Chromatography, Philadelphia, PA US July 27-July 29 2015

Faraji N., Molaei Dehkordi A., 2nd International Conference on Chemical Engineering and Advanced Materials, November 15 – 26 2010